

September 27, 1999  
FINAL REPORT

**SURFACE GEOLOGY BASED STRONG MOTION  
AMPLIFICATION FACTORS FOR THE  
SAN FRANCISCO BAY AND LOS ANGELES AREAS**

Prepared for

**PG&E PEER - TASK 5.B**

by

Walter Silva  
Syliva Li  
Bob Darragh  
Nick Gregor

of

Pacific Engineering and Analysis  
311 Pomona Avenue  
El Cerrito, CA 94530

## **EXECUTIVE SUMMARY**

### **SURFACE GEOLOGY BASED STRONG MOTION AMPLIFICATION FACTORS FOR THE SAN FRANCISCO BAY AND LOS ANGELES AREAS**

**Pacific Engineering and Analysis**

For both the San Francisco Bay and Los Angeles areas, surface geology based amplification factors have been developed for 5% damped response spectra. The factors are computed relative to reference rock site geology,  $K_{fr}$  (Franciscan) for the San Francisco Bay area and  $M_{sb}$  (Granite) for the Los Angeles area. The factors are functions of profile depth (or depth range) as well as expected reference rock peak acceleration values ranging from 0.05g to 1.25g.

The amplification factors are computed using average measured shear-wave velocity profiles at sites located within the surficial geologic units with an RVT (Random Vibration Theory) based equivalent-linear site response approach. Separate  $G/G_{max}$  and hysteretic damping curves are used for San Francisco (North Coast) and Los Angeles (Peninsular Range) cohesionless soils reflecting different degrees of nonlinear response in both regions. These curves, along with  $G/G_{max}$  and hysteretic damping for rock site conditions which are the same for both regions, were validated by modeling recorded motions in both regions.

The analytical amplifications factors are compared to published empirical as well as current NEHRP factors for both regions. Comparisons with the empirical factors show good agreement for empirical factors computed for 5% damped response spectra and reasonable agreement for empirical factors for Fourier amplitude spectra. The analytical factors were generally below the empirical for Fourier amplitude spectra but agreed in shape and general trends: soft alluvium higher than stiff alluvium at low frequency but crossing over at high frequency. Comparisons with the NEHRP provisions showed reasonable agreement for the San Francisco Bay area, except for the Bay Muds ( $Q_m$ ) being classified as NEHRP D (based on actual average shear-wave velocity over the top 100 ft). For the Los Angeles area, good

agreement was seen with the NEHRP amplification factors at low levels of loading (up to about 0.10g). At higher loading levels the low frequency NEHRP factors were significantly exceeded while the high frequency NEHRP factors appear to reflect considerable conservatism at very high loading levels.

The amplification factors developed in this project extend to 1,000 ft for the San Francisco Bay area and 1,500 ft for the Los Angeles area. They may be used to approximately accommodate the effects of near surface geology for seismic hazard evaluations.

## CONTENTS

<b><u>Section</u></b>	<b><u>Page</u></b>
1.0 Introduction	1
2.0 Geology Based Profiles	2
2.1 San Francisco Bay Area Profiles	3
2.2 Los Angeles Area Profiles	4
2.3 Comparison of San Francisco and Los Angeles Profiles	4
2.4 Development of Smooth Profiles For Site Response Analyses	5
3.0 Geology Based Amplification Factors	5
3.1 Methodology	6
3.1.1 Equivalent-Linear Computational Scheme	6
3.1.2 RVT Based Computational Scheme	7
3.2 G/Gmax and Hysteretic Damping Curves	7
3.3 Specification of Control Motions	8
3.4 Development of Site Amplification Factors	10
3.4.1 Amplification Factors for the San Francisco Bay Area	11
3.4.2 Amplification Factors For The Los Angeles Area	13
3.5 Adjustment Factors For Soft Rock Conditions	16
4.0 Summary	16
References	18
Appendix A:	A-1
Appendix B:	B-1

## LIST OF TABLES

<u>Table Number</u>		<u>Page</u>
1	Surface Geology Based Profiles, Site Classes, and Dynamic Material Properties	22
2	Site Classifications	23
3	Loma Prieta Crustal Model (from Wald et Al., 1991)	24
4	Franciscan Reference Site Ground Motion Parameters San Francisco Bay Area	25
5	Depth Categories and Depth Ranges	26

## LIST OF FIGURES

<u>Figure Number</u>		<u>Page</u>
1	Effects of near surface soil conditions on 5% damped response spectral shapes (source: Seed, Ugas, and Lysmor, 1976)	27
2	Effects of hard and soft rock site conditions and magnitude	28
3	Mapped surface geology for the San Francisco Bay Area	29
4	Surface geology based shear-wave velocity profiles for the San Francisco Bay area	30
5	Surface geology based shear-wave velocity profiles for the Los Angeles area	31
6	Comparison of median baserock shear-wave velocity profiles for San Francisco and Los Angeles areas	32
7	Comparison of median Tertiary shear-wave velocity profiles for San Francisco and Los Angeles areas	33
8	Comparison of median Alluvium shear-wave velocity profiles for San Francisco and Los Angeles areas	34
9	Median and $\pm 1 \sigma$ shear-wave velocity profiles for the San Francisco Bay area surface geologic unit $K_{jr}$ , Franciscan	35
10	Median and $\pm 1 \sigma$ shear-wave velocity profiles for the San Francisco Bay area surface geologic unit $TM_{zs}$ , Tertiary Bedrock	25
11	Median and $\pm 1 \sigma$ shear-wave velocity profiles for the San Francisco Bay area surface geologic unit $QT_s$ , Quaternary/Tertiary	
12	Median and $\pm 1 \sigma$ shear-wave velocity profiles for the San Francisco Bay area surface geologic unit $Q_{oa}$ , Older Alluvium	26
13	Median and $\pm 1 \sigma$ shear-wave velocity profiles for the San Francisco Bay area surface geologic unit $Q_a$ , Quaternary Alluvium	
14	Median and $\pm 1 \sigma$ shear-wave velocity profiles for the San Francisco Bay area surface geologic unit $Q_m$ , Bay Mud	

## LIST OF FIGURES

<u>Figure Number</u>		<u>Page</u>
15	Median and $\pm 1 \sigma$ shear-wave velocity profiles for the Los Angeles area surface geologic unit $M_{sb}$ , Granite	41
16	Median and $\pm 1 \sigma$ shear-wave velocity profiles for the Los Angeles area surface geologic unit $T_s$ , Tertiary	42
17	Median and $\pm 1 \sigma$ shear-wave velocity profiles for the San Francisco Bay area surface geologic unit $T_s$ , Saugus	43
18	Median and $\pm 1 \sigma$ shear-wave velocity profiles for the Los Angeles area surface geologic unit $Q_{oa}$ , Older Alluvium	44
19	Median and $\pm 1 \sigma$ shear-wave velocity profiles for the Los Angeles area surface geologic unit $Q_y$ , Younger Alluvium	45
20	Generic $G/G_{max}$ and hysteretic damping curves for rock site conditions	46
21	Generic $G/G_{max}$ and hysteretic damping curves for North Coast cohesionless soil site conditions (EPRI, 1993).	47
22	Generic $G/G_{max}$ and hysteretic damping curves for cohesive soil site conditions (Vucetic and Dobry, 1991)	48
23	Generic $G/G_{max}$ and hysteretic damping curves for Peninsular Range cohesionless soil site conditions (Silva et al., 1997).	49
24	Median and $\pm 1 \sigma$ 5% damped baserock (Franciscan) motions for 5%g (Table 4): $M = 6.5$ , stress drop = 60 bars. Parametric variation includes top 250 ft of the profile (Figure 15) and nonlinear properties	50
25	Comparison of median 5% damped response spectra computed for San Francisco (solid) and Los Angeles (dashed) area baserock site conditions for suite of outcrop peak acceleration values (Table 4): $M = 6.5$ , stress drop: 60 bars	51
26	Comparison of median and $\pm 1 \sigma$ amplification factors (5% damped response spectra) for San Francisco area Quaternary Alluvium ( $Q_w$ ) depth category 4 (30 to 1,000 ft) for reference Franciscan rock outcrop median peak acceleration values of 0.05g and 0.40g	52

## LIST OF FIGURES

<u>Figure Number</u>		<u>Page</u>
27	Comparison of median amplification factors (5% damped response spectra) computed for reference Franciscan outcrop peak acceleration of 0.05g with empirical factors (smoothed Fourier amplitude spectra; Borchardt and Glassmoyer, 1992). Empirical factors were computed using low levels of loading (generally $\leq 0.10g$ )	53
28	Comparison of median amplification factors (5% damped response spectra) computed for reference Franciscan outcrop peak acceleration of 0.40g with empirical factors (smoothed Fourier amplitude spectra; Borchardt and Glassmoyer, 1992). Empirical factors were computed using low levels of loading (generally $\leq 0.10g$ )	54
29	Median amplification factors computed for $QT_s$ , $Q_{\Delta}$ , $Q_m$ , for different depth categories: 30 to 150 ft, dash dots; 150 to 350, solid; 350 to 650, dashes	55
30	Comparison of median amplification factors with NEHRP provisions	56
31	Median and $\pm 1 \sigma$ amplification factors computed for San Francisco area surficial geologic unit $TM_{zs}$	57
32	Median and $\pm 1 \sigma$ amplification factors computed for San Francisco area surficial geologic unit $QT_s$	58
33	Median and $\pm 1 \sigma$ amplification factors computed for San Francisco area surficial geologic unit $Q_{\Delta}$	59
34	Median and $\pm 1 \sigma$ amplification factors computed for San Francisco area surficial geologic unit $Q_{\Delta}$	60
35	Median and $\pm 1 \sigma$ amplification factors computed for San Francisco area surficial geologic unit $Q_m$	61
36	Comparison of median amplification factors computed for units $Q_y$ , $Q_o$ , Saugus ( $T_s$ ), $T_s$ , and $Q_o + T_s$ (Table 1) for the depth categories with the widest depth ranges	62



## LIST OF FIGURES

<u>Figure Number</u>		<u>Page</u>
37	Comparison of median amplification factors (5% damped response spectra) computed for reference Granite outcrop peak acceleration of 0.05g with empirical factors (smoothed Fourier amplitude spectra; Bonilla et al., 1997). Empirical factors are based on small earthquakes	63
38	Deep firm to stiff soil (Geomatrix C + D, Table 2) amplification of 5% damped response spectra relative to soft rock (Geomatrix A + B) from an empirical attenuation relation (Abrahamson and Silva, 1997)	64
39	Comparison of median amplification factors (5% damped response spectra) computed for reference Granite outcrop peak acceleration of 0.10g with empirical factors (5% damped response spectra; Borchardt, 1996) Empirical factors are based on recordings of the 1994 M 6.7 Northridge	65
40	Comparison of median amplification factors (5% damped response spectra) computed for reference Granite outcrop peak acceleration of 0.10g with empirical factors (smoothed Fourier amplitude spectra; Harmsen, 1997). Empirical factors are based on the 1971 San Fernando, 1987 Whittier Narrows, 1991 Sierra Madre, and 1994 Northridge earthquakes	66
41	Comparison of median amplification factors with NEHRP provisions	67
42	Amplification factors computed for Geomatrix site categories A and B (Figure 6, Table 2) relative to San Francisco area reference rock outcrop Franciscan	68
43	Amplification factors computed for Geomatrix site categories A and B (Figure 6, Table 2) relative to Los Angeles area reference rock outcrop Granite	69

# **SURFACE GEOLOGY BASED STRONG MOTION AMPLIFICATION FACTORS FOR THE SAN FRANCISCO BAY AND LOS ANGELES AREAS**

## **1.0 INTRODUCTION**

Observations of the effects of the ground on shaking during earthquakes have a long history. Del Barrio, in the 1855 Proceedings of the University of Chile states<sup>\*</sup> "...a movement.... must be modified while passing through media of different constitutions. Therefore, the earthquake effects will arrive to the surface with higher or lesser violence according to the state of aggregation of the terrain which conducted the movement. This seems to be, in fact, what we have observed in the Colchagua Province (of Chile) as well as in many other cases" (Del Barrio, 1855). In 1862, Mallet (1862) noted the effect of geology upon earthquake damage. Milne (1908) observed that in soft "damp" ground it was easy to produce vibrations of large amplitudes and long duration, while in rock it was difficult to produce vibrations of sufficient amplitude to be recorded.

Wood (1908) and Reid (1910), using apparent intensity of shaking and distribution of damage in the San Francisco Bay area during the 1906 earthquake, gave evidence that the severity of shaking can be substantially affected by the local geology and soil conditions. Gutenberg (1927, 1957) developed amplification factors representing different site geology by examining recordings of microseisms and earthquakes from instruments located on various types of ground. Figure 1 shows average spectral shapes (response spectral acceleration divided by peak acceleration) computed from recordings made on rock and soil sites at close distances to earthquakes in the magnitude range of about M 6 to 7. The differences in spectral shapes are significant and depend strongly upon the general site classifications. These variations in spectral content represent average site dependent ground motion characteristics and result from vertical variations in soil material properties (Hayashi et al., 1971; Mohraz, 1976; Seed et al., 1976). Due primarily to the limited number of records from earthquakes of different magnitudes, spectral content in terms of response spectral shapes was for some time interpreted not to depend upon magnitude nor distance, but primarily on the stiffness and depth of the local soil profile. However, with an increase in the strong motion database, it has become apparent that spectral shapes depend strongly upon magnitude as well as site conditions (Joyner and Boore, 1982, Idriss, 1985; Silva and Green, 1989), and distance (Silva and Green, 1989), and that site effects extend to rock sites as well (Boatwright and Astrue, 1983; Campbell 1981, 1985, 1988; Cranswick et al., 1985; Silva and Darragh, 1995).

Examples of differences in spectral content largely attributable to one-dimensional site effects at rock sites can be seen in comparisons of response spectral shapes computed from motions recorded in both active and stable tectonic regions (Silva and Darragh, 1995). Figure 2 shows average spectral shapes ( $S_a/a_{max}$ ) computed from recordings made on rock at close

---

<sup>\*</sup>Translated from the old Spanish by Professor Ricardo Dobry.

distances to large and small earthquakes. For both magnitudes (moment magnitude  $M$  6.4 and 4.0), the motions recorded in Eastern North America (ENA), a stable tectonic region, show a dramatic shift in the maximum spectral amplification toward higher frequencies compared to the Western North American (WNA) motions. These differences in spectral content are significant and are interpreted as primarily resulting from differences in the shear-wave velocity and damping in the rocks directly beneath the site (Boore and Atkinson, 1987; Toro and McGuire, 1987; Silva and Green, 1989; Silva and Darragh, 1995). Also evident in Figure 2 is the strong magnitude dependency of the response spectral shapes. The smaller earthquakes show a much narrower bandwidth. This is a consequence of higher corner frequencies for smaller magnitude earthquakes (Boore, 1983; Silva and Green, 1989; Silva and Darragh, 1995).

The difference in spectral content due to soil site effects, as shown in Figure 1, and due to rock site effects, as shown in Figure 2, are dramatic and illustrate the degree to which one-dimensional site conditions (vertical variations in dynamic material properties) control strong ground motions.

In order to capture these geologically controlled differences in ground motions, site amplification factors are developed in a manner that is appropriate for San Francisco Bay area and Los Angeles area soil and rock-sites. For wide applicability, both the rock and soil conditions are based upon mapped surface geology with appropriate shear-wave velocity profiles developed for each geology type. The amplification factors are developed for 5% damped response spectra (values at 100 Hz apply to peak acceleration) and are relative to a generic Franciscan rock site for the San Francisco Bay area and a generic granitic rock site for the Los Angeles region. The factors accommodate nonlinear soil/rock response and are produced as a function of expected Franciscan or granitic rock peak acceleration values. Because of this, they may be applied to any size earthquake at any distance with knowledge only of the expected rock peak acceleration. The factors are considered appropriate for rock outcrop peak accelerations up to 1.25g and over the frequency range of 0.1 to 100.0 Hz. At long periods, due to possible basin effects, care should be exercised in applying the factors to deep soil sites at frequencies less than about 0.5 Hz for distant ( $> 50$  km) earthquakes.

## 2.0 GEOLOGY BASED PROFILES

The development of shear-wave velocity profiles appropriate for the mapped surface geology of the San Francisco Bay and Los Angeles areas was a cooperative effort between Pacific Engineering and Analysis (PE&A) and Chris Wills of the California Division of Mines and Geology (CDMG). As part of the CDMG effort in developing state-wide probabilistic seismic shaking maps, Mr. Wills was tasked with associating site categories based on average velocity over the top 30m with surface geology. To accomplish this task, he was planning on developing a shear-wave velocity profile database to correlate the profile averages with the mapped geology at the profile locations. Since PE&A already possessed a large proprietary database, an agreement was reached such that the CDMG could use the database provided any augmentation was shared with PE&A. As a result, Mr. Wills added many profiles along with missing profile coordinates, merged the database with a GIS system, and plotted the profiles on a basemap map of surface geology (Figure 3). The result is a tabulation of profiles for each

geology type. Rock units consist of Franciscan, Quaternary-Tertiary, and Tertiary for the San Francisco area and Granite, Tertiary, and Saugus (Tertiary) for the Los Angeles area. Soil units consist of Quaternary and Older Alluvium, and Bay Mud for the San Francisco Bay area and Quaternary and Older Alluvium for the Los Angeles area. Table 1 lists the geology types, average shear-wave velocity to 30m, the corresponding USGS and NEHRP site categories (Table 2), and number of shear-wave velocity profiles currently in each category.

To develop profiles appropriate for the different geology types, median and  $\pm 1\sigma$  (lognormal) profiles were computed for the profiles in each geology group. Figures 4 and 5 show median profiles for the San Francisco and Los Angeles areas respectively. For the San Francisco area, the geologic units generally show distinct median profiles with the exception of Quaternary Alluvium ( $Q_u$ ) and Older Alluvium ( $Q_o$ ). Distinct NEHRP categories include Franciscan ( $K_f$ , NEHRP B), Tertiary Bedrock ( $TM_{zs}$ , C) and Quaternary/Tertiary Rock ( $QT_s$ , C) and the stiff to firm soils (all NEHRP category D). Unfortunately, the median Bay Mud profile ( $Q_m$ ), with its 30m average shear-wave velocity of about 188m/sec, is placed in NEHRP Category C, with the firm to stiff soils (Table 2).

## 2.1 San Francisco Bay Area Profiles

The profile figures show several features of interest. For the rock classes, Franciscan and Tertiary, a significant difference exists with the Tertiary profile being much softer (NEHRP site class C) than the Franciscan and resembling a stiff soil (Older Alluvium) at shallow depths. The Franciscan is considered soft rock but is stiff enough (NEHRP site class B) to form the basis for the San Francisco area amplification factors. That is, the site amplification factors will be computed relative to Franciscan rock outcropping as defined by the Franciscan profile in Figure 4.

For the alluvium, little difference in stiffness is seen between the Older and Quaternary Alluvium profiles. This suggests that, in view of uncertainty in the median profiles, there may be no statistically significant differences in the amplification factors. This is examined in Section 3 resulting in the combining of the two sets of amplification factors into one set, reflecting the broader class of alluvium.

The Bay Mud profile shows a shallow low velocity zone with higher shear-wave velocities at the surface than at a depth of about 20 ft. This velocity reversal is likely due to the presence of fill material which is a common occurrence in the built environment near San Francisco Bay. This profile is not unexpected since velocity measurements (boreholes) are generally associated with structures of some kind. Because such features can have a strong effect on ground motions at high levels of loading, they are most appropriately addressed on a site-specific basis. The base case profile was smoothed through this feature. The amplification factors for Bay Mud surface geology should then be considered to have higher uncertainty at higher loading levels (expected Franciscan  $PGA \geq 40\%$ ) and at short periods ( $\leq 0.2$  sec).

## 2.2 Los Angeles Area Profiles

For the Los Angeles area, Figure 5 compares the median surface geology based profiles and shows several features of interest as well. For the alluvium, the Older Alluvium ( $Q_o$ ) profile is significantly stiffer than the Quaternary Alluvium ( $Q_y$ ) profile, unlike the corresponding profiles for the San Francisco Bay area (Figure 4).

The three rock classes (Table 1): Granite, Tertiary, and Saugus show significant differences in shear-wave velocities since both the Tertiary and Saugus (NEHRP site class C) are much softer than the Granite (NEHRP site class B). The shallow portion of the Tertiary resembles a firm soil (Older Alluvium). Interestingly, in the top 50 to 100 feet, the Saugus profile is stiffer than either Tertiary or Older Alluvium. This suggests that, in view of the uncertainty and variability in the shear-wave velocity profiles, there may be no statistically significant differences in the amplification factors. This is examined in Section 3 resulting in a combining of the three sets of amplification factors into one, reflecting a broader classification.

## 2.3 Comparison of San Francisco and Los Angeles Profiles

To compare median profiles for the two regions, Figures 6 to 8 show profiles for the corresponding surface geology. Figure 6 compares the two hard (California) rock profiles, Franciscan and Granite. For the depth range of overlap, the two profiles are similar suggesting similar strong ground motion response, all else being comparable. Unfortunately, only 8 Granite profiles are available (Table 1) compared to 30 for the Franciscan surficial geology, as a result a bias may exist for the Los Angeles area Granite profile. For the available data, these profiles may suggest very similar dynamic material properties for the Franciscan and Granite site geologies for the two regions. Since these profiles represent the stiffest materials, they are taken as the reference rock site conditions, consistent with regional empirical site response studies (Borcherdt and Glassmoyer, 1992; Harmsen, 1997; Bonilla et al., 1997).

It is important to point out that this rock category (Franciscan and Granite) is likely significantly stiffer than “rock” site conditions which characterize most empirical attenuation relation for tectonically active regions (Abrahamson and Shellok, 1997). As a result, the “soil” amplification factors may not be strictly appropriate for application to rock motions estimated using generic rock attenuation relations.

To illustrate the differences in shallow shear-wave velocities between the Franciscan and Granite baserock geologies and those implied in WNA rock empirical attenuation relations, the median profile for Geomatrix site category A and B was added to Figure 6. The Geomatrix A and B profile reflects rock and very shallow soil (< 10m) which are traditionally interpreted as “rock” site conditions in the development of empirical attenuation relations. In general, both the Franciscan and Granite baserock profiles are stiffer than the Geomatrix A and B category suggesting a possible difference in site response. As a result, amplification factors are developed for a Geomatrix A and B site category (Section 3.5) to provide an assessment of potential differences in response. The amplification factors may be used to “adjust” the soil factors as well.

Figure 7 shows corresponding median Tertiary profiles for the two regions. Apart from the Saugus profile, the  $T_s$  profile for the Los Angeles Area is intermediate between the San Francisco  $TM_{zs}$ , and  $QT_s$  profiles. Although the three profiles are similar for depths less than about 100 ft, the differences shown by the velocity trends at greater depths result in significant differences in mean response (amplification).

Figure 8 shows median alluvial profiles for both regions. The  $Q_y$ ,  $Q_{al}$ , and  $Q_{oa}$  (below about 100 ft) are very similar with  $Q_o$  (Older Alluvium for Los Angeles) showing significantly higher velocities. Conversely, the Bay Muds ( $Q_m$ ) show very low velocities throughout the entire depth range. While profiles of similar very soft soils for the Los Angeles Area (e.g. Los Angeles Harbor area) were not available, amplification factors computed for Bay Mud would be more appropriate than those computed for either  $Q_y$  or  $Q_o$  for these very soft soils in the Los Angeles Area.

## 2.4 Development of Smooth Profiles For Site Response Analyses

Smooth profiles were drawn through the median values and, where necessary, extrapolated to deeper depths to develop profiles for computing strong ground motions (PGA, PGV, PGD, and 5% damped response spectra). Both median and  $\pm 1 \sigma$  surface geology based profiles as well as smooth and extrapolated versions for site response calculations are shown in Figures 9 to 14 for the San Francisco Bay region and Figures 15 to 19 for the Los Angeles area. For source-to-site modeling in the San Francisco area, the shallow profiles are merged with the Wald et al. (1991) Loma Prieta crustal model (Table 3). For the Franciscan unit, the profile is merged with the second layer of the Wald et al. (1991) crust (Figure 9). The remaining geologic unit profiles are simply placed on top of the Wald crust which has a shear-wave velocity of 3,281 ft/sec in the top layer (Table 3).

For the Los Angeles area, the Granitic unit profile is considered the same as the Franciscan (Figure 6), replacing the properties of the top layer of the Wald et al. (1996) crust (Table 3, Figure 15). As with the San Francisco area profile, the remaining geologic unit profiles are simply placed on top of the Wald et al. (1996) crust that again has a shear-wave velocity of 3,281 ft/sec (1.0 km/sec) in the top layer (Table 3).

## 3.0 GEOLOGY BASED AMPLIFICATION FACTORS

Certainly the most satisfying approach to account for the effects of surficial materials on strong ground motion is empirical. Ideally, amplification factors could be developed based entirely upon observation of strong ground motion. Studies using data recorded on rock and on different classes of soil profiles, such as stiff soils and deep cohesionless soils, have demonstrated large differences in spectral amplification ( $S_a/a_{max}$ ) and in spectral velocity due to the presence of the soils (Seed et al., 1976; Mohraz, 1976; Joyner and Fumal, 1984; Abrahamson and Silva, 1997). Empirical studies of geologically based amplification factors for the San Francisco Bay area have shown large and stable differences in weak motion Fourier amplitude spectra (Borcherdt, 1970; Borcherdt and Glassmoyer, 1992). While these studies are

extremely useful in a general sense, the limited number and size of earthquakes and different types of profiles as well as poorly known recording site conditions preclude relying directly upon empirical results. In particular, few data are available for very high levels of shaking and for a variety of site conditions. Also, few ground motion recording sites have detailed soil/rock profiles for which reliable soil/rock properties are available. Because of these limitations, some form of computational analysis is desirable and direct observations of soil response can then be used as calibrations and to provide a basis for assessing the reasonableness of the results of analytical computations.

### 3.1 Methodology

The conventional computational approach in developing spectral amplification factors appropriate for specific profiles would involve selection of suitable time histories to serve as control or rock outcrop motions and a suitable nonlinear computational formulation to transmit the motion through the profile.

#### 3.1.1 *Equivalent-Linear Computational Scheme*

The computational scheme which has been most widely employed to evaluate one-dimensional site response assumes vertically-propagating plane shear waves. Departures of soil response from a linear constitutive relation are treated in an approximate manner through the use of the equivalent-linear approach.

The equivalent-linear approach, in its present form, was introduced by Seed and Idriss (1970). This scheme is a particular application of the general equivalent linear theory introduced by Iwan (1967). Basically, the approach is to approximate a second order nonlinear equation, over a limited range of its variables, by a linear equation. Formally this is done in such a way that an average of the difference between the two systems is minimized. This was done in an ad-hoc manner for ground response modeling by defining an effective strain which is assumed to exist for the duration of the excitation. This value is usually taken as 65% of the peak time-domain strain calculated at the midpoint of each layer, using a linear analysis. Modulus and damping curves are then used to define new parameters for each layer based on the effective strain computations. The linear response calculation is repeated, new effective strains evaluated, and iterations performed until the changes in parameters are below some tolerance level. Generally a few iterations are sufficient to achieve a strain-compatible linear solution.

This stepwise analysis procedure was formalized into a one-dimensional, vertically propagating shear-wave code called SHAKE (Schnabel et al., 1972). Subsequently, this code has easily become the most widely used analysis package for one-dimensional site response calculations.

The advantages of the equivalent-linear approach are that parameterization of complex nonlinear soil models is avoided and the mathematical simplicity of linear analysis is preserved. A truly nonlinear approach requires the specification of the shapes of hysteresis curves and their

cyclic dependencies. In the equivalent-linear methodology the soil data are utilized directly and, because at each iteration the problem is linear and the material properties are frequency independent, the damping is rate independent and hysteresis loops close.

While the assumptions of vertically propagating shear waves and equivalent-linear soil response certainly represent approximations to actual conditions, their combination has achieved demonstrated success in modeling observations of site effects (Schnabel et al., 1972; Silva et al., 1988; Schneider et al., 1993; EPRI, 1993).

### ***3.1.2 RVT Based Computational Scheme***

The computational scheme employed to compute the site response uses the stochastic model to generate the power spectral density and spectral acceleration of the rock or control motion. This motion or power spectrum is then propagated through the one-dimensional soil profile using the plane-wave propagators of Silva (1976). In this formulation only SH waves are considered. Arbitrary angles of incidence may be specified but normal incidence is used throughout the present analyses.

In order to treat possible material nonlinearities, an RVT (Random Vibration Theory) based equivalent-linear formulation is employed. Random process theory is used to predict peak time domain values of shear strain based upon the shear strain power spectrum. In this sense the procedure is analogous to the program SHAKE except that peak shear strains in SHAKE are measured in the time domain. The purely frequency domain approach obviates a time domain control motion and, perhaps just as significant, eliminates the need for a suite of analyses based on different input motions. This arises because each time domain analysis may be viewed as one realization of a random process. In this case, several realizations of the random process must be sampled to have a statistically stable estimate of site response. The realizations are usually performed by employing different control motions with approximately the same level of peak acceleration and response spectrum.

In the case of the frequency domain approach the estimates of peak shear strain as well as oscillator response are, as a result of the random process theory, fundamentally probabilistic in nature. Stable estimates of site response can then be computed by forming the ratio of spectral acceleration predicted at the surface of a soil profile to the spectral acceleration predicted for the control motion.

The procedure of generating the point-source stochastic power spectrum computing the equivalent-linear layered-soil response, and estimating peak time domain values has been incorporated into a single code termed RASCALS (Schneider et al., 1993).

## **3.2 G/Gmax and Hysteretic Damping Curves**

Four sets of G/Gmax and hysteretic damping curves are used: generic rock ( $K_{jf}$ ,  $TM_{zs}$ ,  $M_{xb}$  and  $T_s$ ), cohesionless soils ( $QT_s$ ,  $Q_u$ ,  $Q_o$ ,  $Q_y$ ,  $QT_s$ ,  $T_s$  (Saugus)), and cohesive soils ( $Q_m$ )



(Table 1). The rock curves (Figure 20) are based on point-source modeling of the rock site empirical attenuation relation of Abrahamson and Silva (1997) for a range in magnitudes and distances using a generic rock profile (Geomatrix A and B, Figure 6) (Silva et al., 1997).

For the geologic units which are considered cohesionless soils in the San Francisco Bay area (gravels, sands, and low PI clays) in terms of high-strain dynamic material properties (QTs, Qal), the recent EPRI (1993) G/Gmax and hysteretic damping curves are used (Figure 21). These curves were developed for generic applications to cohesionless soils in the general range of gravelly sands to low plasticity silts or sandy clays. For application to Quaternary/Tertiary rocks (QT<sub>s</sub>), the implied assumption is that these sites behave more like a stiff soil (gravelly sand) than rock. A not unreasonable assumption considering a surface velocity of about 800 ft/sec (Figure 4) and a NEHRP site class C (Table 1). The EPRI (1993) curves have recently been validated at 48 San Francisco Bay area cohesionless soil sites (Geomatrix site class C or D, Table 2) through modeling strong ground motions from the Coyote Lake, Morgan Hill, and Loma Prieta earthquakes (Silva et al., 1997).

For the Bay Mud (Q<sub>m</sub>) categories, generic sections of Fill (15 ft), young Bay Mud (50 ft) and old Bay Clay (30 ft) over Quaternary Alluvium (Q<sub>a</sub>) are assumed. These generic zones are based on an examination of several CALTRANS boreholes located near highway bridges (Cliff Roblee, personal communication) and are used only to assign G/Gmax and hysteretic damping curves. For the Fill material and the Alluvium, EPRI (1993) curves are used. For the young Bay Muds and Old Bay Clay, the Vucetic and Dobry (1991) cohesive soil curves for a PI of 40%, an average value for these cohesive soils, are used (Figure 22).

For the geologic units which are considered cohesionless soils in the Los Angeles area (QT<sub>s</sub>, Q<sub>a</sub>, Q<sub>y</sub>, Saugus), recent strong ground motion analyses for about 80 sites which recorded the 1994 Northridge earthquake found the EPRI G/Gmax and hysteretic damping curves showed too much nonlinearity (Silva et al., 1997). As a result, a revised set of G/Gmax and hysteretic damping curves were developed for Peninsular Range cohesionless soils and are shown in Figure 23.

### 3.3 Specification of Control Motions

The Franciscan K<sub>r</sub> and Granite (M<sub>xb</sub>) profiles (Figures 9 and 15) represent the stiffest of the suite of geologically based profiles, and are taken as the reference site geology (Table 1). The Franciscan unit was also used as a reference site condition by Borchardt and Glassmoyer (1992) and the Granite unit by Harmsen (1997) and Bonilla et al. (1997). The common reference permits a comparison of analytical to empirical amplification factors developed from either recordings of the M 6.9 1989 Loma Prieta or several Los Angeles area earthquakes using generally low levels of reference rock motions.

Since time histories are not required for the RVT based equivalent-linear site response analyses, the stochastic point-source model is used to compute the motions at the surface of the baserock or reference rock as well as the other profiles. Both qualitative assessments and quantitative validations of the stochastic point-source model (Hanks and McGuire, 1981; Boore,

1983, 1986; McGuire et al., 1984; Boore and Atkinson, 1987; Silva and Lee, 1987; Toro and McGuire, 1987; Silva et al., 1990; EPRI, 1993; Schneider et al., 1993; Silva and Darragh, 1995; Silva et al., 1997) have demonstrated that it provides accurate ground motion estimates, making it an appropriate choice to produce ground motions representative of the geologic based profiles.

To generate the motions, a M 6.5 earthquake is used with the distance (epicentral) varied to produce a suite of distinct peak acceleration values at the surface of the reference rock unit (Table 4). The same source and path parameters are then used for the other unit profiles resulting in a suite of amplification factors as a function of reference rock outcrop peak acceleration values (EPRI, 1993; Toro et al., 1992). For the point-source, a stress drop of 60 bars (Silva and Darragh, 1995) and a small strain total kappa value of 0.04 sec are used for all the profiles. The total kappa value includes the small strain damping in the nonlinear zone. These values were determined in an inversion of the Abrahamson and Silva (1997) empirical attenuation relation (Silva et al., 1997). The rock profiles (Franciscan, Tertiary, and Granite) are permitted to exhibit material nonlinearity to depths where the velocities exceed about 3,400 ft/sec (Figures 9, 10, 15, and 16). This occurs at about 70 ft for the Franciscan and Granite profiles and at about 250 ft for the Tertiary profiles. The soil sites are treated as potentially nonlinear to the top of the Wald et al. (1991, 1996) crusts (Table 3) provided this depth is  $\leq$  500 ft. The depth to this assumed basement material varies from 30 to 1,500 ft, depending upon category depth (Table 5). All soils are constrained to be linear in response below 500 ft.

The  $Q(f)$  model is  $176 f^{0.6}$  for the San Francisco Bay area and  $275 f^{0.6}$  for the Los Angeles area. These values were determined from inversions of northern California earthquakes Loma Prieta, Coyote Lake, and Morgan Hill recorded at about 90 sites over the fault distance range of about 12 to 90 km and Peninsular Range earthquakes Northridge, San Fernando, and Whittier Narrows at 180 sites over the fault distance range of about 10 to 200 km (Silva et al., 1997).

To generate motions which cover the range from linear response to the potentially largest horizontal motions to be expected, six distances are run with reference rock outcrop peak accelerations ranging from 0.05g to 1.25g (Table 4). The magnitude and stress drop is fixed at M 6.5 and 60 bars respectively with the assumption that the amplification factors (ratios) are not highly sensitive to either magnitude or stress drop (EPRI, 1993). Since the profiles are randomized in velocity and layer thickness, the median peak acceleration does not exactly correspond to the target peak acceleration (Table 4). In general, the median values are very close, within about 10% of the target which is considered acceptable since the amplifications vary little for a 10% change in input motions.

The profile randomization scheme, which varies both layer velocity and thickness, is based on a correlation model developed from an analysis of variance on about 500 measured shear-wave velocity profiles (EPRI, 1993; Silva et al., 1997). Figure 24 shows the Franciscan outcrop 5% damped pseudo acceleration spectra (median and  $\pm 1 \sigma$  for the lowest level of motion, 0.05g). The profile is varied to the top layer of the Wald et al., (1991) Loma Prieta crust, a depth of about 250 ft. The parametric variation, reflected in the sigma ( $\sigma_h = 0.15$  for PGA), includes profile velocity and layer thickness variation in addition to variability in the

## G/Gmax and hysteretic damping curves.

To accommodate variability in the modulus reduction and damping curves on a generic basis, the curves were independently randomized about the base case values. A log normal distribution was assumed with a  $\sigma_{\ln}$  of 0.35 at a cyclic shear strain of  $3 \times 10^{-2}\%$  with upper and lower bounds of  $2\sigma$ . The truncation was necessary to prevent modulus reduction or damping models that are not physically possible. The random curves are generated by sampling the transformed normal distribution with a  $\sigma_{\ln}$  of 0.35, computing the change in normalized modulus reduction or percent damping at  $3 \times 10^{-2}\%$  shear strain, and applying this factor at all strains. The random perturbation factor is reduced or tapered near the ends of the strain range to preserve the general shape of the median curves (Silva, 1992). The parametric variability shown in Figure 24 then represents the contribution to the uncertainty in strong ground motions due to the top 200 to 300 ft at hard California rock (Franciscan) sites in the San Francisco Bay (and Los Angeles) area.

The remaining reference rock outcrop median spectra are shown in Figure 25. These median spectra then represent the denominator or reference geologic unit in the amplification factors. Since the shallow profile is taken as the same for both Franciscan and Granite reference rock conditions, the differences in median motions are due only to differences in the deep crust (Table 3).

### 3.4 Development of Site Amplification Factors

Site amplification factors are computed as the ratio of 5% damping response spectral acceleration ( $S_a$ ) computed at the surface of each site for each randomized profile to the median 5% damping response spectral acceleration ( $S_a$ ) computed for the reference rock outcrop motion (Figure 25). In addition, peak acceleration, peak particle velocity, and peak particle displacement were computed for the site and reference outcrop as well. Levels of reference rock outcrop peak acceleration values of 0.05, 0.1, 0.2, 0.4, 0.75, 1.0, and 1.25g were used to accommodate the effects of material nonlinearity upon site response. Table 4 shows the magnitude ( $M$ ), distance ( $R$ ), peak acceleration, peak particle velocity, and peak particle displacement computed for the outcrop motions.

To accommodate likely profile depth ranges appropriate for the two areas, categories based upon depth to basement (taken here as top of Wald et al., 1991, 1996 crusts; Table 3) were developed. The categories reflect a mean depth and a range over which the amplification factors are considered applicable. Table 5 lists the categories, depth ranges, and the corresponding geologic units which are considered to have underlying basement material. The range in depth to basement material over which the amplification factors for each depth category are considered applicable are based on the randomization (uniform distribution) depth range. While the depth randomization is intended to capture the profile depth range over which the amplification factors may be applied, the factors are strictly only applicable for a reduced range about the mean depth. That is, averaging amplifications computed for deep profiles with those computed for shallow profiles broadens the amplification but tends to lower the values at frequencies above and below the fundamental frequency of the mean profile depth. This effect

becomes more pronounced as the depth range is increased. An enveloping scheme needs to be developed over amplification factors developed using overlapping depth ranges to produce factors strictly appropriate for applications to wide depth ranges. As a result, care must be exercised in implementing the factors for depths exceeding about  $\pm 50\%$  of the mean category depths (Table 5). This averaging artifact partially motivated the approximately  $\pm 50\%$  ranges in depth categories 1 to 3 (and 5 for Los Angeles, Table 5) and is not considered a significant issue for these cases. For the wide depth bins however, one should use conservative factors based on estimated profile depth and an examination of the suite of factors plotted in Appendices A and B.

For the soils, the existence of basement material is clear. However for the QT<sub>s</sub> (Quaternary/Tertiary) rock unit in the San Francisco Bay area, which consists of conglomerates, lesser sandstones, siltstones, and claystones of the Santa Clara, Ukiah, and Paso Robles formations and for the T<sub>s</sub> and combined Q<sub>o</sub> and T<sub>s</sub> in the Los Angeles area, the existence of a basement complex is doubtful. It should be pointed out however, that we are defining basement in terms of a steep shear-wave velocity gradient (approximated as a step) which, for shallow depths (category 1) may represent weathering. For the deeper categories, the rapid increase in shear-wave velocity may be interpreted as a transition to much more competent QT<sub>s</sub> over a fairly narrow depth zone. Sufficient deep borehole data are simply not currently available to resolve this issue.

#### *3.4.1 Amplification Factors For The San Francisco Bay Area*

The amplification factors, 5% damped Sa/Sa (reference rock), were computed at approximately 90 frequencies from approximately 0.10 Hz to 100 Hz.

As an example of the general shape of the amplification factors, Figure 26 shows the median factors and  $\pm 1 \sigma$  sigma values computed for Quaternary Alluvium Category 4 (30 to 1,000 ft, Table 5) for Franciscan outcrop peak acceleration values of 0.05 and 0.40g (solid and dashed lines respectively). Due to the randomizing over depth, only a minor contribution of the fundamental resonance is present. The variability reflects parametric uncertainty in the profile, and includes profile layer thickness, shear-wave velocity, profile depth (30 to 1,000 ft), and G/Gmax and hysteretic damping curves. The first layer of the Wald et al. (1991) crust (base of the profiles) is also randomly varied assuming a lognormal distribution with a  $\sigma_w$  of 0.3 (EPRI, 1993). The depth variation assumes a uniform distribution resulting in a mean profile depth (depth to first layer of the Wald crust) of 515 ft (Table 5).

The effects of nonlinearity are seen in the reduction of amplification at high frequency and the shifting of amplification to lower frequency for the 40%g Franciscan outcrop motions. The increase in variability apparent in the higher motions is likely due to the effects of variability in the G/Gmax and hysteretic damping curves.

To assess the actual number of potentially distinct geologic units in terms of site response for the San Francisco Bay area, Figures 27 and 28 show median amplification factors computed for Bay Mud, Quaternary Alluvium, Older Alluvium, and Quaternary/Tertiary units for

outcropping Franciscan of 0.05g and 0.40g respectively. Also shown in the Figures are the empirical amplification factors computed for Fourier amplitude spectra by Borchardt and Glassmoyer (1992). These factors were estimated from low level recordings of the M 6.9 1989 Loma Prieta earthquake at sites located in the same geologic units. For both the low- and high-strain analytical factors (Figures 27 and 28), little difference is seen between the Older Alluvium ( $Q_{ol}$ ) and Quaternary Alluvium ( $Q_u$ ). As a result, the factors are combined into one  $Q_a$  unit (Table 1). For the low-strain factors shown in Figure 27, the comparison between the analytical and empirical results is surprisingly good. Since the analytical factors are computed for 5% damped response spectra, to allow direct use in hazard assessment, and the empirical factors were computed for Fourier amplitude spectra which results in an amplitude dependence upon degree of smoothing, the close agreement is particularly encouraging.

The effects of nonlinear response are evident in the higher-motion analytical factors computed for Franciscan outcrop motions of 40%g. Figure 28 shows a significant reduction in motions, mostly at high frequency ( $\geq 3$  Hz), for the Bay Mud and Alluvial soils and for the Quaternary/Tertiary rock units. The Tertiary unit, being quite stiff, remain largely linear in response (relative to Franciscan). The accompanying shift in dominate frequency is also apparent, moving from about 1 to 2 Hz to below 1 Hz as the Franciscan outcrop peak acceleration increases from 0.05g to 0.40g. These trends are not apparent in the empirical factors, being based on generally low levels of input (Franciscan) motions.

To illustrate the important effects of depth to bedrock or basement material, Figure 29 shows  $Q_{ts}$ ,  $Q_a$ , and  $Q_m$  median amplification factors computed for Franciscan outcrop peak acceleration of 0.20g and 0.40g for depth Categories 1, 2, and 3 (Table 5). The mean category depths are 90, 250, and 500 feet, respectively. Figure 29 shows the broadening and shifting of peak amplification to lower frequencies as depth to basement increases. There is also an accompanying decrease in high frequency amplification due to material damping. These results show that depth to basement material is a first order effect in amplification factors and should be accommodated in their development as well as implementation.

To illustrate the differences between the current NEHRP amplification factors and those based on surface geology, Figure 30 shows median factors computed for the broadest depth categories along with corresponding NEHRP recommendations. Except for the  $Q_m$  category, which classifies as NEHRP category D based on velocity (but should be NEHRP category E based on surface geology and response), favorable agreement is seen for reference Franciscan (NEHRP category B, Table 1) and for peak acceleration values up to about 0.20g. At higher loading levels, however, Figure 30\* shows departures which are both conservative and unconservative. The high frequency NEHRP factors (2.0 Hz to 10.0 Hz) are conservative for NEHRP profile D but appear to be low for profile NEHRP profile C. For the low frequency NEHRP factors (0.5 Hz to 2.5 Hz), profile D appears low compared to  $Q_a$  (combined  $Q_o$  and  $Q_u$ , Table 5).

---

\*For reference rock peak accelerations exceeding 0.4g, NEHRP recommends site specific evaluations for category E.

The final set of median amplification factors covering the complete range in Franciscan outcrop peak accelerations (0.05 to 1.25g) are shown in Figures 31 to 35 for the categories reflecting the widest depth ranges (Table 5). Each Figure shows median and  $\pm 1 \sigma$  amplification factors (5% damped response spectra) computed for the Bay Mud, Older Alluvium, Quaternary Alluvium, Quaternary/Tertiary, and Tertiary surface geologic units. Interestingly, for the widest depth ranges, there is a distinction between Older Alluvium and Quaternary Alluvium (Figures 33 and 34 respectively). As a result, the categories are retained. The units may be combined by averaging the separate amplification factors for applications where the distinction is small (e.g. 350 to 650 ft depth range, Figures 27 and 28).

The amplification of peak acceleration (100 Hz on the plots) is large, about a factor of 2 for the soil profiles at low levels of motions (Figures 33 to 35). At around 0.20 to 0.40g, the effects of nonlinearity become significant, reducing high frequency motions ( $f \geq 10$  Hz) and increasing low frequency ( $f \leq 1$  Hz) motions. These trends are, as expected, more pronounced as profile stiffness decreases and are reflected in a change in shape of soil spectra with increasing loading levels. For the highest levels of motions (0.075g and 1.25g for outcropping Franciscan) the Quaternary Alluvium and Bay Mud profiles show extreme nonlinearity. These results must be viewed in the context of the equivalent-linear approximation and may be overdamped compared to appropriate equivalent fully nonlinear analyses. These levels of motions are beyond the current sampling in the empirical strong motion database and a reasonable lower limit of amplification for these generic results is about 0.5 to 0.6, a value supported empirically for generic deep soil (Abrahamson and Silva, 1997).

The complete suite of amplification factors is included in Appendix A. These amplification factors are designed to serve as a means of approximately accounting for the effects of surficial geology and depth to basement for seismic hazard estimation. Although detailed site specific results could produce results different from those predicted for these generalized categories, we believe that the results presented are appropriate and represent a useful tool for use in seismic hazard estimation for applications to the San Francisco Bay area. Linear interpolation may be used to provide amplifications between frequency and reference rock peak acceleration values.

### ***3.4.2 Amplification Factors For The Los Angeles Area***

Although median shear-wave velocity profiles for baserock conditions are quite similar for the San Francisco Bay ( $K_r$ ) and Los Angeles ( $M_{sb}$ ) areas (Figure 6) resulting in similar rock motions (Figure 25), differences in both the soil profiles and nonlinear properties between the regions suggest that important differences in response will occur. As a result, separate amplification factors are developed for Los Angeles area soils and soft rock. Since profiles were not available for very soft Los Angeles area materials (e.g., Los Angeles Harbor area), the use of San Francisco Bay area amplification factors computed for Bay Mud ( $Q_m$ ) site conditions are recommended.

To assess the actual number of distinct geologic units in terms of site response, Figure 36 shows median amplification factors computed for Quaternary Alluvium, Older Alluvium,

Quaternary + Tertiary, Saugus, and Tertiary units for outcropping Granite in the range of 0.05g to 1.25g.

The depth range is 30 to 1,000 ft (average depth 515 ft), except for Tertiary as it reaches about 3,000 ft/sec at a depth of 200 ft (Figure 16). The Saugus (Tertiary rock) category is retained as a distinct category for comparison but is also included in the combined  $QT_s$  category. From a visual qualitative analysis, it appears that  $Q_y$  (solid lines) and  $T_s$  (solid dotted) are distinct categories along with the Saugus (crosses). There is also an indication of differentiation of these categories and the combined  $QT_s$  category (dots). Larger depth ranges generally result in fewer distinct (resolvable) categories due to the inherent smoothing or averaging, so care is warranted in such qualitative assessments. Over most of the frequency range and loading levels up to about 0.40g, Quaternary Alluvium ( $Q_y$ ) provides a reasonable suite of factors for general applicability for sites with depths not exceeding around 700 ft (depths not exceeding about 50% of the mean depth). For applications to profiles of greater depths, a deeper depth category should be used. At higher loading levels, due to nonlinearity the stiffer Tertiary ( $T_s$ ) profile is significantly above the  $Q_y$  amplification for frequencies above about 1 Hz.

While a statistically quantitative measure of distinct categories is desirable, with analytical factors such an assessment remains an elusive objective. Statistically significant differences in mean amplification must ultimately be assessed with ground motion (recordings) of sufficient quantity and quality (range in loading levels, and accurate site categorizations). Probably the most complete set of data in this respect is in southern California and several empirical site response analyses have been performed using similar surficial geologic units (Bonilla et al., 1997; Borchardt, 1996; and Harmsen, 1997). Figure 37 compares empirical amplification factors (Bonilla et al., 1997) computed for Fourier amplitude spectra to the analytical factors for surficial geologic units  $Q_y$  (Quaternary Alluvium) and the combined  $Q_o + T_s$  (Older Alluvium plus Tertiary "rock"). The empirical factors are relative to Granite ( $M_{xb}$ ) and are based upon aftershocks of the 1994 M 6.7 Northridge earthquake, generally reflecting low levels of motion. The two geologic units ( $Q_y$  and  $Q_o + T_s$ ) were found by Bonilla et al. (1997) to have significantly different response, based up analyses of multiple earthquakes and multiple sites. The analytical factors are for deep soil conditions (average depth of 500 ft) as most of the stations are assumed to reflect deep basement conditions. Both the trends and relative levels between the  $Q_y$  and  $Q_o + T_s$  amplifications are reflected in the analytical factors. Both empirical factors exceed the analytical, possibly due to the mixture of Fourier and response spectra. Additionally, few rock sites ( $M_{xb}$ ) were available for the empirical analyses which may result in a bias in the baserock motions. Stable levels of amplification of 5% damped response spectra of strong ground motion at firm to stiff soil sites relative to soft rock sites generally do not exceed factors of about 2 to  $2\frac{1}{2}$  (at low frequency). This is supported by Figure 38 which shows soil site amplification (Geomatrix C + D, Table 2) relative to soft rock (Geomatrix A + B) from the empirical attenuation relation of Abrahamson and Silva (1997). The maximum amplification occurs at low frequency and is near 2. For low levels of expected rock peak acceleration, the shape of the empirical amplification factors for generic firm soil, based solely on strong ground motions (Figure 38), is similar to the analytical factors (Figure 37) and of comparable levels.

For the same surficial geologic units, Borchardt (1996) developed amplification factors (for 5% damped response spectra) from strong ground motion recording of the 1994 M 6.7 Northridge earthquake. The comparison of the analytical factors to the empirical factors of Borchardt (1996) are shown in Figure 39. For this comparison a reference rock peak acceleration of 0.10g is used to reflect average levels for the recordings. As with the previous comparison, analytical factors were computed for a depth range of 30 to 1,000 ft (average depth of 515 ft) and are most appropriate for profiles with depth less than about 700 ft. In this comparison, the agreement is more favorable. The underprediction at low frequency (0.20 to 0.67 Hz) would largely be eliminated using the 500 to 1,500 ft suite of factors (Appendix B). Interestingly, the high frequency crossover seen in the empirical factors is reflected in the analytical factors as well.

A final comparison with empirical factors is shown in Figure 40. These empirical amplification factors were estimated by Harmsen (1997) from accelerograph recordings of the 1971 San Fernando, 1987 Whittier Narrows, 1991 Sierra Madre, and 1994 Northridge earthquakes. The factors are relative to granite outcropping ( $M_{xb}$ ) and were computed for Fourier amplitude spectra. In this case Older Alluvium was considered distinct from Tertiary ( $T_s$ ) in mean amplification. This distinction in amplification based on surface geology is not resolved by categories based on average shear-wave velocity over the top 100 ft as  $Q_o$  and  $T_s$  (along with Saugus) are NEHRP category C (Table 1, Figure 40).

As with the other comparison with Fourier amplitude amplification (Figure 37), the general trends are captured (along with the high frequency crossover) but with a low frequency underprediction. A similar consistent difference is also seen between the empirical Fourier amplitude and empirical 5% damped response spectra amplification factors.

To examine the comparison of the NEHRP amplification factors, Figure 41 shows the  $Q_y$  (NEHRP D) and  $Q_o + T_s$  (NEHRP C) for the depth range of 30 to 1,000 ft (mean depth of 515 ft) along with the recommended provisions. Close agreement is seen at low loading levels (0.05 and 0.10g) but the low-frequency factors (0.50 to 2.5 Hz) appear to reflect too much nonlinearity at the higher levels.

This trend was also found by both Silva and Toro (1998) and Crouse and McGuire (1996) who also concluded that the NEHRP factors probably reflected too much nonlinear response. Interestingly, the high-frequency NEHRP provisions for loading levels of 0.75g and above appear conservative, showing less nonlinear response than the factors computed here, particularly for frequencies exceeding about 5 Hz.

The complete suite of amplification factors is included in Appendix A. These amplification factors are designed to serve as a means of approximately accounting for the effects of surficial geology and depth to basement for seismic hazard estimation. Although detailed site specific results could produce results different from those predicted for these generalized categories, we believe that the results presented are appropriate and represent a useful tool for use in seismic hazard estimation for applications to the Los Angeles area. Linear interpolation may be used to provide amplifications between frequency and reference rock peak acceleration values.



### 3.5 Adjustment Factors For Soft Rock Conditions

As previously mentioned, reference rock site conditions for both the San Francisco ( $K_{jr}$ ) and Los Angeles ( $M_{xb}$ ) areas reflect somewhat stiffer shallow site conditions than typical rock site conditions implicit in WNA empirical attenuation relations (assumed Geomatrix Category A + B, Figure 6). Since the amplification factors (Appendices A and B) are computed relative to the baserock surface geology (to compare with site response studies), another suite of factors has been computed as Geomatrix site Category A + B relative to  $K_{jr}$  (San Francisco area) and  $M_{xb}$  (Los Angeles area). Figures 42 and 43 show the soft rock to reference rock amplification factors for the San Francisco and Los Angeles areas respectively. The factors are nearly identical for the two regions since the same shallow reference rock profiles are used to generate the outcrop motions. These factors show a slight amplification near 3 Hz at all loading levels and deamplification near 10 Hz at high levels of loading. These effects are attributed to the softer Geomatrix A + B profiles compared to  $K_{jr}$  and  $M_{xb}$  profile. Since peak acceleration is affected very little, hazard results from empirical rock site attenuation relations may be used to select appropriate amplification factors. These adjustment factors may then be used to condition the amplification factors to soft rock conditions by division prior to applying the empirical rock spectrum.

## 4.0 SUMMARY

For both the San Francisco Bay and Los Angeles areas, surface geology based amplification factors have been developed for 5% damped response spectra. The factors are computed relative to reference rock site geology,  $K_{jr}$  (Franciscan) for the San Francisco Bay area and  $M_{xb}$  (Granite) for the Los Angeles area. The factors are functions of profile depth (or depth range) as well as expected reference rock peak acceleration values ranging from 0.05g to 1.25g.

The amplification factors are computed using average measured shear-wave velocity profiles at sites located within the surficial geologic units with an RVT (Random Vibration Theory) based equivalent-linear site response approach. Separate  $G/G_{max}$  and hysteretic damping curves are used for San Francisco (North Coast) and Los Angeles (Peninsular Range) cohesionless soils reflecting different degrees of nonlinear response in both regions. These curves, along with  $G/G_{max}$  and hysteretic damping for rock site conditions which are the same for both regions, were validated by modeling recorded motions in both regions.

The analytical amplifications factors are compared to published empirical as well as current NEHRP factors for both regions. Comparisons with the empirical factors show good agreement for empirical factors computed for 5% damped response spectra and reasonable agreement for empirical factors for Fourier amplitude spectra. The analytical factors were generally below the empirical for Fourier amplitude spectra but agreed in shape and general trends: soft alluvium higher than stiff alluvium at low frequency but crossing over at high frequency. Comparisons with the NEHRP provisions showed reasonable agreement for the San Francisco Bay area, except for the Bay Muds ( $Q_m$ ) being classified as NEHRP D (based on actual average shear-wave velocity over the top 100 ft). For the Los Angeles area, good agreement was seen with the NEHRP amplification factors at low levels of loading (up to about

0.10g). At higher loading levels the low frequency NEHRP factors were significantly exceeded while the high frequency NEHRP factors appear to reflect considerable conservatism at very high loading levels.

The amplification factors developed in this project extend to 1,000 ft for the San Francisco Bay area and 1,500 ft for the Los Angeles area. They may be used to approximately accommodate the effects of near surface geology for seismic hazard evaluations.

## REFERENCES

- Abrahamson, N.A and K.M. Shedlock (1997). "Overview." *Seis. Research Lett.*, 68(1), 9-23.
- Abrahamson and Silva (1997). "Empirical response spectral attenuation relations." to appear in *Seismological Research Letters*.
- Boatwright, J., and Astrue, M. (1983). "Analysis of the aftershocks of the New Brunswick earthquake." *Workshop on Site-Specific Effects of Soil and Rock on Ground Motion and the Implications for Earthquake-Resistant Design*. USGS Open-File Rept. 83-245.
- Bonilla, L.F., J.H. Steidl, G.T., Lindley, A.G Tumarkin and R.J. Archuleta (1997). "Site amplification in the San Fernando Valley, California: Variability of Site-effect estimation using the S-wave, coda, and H/V methods. *Bull. Seism. Soc. Am.*, 87(3), 710-730.
- Boore, D.M., and Atkinson, G.M. (1987). "Stochastic prediction of ground motion and spectral response parameters at hard-rock sites in eastern North America." *Bull. Seism. Soc. Am.*, 77(2), 440-467.
- Boore, D.M. (1986). "Short-period P- and S-wave radiation from large earthquakes: implications for spectral scaling relations." *Bull. Seism. Soc. Am.*, 76(1) 43-64.
- Boore, D.M. (1983). "Stochastic simulation of high-frequency ground motions based on seismological models of the radiated spectra." *Bull. Seism. Soc. Am.*, 73, 1865-1894.
- Borcherdt, R. D. (1996). "Preliminary amplification estimates inferred from strong ground-motion recordings of the Northridge earthquake of January 17, 1994." *Proceedings of the International Workshop on Site Response Subjected to Strong Earthquake Motions*. Yokosuka Japan, 1-26.
- Borcherdt, R. D. and Glassmoyer, G. (1992). "On the Characteristics of Local Geology and Their Influence on Ground Motions Generated by the Loma Prieta Earthquake in the San Francisco Bay region, California." *Bull. Seism. Soc. Am.*, 82(2), 603-641.
- Borcherdt, R.D. (1970). "Effects of local geology on ground motion near San Francisco Bay." *Bull. Seism. Soc. Am.*, 60:29-61.
- Campbell, K.W. (1988). "Predicting strong ground motion in Utah." *Evaluation of Regional and Urban Earthquake Hazards and Risk in Utah*, edited by W.W. Hays and P.L. Gori, USGS Prof. Paper.
- Campbell, K.W. (1985). "Near-source estimation of strong ground motion for the Eastern United States: second quarter progress report - FY 1985." Submitted to *Nuclear Regulatory Commission*, 14 pages.
- Campbell, K.W. (1981). "Near-source attenuation of peak horizontal acceleration." *Bull. Seism. Soc. Am.*, 71(6), 2039-2070.

- Cranswick, E., Wetmiller, R., and Boatwright, J. (1985). "High-frequency observations and source parameters of microearthquakes recorded at hard-rock sites." *Bull. Seism. Soc. Am.*, 75(6), 1535-1567.
- Crouse, C. B. and McGuire, J.W. (1996). "Site response studies for purpose of revising NEHRP seismic provisions." *Earthquake Spectra*, 12(3), 407-439.
- Electric Power Research Institute (1993). "Guidelines for determining design basis ground motions." Palo Alto, Calif: Electric Power Research Institute, vol. 1-5, EPRI TR-102293.  
 vol. 1: Methodology and guidelines for estimating earthquake ground motion in eastern North America.  
 vol. 2: Appendices for ground motion estimation.  
 vol. 3: Appendices for field investigations.  
 vol. 4: Appendices for laboratory investigations.  
 vol. 5: Quantification of seismic source effects.
- Gutenberg, B. (1927). *Grundlagen der Erdlebenskunde*. Berlin.
- Gutenberg, B. (1957). "Effects of ground on earthquake motion." *Bull. Seism. Soc. Am.*, 47(1), 221-250.
- Hanks, T.C., and McGuire, R.K. (1981). "The character of high-frequency strong ground motion." *Bull. Seism. Soc. Am.*, 71, 2071-2095.
- Harmsen, S.C. (1997). "Determination of site amplification in the Los Angeles urban area from inversion of strong-motion records." *Bull. Seism. Soc. Am.*, 87(4), 866-887.
- Hayashi, S., H. Tsuchida, and E. Kurata (1971). "Average response spectra for various subsoil conditions." *Third Joint Meeting, US-Japan Panel on Wind and Seismic Effects*, UJNR, Tokyo.
- Idriss, I.M. (1985). "Evaluating seismic risk in engineering practice." *Proc. Eleventh Internat. Conf. on Soil Mech. and Foundation Eng.*, San Francisco, edited by A.A. Balkema, Rotterdam, 1, 255-320.
- Iwan, W.D. (1967). "On a class of models for the yielding behavior of continuous and composite systems." *J. Appl. Mech.*, 34, 612-617.
- Joyner, W.B., and Fumal, T.E. (1984). "Use of measured shear-wave velocity for predicting geologic site effects on strong ground motion." *Proc. Eighth World Conf. on Earthq. Engin.*, San Francisco, 2, 777-783.
- Joyner, H.B. and D.M. Boore (1982) "Prediction of earthquake response spectra." *USGS, Open-File Rept. 82-977*.
- Mallet, R. (1862). *Great Neopolitan earthquake of 1857, London.* " 2 vols.

- Milne, J. (1908). *"Seismology, London."* 2nd edition.
- McGuire, R.K., A.M. Becker, and N.C. Donovan (1984). "Spectral estimates of seismic shear waves." *Bull. Seism. Soc. Am.*, 74(4), 1427-1440.
- Mohraz, B. (1976). "A study of earthquake response spectra for different geological conditions." *Bull. Seism. Soc. Am.*, 66(3) 915-935.
- Reid, H.F. (1910). *"The California earthquake of April 18, 1907."* The Mechanics of the Earthquake, Carnegie Inst. of Washington, Publ. 87, 21.
- Schnabel, P.B., Lysmer, J., and Seed, H.B. (1972). *SHAKE: a Computer Program for Earthquake Response Analysis of Horizontally Layered Sites.* Earthq. Engin. Res. Center, Univ. of Calif. at Berkeley, EERC 72-12.
- Schneider, J.F., W.J. Silva, and C.L. Stark (1993). Ground motion model for the 1989 M 6.9 Loma Prieta earthquake including effects of source, path and site. *Earthquake Spectra*, 9(2), 251-287.
- Seed, H.B., C. Ugas and J. Lysmer. (1976). "Site-dependent spectra for earthquake resistant design." *Bull. Seism. Soc. Am.*, 66(1), 221-243.
- Seed, H.B. and I.M. Idriss (1970). *"Soil moduli and damping factors for dynamic response analyses."* Earthq. Eng. Res. Center, Univ. of Calif. at Berkeley, Report No. UCB/EERC-70/10.
- Silva, W.J. and G. Toro (1998) "Verification of response spectral shapes and anchor points for different site categories for building design codes." California Department of Conservation, Division of Mines and Geology, Report CSMIP/97-08.
- Silva, W.J., N. Abrahamson, G. Toro and C. Costantino. (1997). "Description and validation of the stochastic ground motion model." Report Submitted to Brookhaven National Laboratory, Associated Universities, Inc. Upton, New York 11973, Contract No. 770573
- Silva, W.J. and R. Darragh (1995). "Engineering characterization of earthquake strong ground motion recorded at rock sites." Palo Alto, Calif:Electric Power Research Institute, TR-102261.
- Silva, W.J. (1992). "Factors controlling strong ground motions and their associated uncertainties." *Dynamic Analysis and Design Considerations for High Level Nuclear Waste Repositories*, ASCE 132-161.
- Silva, W.J., Darragh, R.B., and Wong, I.G. (1990). "Engineering characterization of earthquake strong ground motions with applications to the Pacific Northwest." in Hays, W.W., ed., *Proceedings of the Third NEHRP Workshop on earthquake Hazards in the Puget sound/Portland region*, U.S. geological Survey Open-File report (in press).

- Silva, W.J., and Green, R.K. (1989). "Magnitude and distance scaling of response spectral shapes for rock sites with applications to North American tectonic environment." *Earthquake Spectra*, 5(3), 591-624.
- Silva, W. J.; Turcotte, T.; Moriwaki, Y. (1988). "Soil Response to Earthquake Ground Motion," Electric Power Research Institute, Walnut Creek, California, Report No. NP-5747.
- Silva, W.J., and Lee, K. (1987). "*WES RASCAL code for synthesizing earthquake ground motions.*" State-of-the-Art for Assessing Earthquake Hazards in the United States, Report 24, U.S. Army Engineers Waterways Experiment Station, Misc. Paper S-73-1.
- Silva, W.J. (1976). "Body Waves in a Layered Anelastic solid." *Bull. Seis. Soc. Am.*, vol. 66(5), 1539-1554.
- Toro, G.R., Silva, W.J., McGuire, R.K., and Herrmann, R.B. (1992). "Probabilistic seismic hazard mapping of the Mississippi embayment." *Seism. Res. Letters*, 63(3), 449-??.
- Toro, G.R., and McGuire, R.K. (1987). "An investigation into earthquake ground motion characteristics in eastern North America." *Bull. Seism. Soc. Am.*, 77, 468-489.
- Vucetic, M.; Dobry, R. (1991). "Effects of Soil Plasticity on Cyclic Response," *Journal of Geotechnical Engineering, ASCE*, 117(1), 89-107.
- Wald, D.J., T.H. Heaton and K.W. Hudnut (1996). "The slip history of the 1994 Northridge, California, earthquake determined from strong-motion, teleseismic, GPS, and leveling data." *Bull. Seism. Soc. Am.*, 86(1B), S49-S70.
- Wald, D.J., D.V. Helmberger, and T.R. Heaton (1991). "Rupture model of the 1989 Loma Prieta Earthquake from the inversion of strong motion and broadband teleseismic data." *Bull. Seism. Soc. Amer.*, 81(5), 1540-1572.
- Wood, H.O. (1908). "Distribution of apparent intensity in San Francisco, in the California earthquake of April 18, 1906." *Report of the State Earthquake Investigation Commission*, Wash., D.C.: Carnegie Institute, 1, 220-245.

September 27, 1999  
FINAL REPORT

**SURFACE GEOLOGY BASED STRONG MOTION  
AMPLIFICATION FACTORS FOR THE  
SAN FRANCISCO BAY AND LOS ANGELES AREAS**

Prepared for

PG&E PEER - TASK 5.B

by

Walter Silva  
Syliva Li  
Bob Darragh  
Nick Gregor

of

Pacific Engineering and Analysis  
311 Pomona Avenue  
El Cerrito, CA 94530

Table 1					
SURFACE GEOLOGY BASED PROFILES, SITE CLASSES, AND DYNAMIC MATERIAL PROPERTIES					
SAN FRANCISCO BAY AREA					
Geology	Average Velocity over 30m	Site Classes		Number of Profiles	G/Gmax and Hysteretic Damping
		USGS	NEHRP		
K <sub>fr</sub> (Franciscan)	771.44 m/s	A	B	30	Generic rock
TM <sub>u</sub> (Tertiary Bedrock)	506.13 m/s	B	C	18	Generic rock
QT <sub>u</sub> (Quaternary/Tertiary)	466.12 m/s	B	C	9	EPRI
Q <sub>oa</sub> (older alluvium)	353.44 m/s	C	D	16	EPRI
Q <sub>al</sub> (Quaternary alluvium)	296.49 m/s	C	D	37	EPRI
Q <sub>oa</sub> + Q <sub>al</sub>	312.15 m/s	C	D	53	EPRI
Q <sub>m</sub> (Bay mud)	187.87 m/s	C	D	60	Vucetic/Doby, EPRI
				170	
LOS ANGELES AREA					
Geology	Average Velocity over 30m	Site Classes		Number of Profiles	G/Gmax and Hysteretic Damping
		USGS	NEHRP		
M <sub>ab</sub> (Granite)	843.78 m/s	A	B	8	Generic rock
T <sub>s</sub> (Saugus)	576.81 m/s	B	C	4	Peninsular Range
T <sub>s</sub> (Tertiary)	436.39 m/s	B	C	43	Generic rock
Q <sub>o</sub> (Older alluvium)	391.24 m/s	B	C	124	Peninsular Range
QT <sub>s</sub> (Q <sub>o</sub> + T <sub>s</sub> )	508.61 m/s	B	C	171	Peninsular Range
Q <sub>y</sub> (Quaternary alluvium)	317.68 m/s	C	D	219	Peninsular Range
				398	



Table 2

# **SITE CLASSIFICATIONS**

Average shear-wave velocity to a depth of 30m is:

USGS Site Classification (Boore et al., 1994)	NEHRP 1994	UBC 1997
A = > 750 m/s	A = > 1,500 m/s	> 5,000 ft/sec
B = 360 - 750	B = 760 - 1,500	2,500 - 5,000
C = 180 - 360	C = 360 - 760	1,200 - 2,500
D = < 180 m/s	D = 180 - 360	600 - 1,200
	E = < 180	< 600 ft/sec

## **GEOMATRIX Site Classification**

Geotechnical subsurface characteristics (Robert Youngs, personal communications)

- A = Rock. Instrument on rock ( $V_s > 600$  mps or < 5m of soil over rock).
- B = Shallow (stiff) soil. Instrument on/in soil profile up to 20m thick overlying rock.
- C = Deep narrow soil. Instrument on/in soil profile at least 20m thick overlying rock, in a narrow canyon or valley no more than several km wide.
- D = Deep broad soil. Instrument on/in a soil profile at least 20m thick overlying rock, in a broad valley.
- E = Soft deep soil. Instrument on/in deep soil profile with average  $V_s < 150$  mps.

## **Relations To Building Code Classifications**

UBC	USGS	NEHRP	GEOMATRIX
S1	A + B	B + C	A + B
S2	B + C	C + D	C + D
S3	D	E	E
S4	E		

Table 3		
LOMA PRIETA CRUSTAL MODEL (from Wald et al., 1991)		
Thickness (km)	V <sub>s</sub> (km/sec)	Density (cgs)
0.1	1.00	2.00
0.4	1.95	2.30
0.5	2.48	2.35
2.0	2.77	2.35
2.0	3.10	2.35
2.0	3.31	2.45
2.0	3.55	2.58
4.0	3.61	2.62
5.0	3.62	2.63
7.0	3.85	2.77
	4.62	3.28
NORTHRIDGE CRUSTAL MODEL (from Wald et al., 1996)		
Thickness (km)	V <sub>s</sub> (km/sec)	Density (cgs)
0.5	1.00	2.10
1.5	2.00	2.30
2.5	3.20	2.50
23.0	3.60	2.60
5.0	3.90	2.90
	4.50	3.00

Table 4

**FRANCISCAN REFERENCE SITE GROUND MOTION PARAMETERS  
SAN FRANCISCO BAY AREA**

Target Outcrop* PGA(g)	Median Outcrop* PGA(g)	Median Outcrop* PGV(cm/sec)	Median Outcrop* PGD(cm)	Median Outcrop* V/A (cm/sec/g)	Median Outcrop* AD/V <sup>2</sup> (gcm/cm <sup>2</sup> /sec <sup>2</sup> )	Dist. (km)	Depth (km)	M	$\Delta\sigma$ (bars)
0.05	0.05	5.08	2.30	101.63	4.35	42.00	8.00	6.5	60
0.10	0.11	10.16	4.45	92.42	4.63	22.00	8.00	6.5	60
0.20	0.20	17.46	7.51	88.14	4.76	11.80	8.00	6.5	60
0.40	0.39	33.03	14.00	84.96	4.87	0.00	7.80	6.5	60
0.75	0.74	65.22	28.80	87.82	4.94	0.00	4.50	6.5	60
1.25	1.30	122.25	52.93	94.12	5.01	0.00	2.54	6.5	60

$Q(f) = 176 f^{0.6}$  (San Francisco; based on regional inversions, Silva et al., 1997)

**GRANITE REFERENCE SITE GROUND MOTION PARAMETERS  
LOS ANGELES AREA**

Target Outcrop** PGA(g)	Median Outcrop** PGA(g)	Median Outcrop** PGV(cm/sec)	Median Outcrop** PGD(cm)	Median Outcrop** V/A (cm/sec/g)	Median Outcrop** AD/V <sup>2</sup> (gcm/cm <sup>2</sup> /sec <sup>2</sup> )	Dist. (km)	Depth (km)	M	$\Delta\sigma$ (bars)
0.05	0.05	4.84	2.15	95.34	4.56	46.00	8.00	6.5	60
0.10	0.10	9.16	3.97	89.29	4.75	25.00	8.00	6.5	60
0.20	0.20	17.29	7.39	85.89	4.87	12.00	8.00	6.5	60
0.40	0.40	33.57	14.22	83.95	4.95	0.00	7.60	6.5	60
0.75	0.77	67.34	26.30	87.47	4.96	0.00	4.49	6.5	60
1.25	1.26	110.55	48.76	87.44	5.01	0.00	2.77	6.5	60

$Q(f) = 275 f^{0.6}$  (Los Angeles; based on regional inversions, Silva et al., 1997)

Kappa = 0.04 sec, low strain

\*Top of Franciscan Profile

\*\*Top of Granitic Profile

Table 5  
DEPTH CATEGORIES AND DEPTH RANGES

SAN FRANCISCO BAY AREA		
Category	Mean Depth (ft)	Range* (ft)
1	90	30 - 150
2	250	150 - 350
3	500	350 - 650
4	515	30 - 1,000
5	250	30 - 450
6	340	30 - 650
Geologic Units and Depth Categories		
Geologic Unit		Depth Categories
Quaternary/Tertiary (QT <sub>s</sub> )		1, 2, 3, 6
Older Alluvium (Q <sub>oa</sub> )		1, 2, 3, 4, 5
Quaternary Alluvium (Q <sub>al</sub> )		1, 2, 3, 4, 5
Bay Mud (Q <sub>m</sub> )		1, 2, 3, 6
LOS ANGELES AREA		
Category	Mean Depth (ft)	Range* (ft)
1	90	30 - 150
2	250	150 - 350
3	500	350 - 650
4	515	30 - 1000
5	1,000	500 - 1,500
Geologic Units and Depth Categories		
Geologic Unit		Depth Categories
Saugus (T <sub>s</sub> )		1, 2, 3, 4
Old Alluvium + Tertiary (Q <sub>o</sub> + T <sub>s</sub> )		1, 2, 3, 4, 5
Old Alluvium (Q <sub>o</sub> )		1, 2, 3, 4
Quaternary Alluvium (Q <sub>y</sub> )		1, 2, 3, 4, 5

\*Range of profile depth over which category applies as well as range of depth randomization for each category. Profile depth is defined as depth to basement material: top of Wald et al. (1991; 1996) crusts (Table 3).

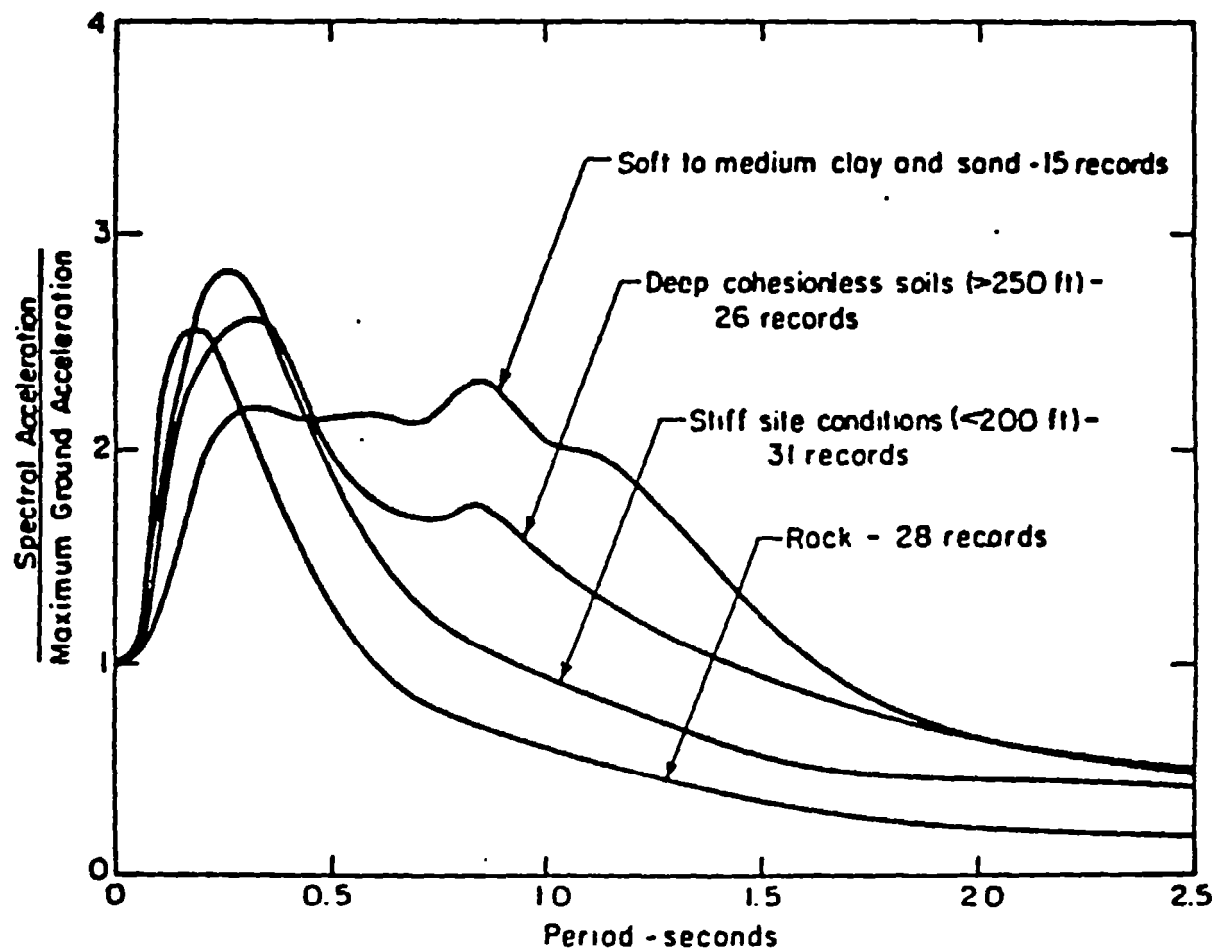


Figure 1. Effects of near surface soil conditions on 5% damped response spectral shapes (source: Seed, Ugas, and Lysmor, 1976).

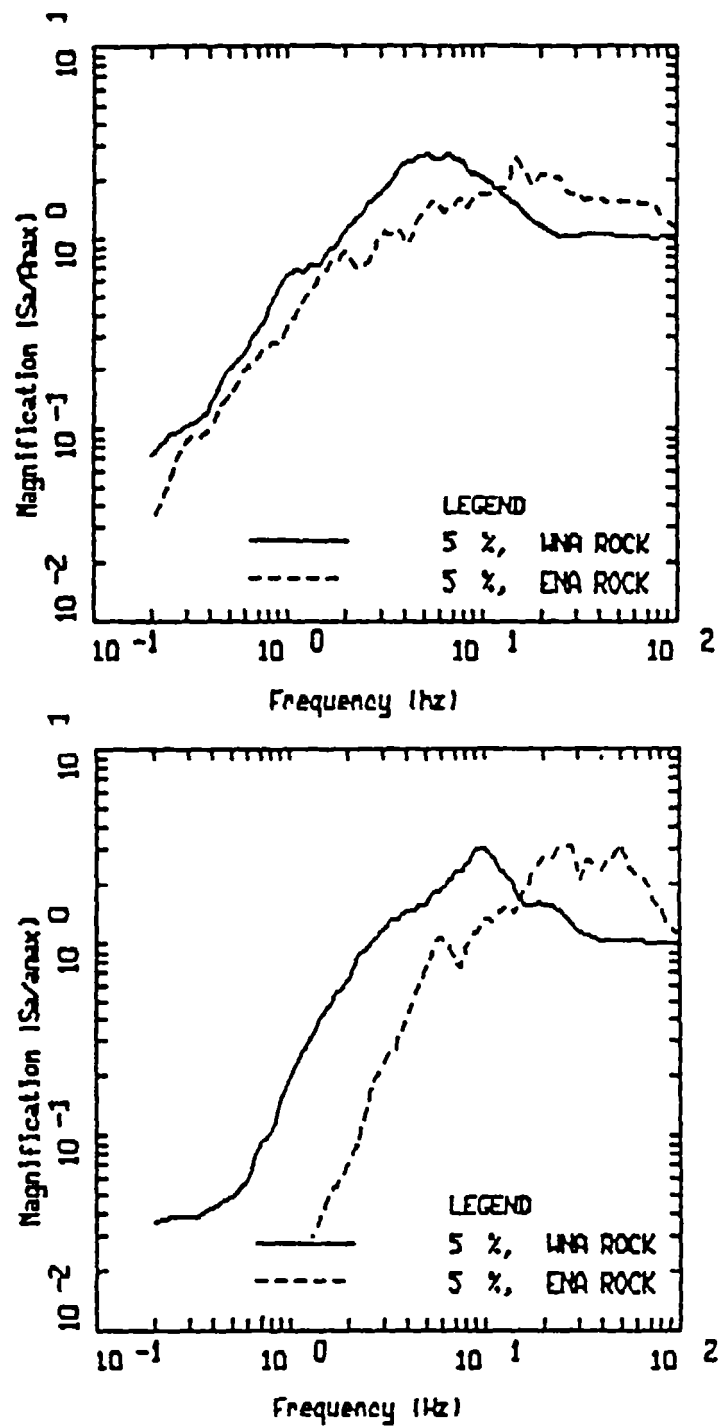


Figure 2. Effects of hard and soft rock site conditions and magnitude on 5% damped response spectral shapes for earthquakes with  $M \approx 6.5$  (upper) and  $M \approx 4.5$  (lower) (source: Silva and Darragh, 1995).

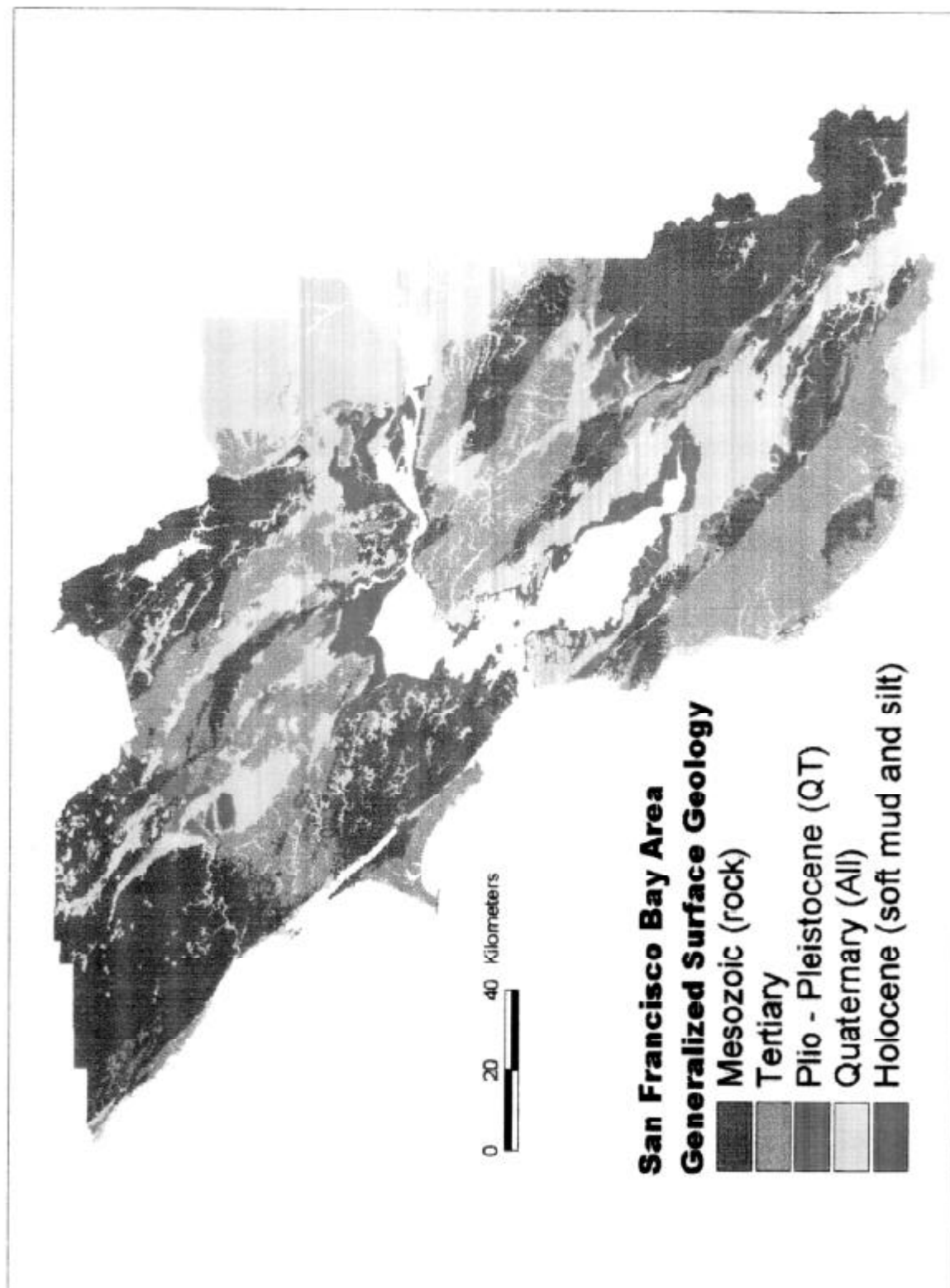
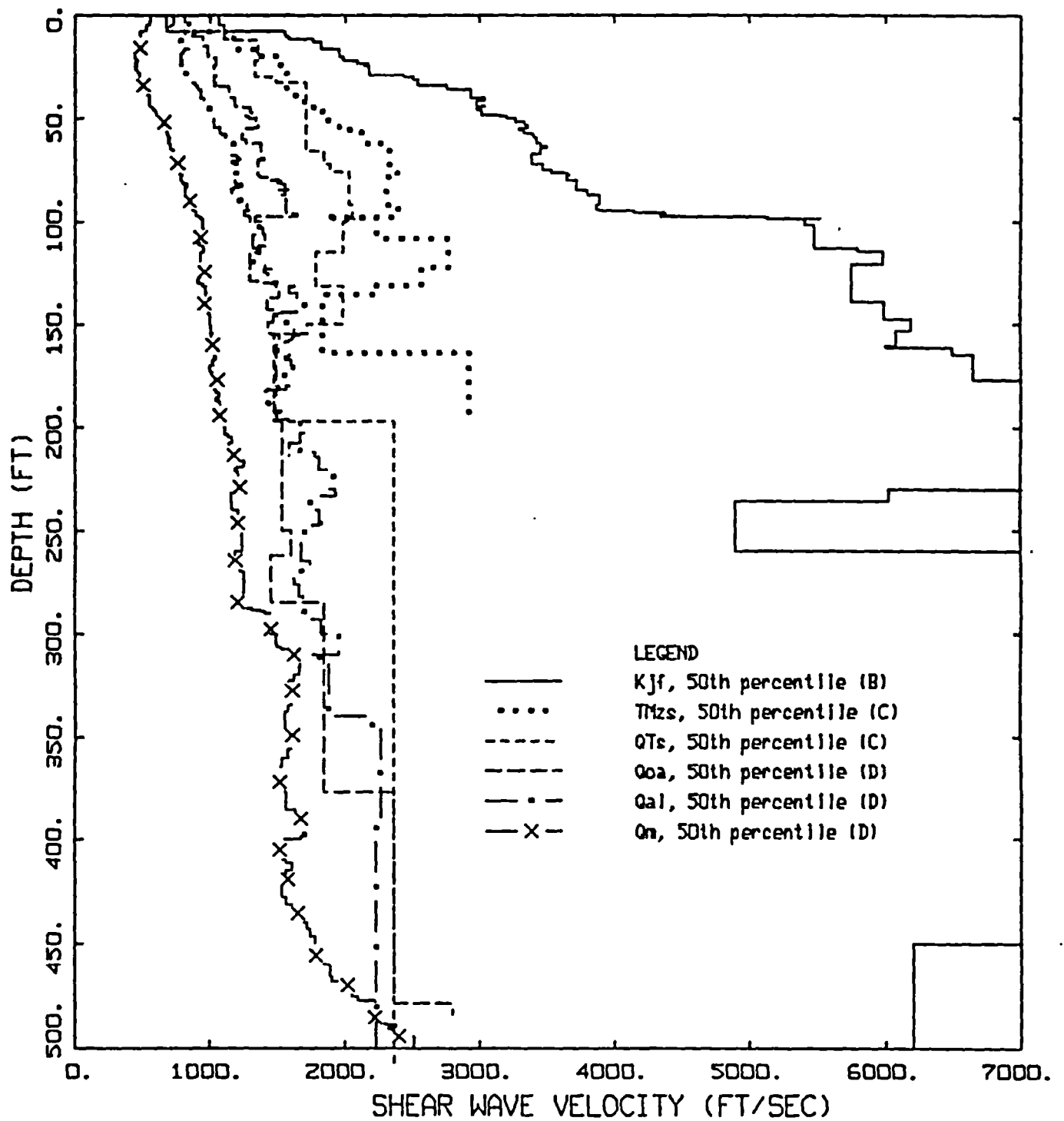


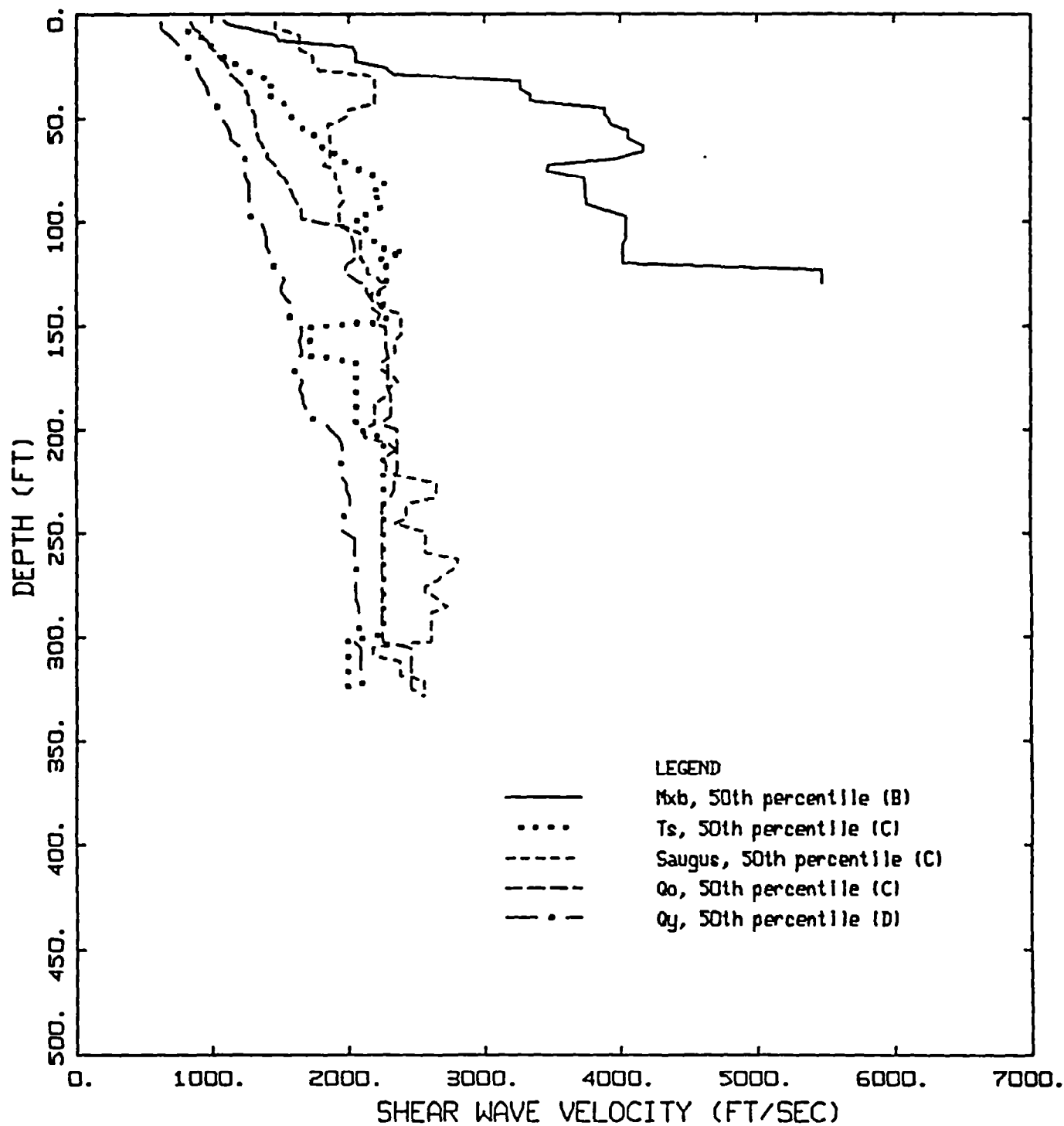
Figure 3. Mapped surface geology for the San Francisco Bay Area showing categories Bay Mud ( $Q_m$ ) Quaternary Alluvium ( $Q_a + Q_m$ ), Quaternary/Tertiary ( $Q_{ts}$ ), Tertiary Bedrock ( $T_s$ ), and Franciscan ( $K_p$ ) (source: Wentworth (1997)).



## SHEAR WAVE VELOCITY PROFILES SAN FRANCISCO

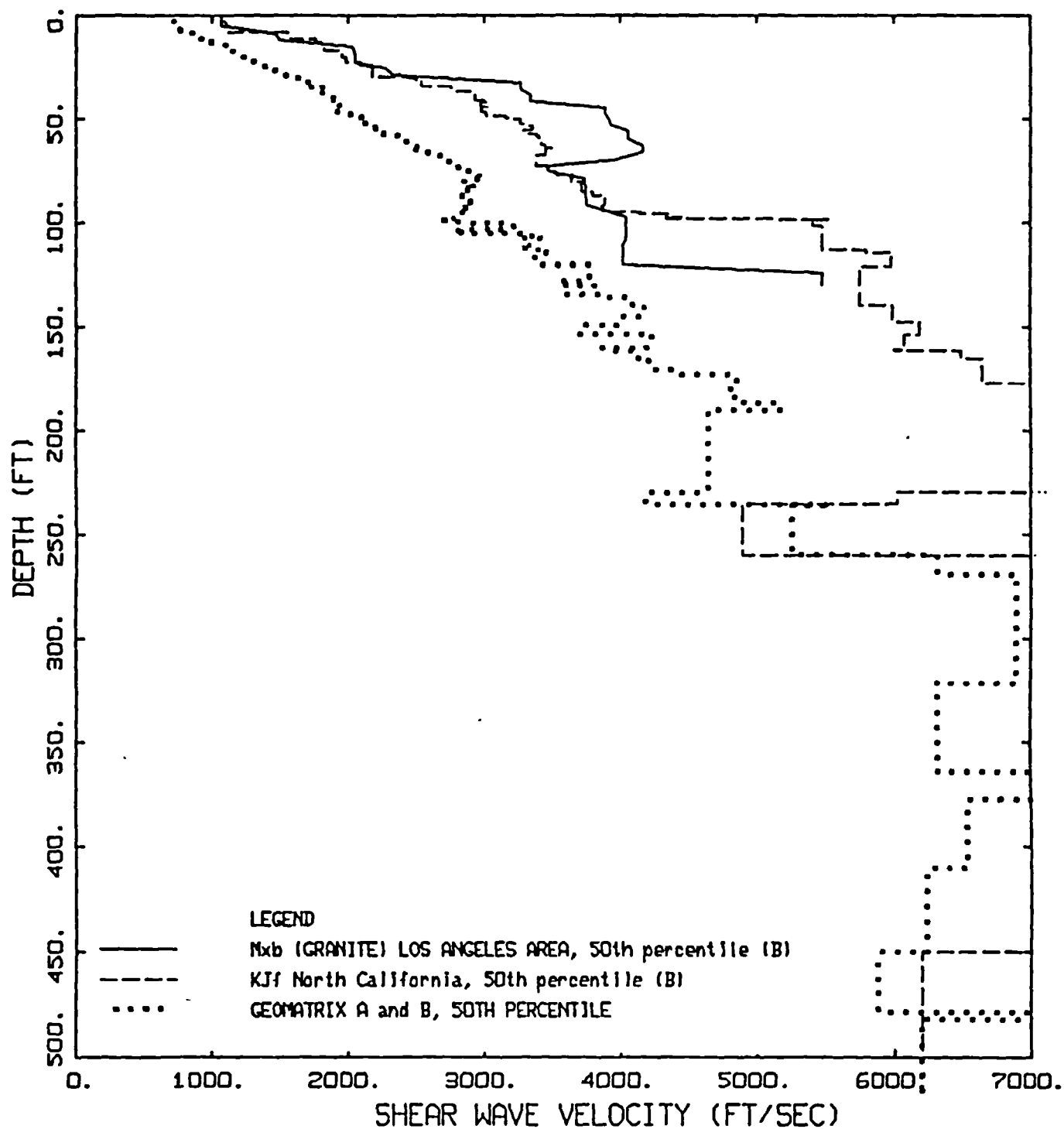
Figure 4. Surface geology based shear-wave velocity profiles for the San Francisco Bay area. Profiles are median estimates based on borehole measurements. Corresponding NEHRP categories are shown (Table 1).





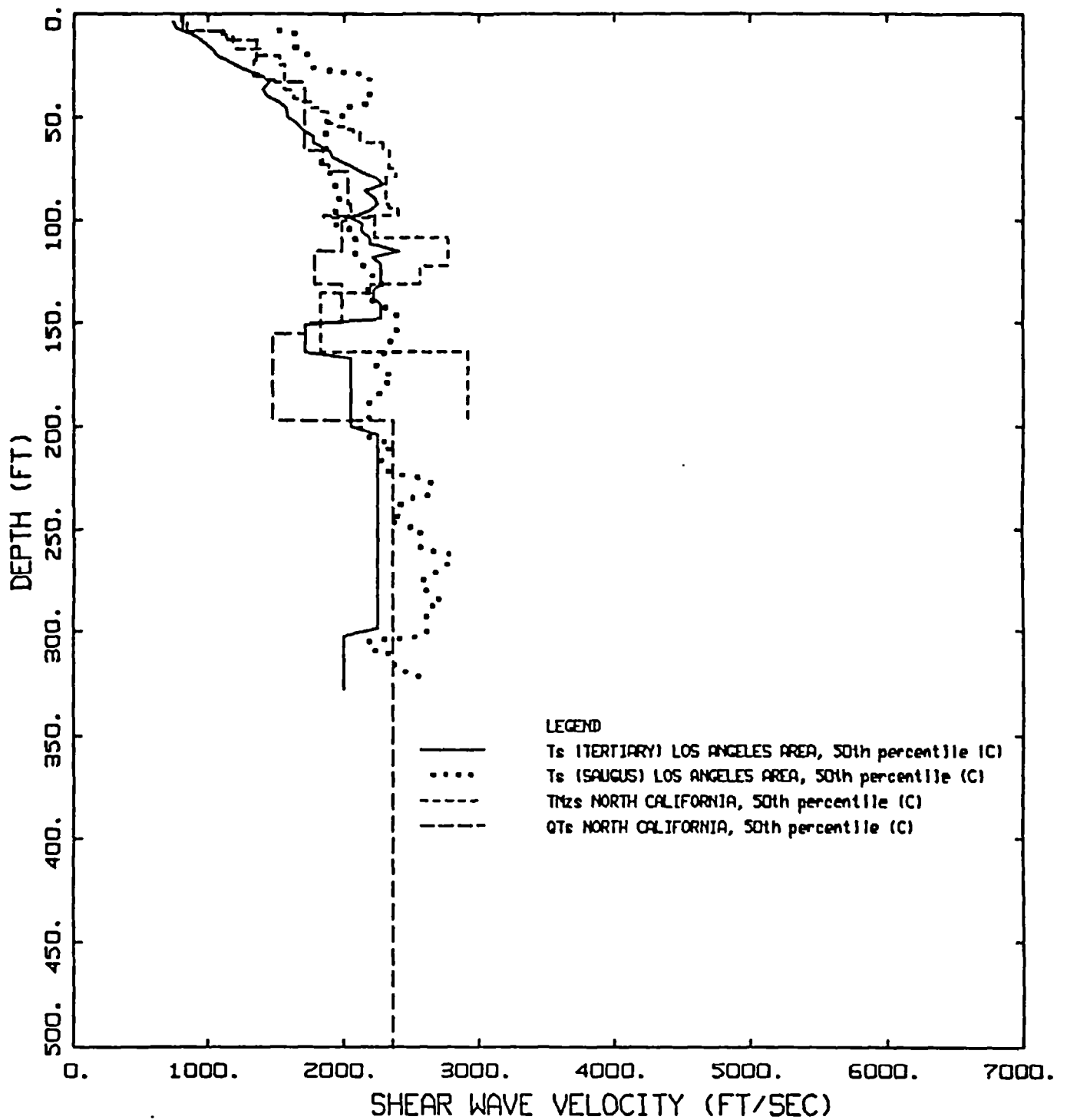
## SHEAR WAVE VELOCITY PROFILES LOS ANGELES

Figure 5. Surface geology based shear-wave velocity profiles for the Los Angeles area. Profiles are median estimates based on borehole measurements. Corresponding NEHRP categories are shown (Table 1).



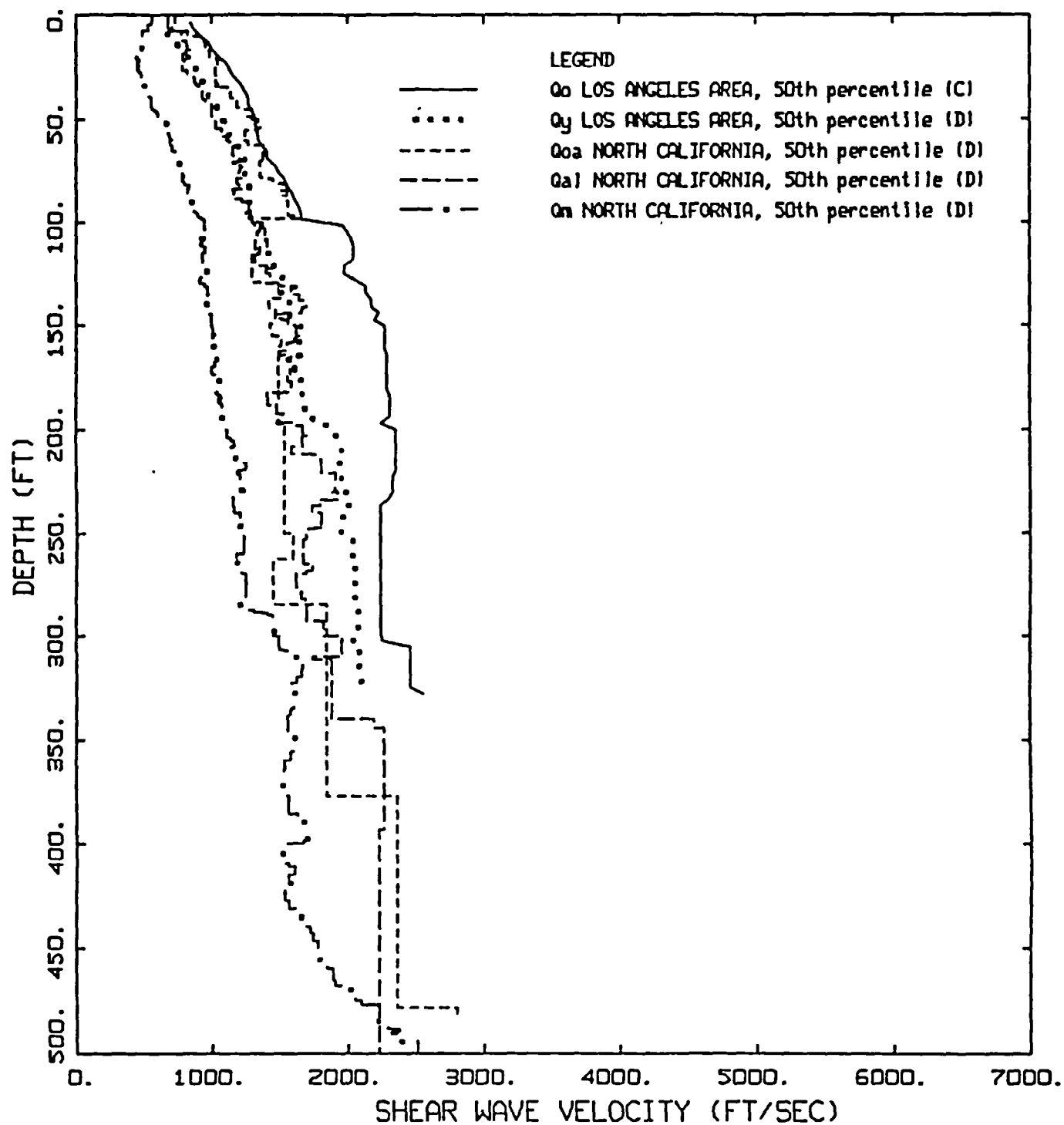
## SHEAR WAVE VELOCITY PROFILES SF, LA BASE ROCK COMPARISON

Figure 6. Comparison of median baserock shear-wave velocity profiles for San Francisco (Figure 4) and Los Angeles (Figure 5) areas. Dotted line is median profile for Geomatrix Category A and B, generally reflecting soft rock site conditions for California based empirical attenuation relations (Silva et al., 1997).



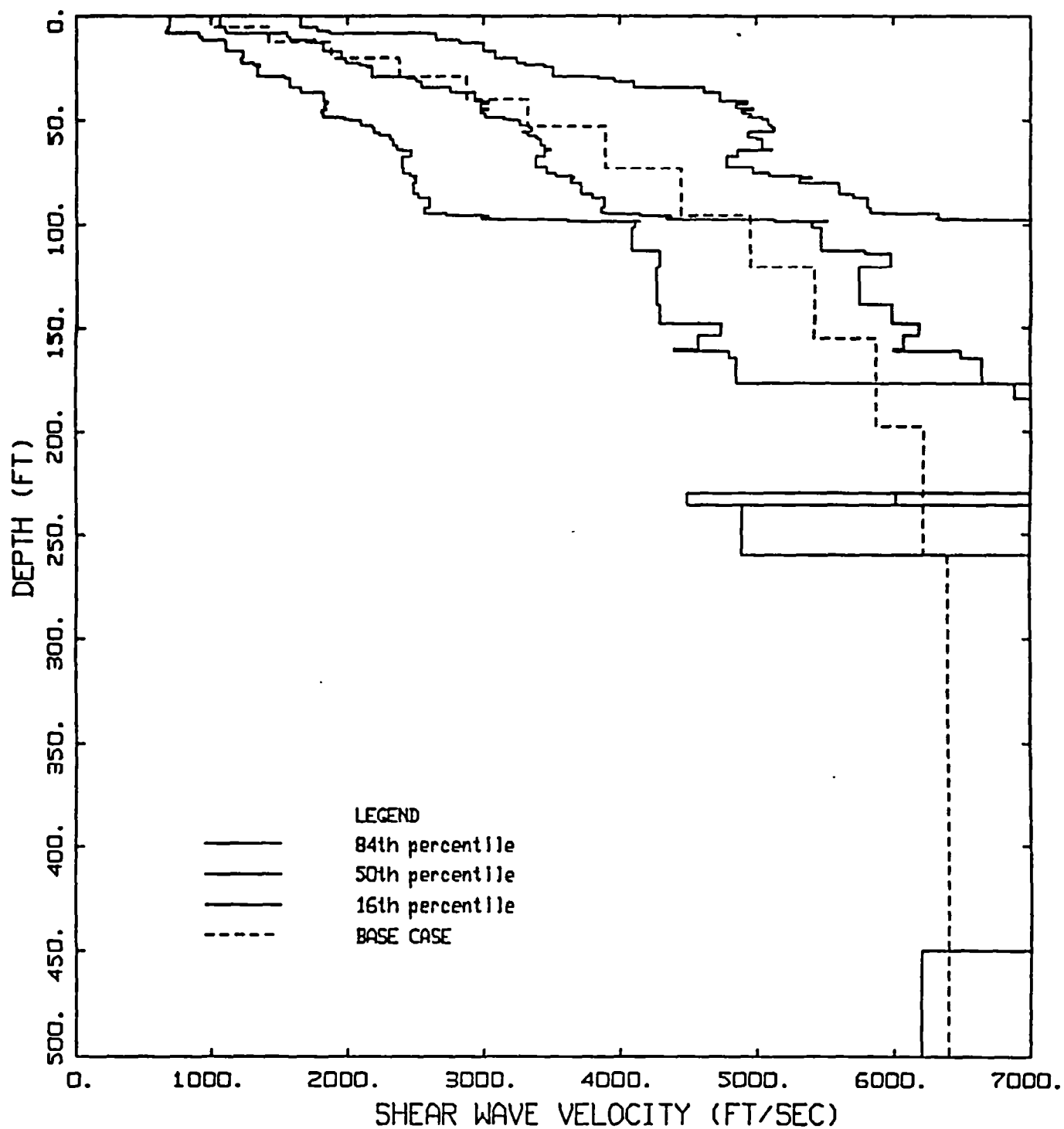
## SHEAR WAVE VELOCITY PROFILES SF, LA TERTIARY COMPARISON

Figure 7. Comparison of median Tertiary shear-wave velocity profiles for San Francisco (Figure 4) and Los Angeles (Figure 5) areas.



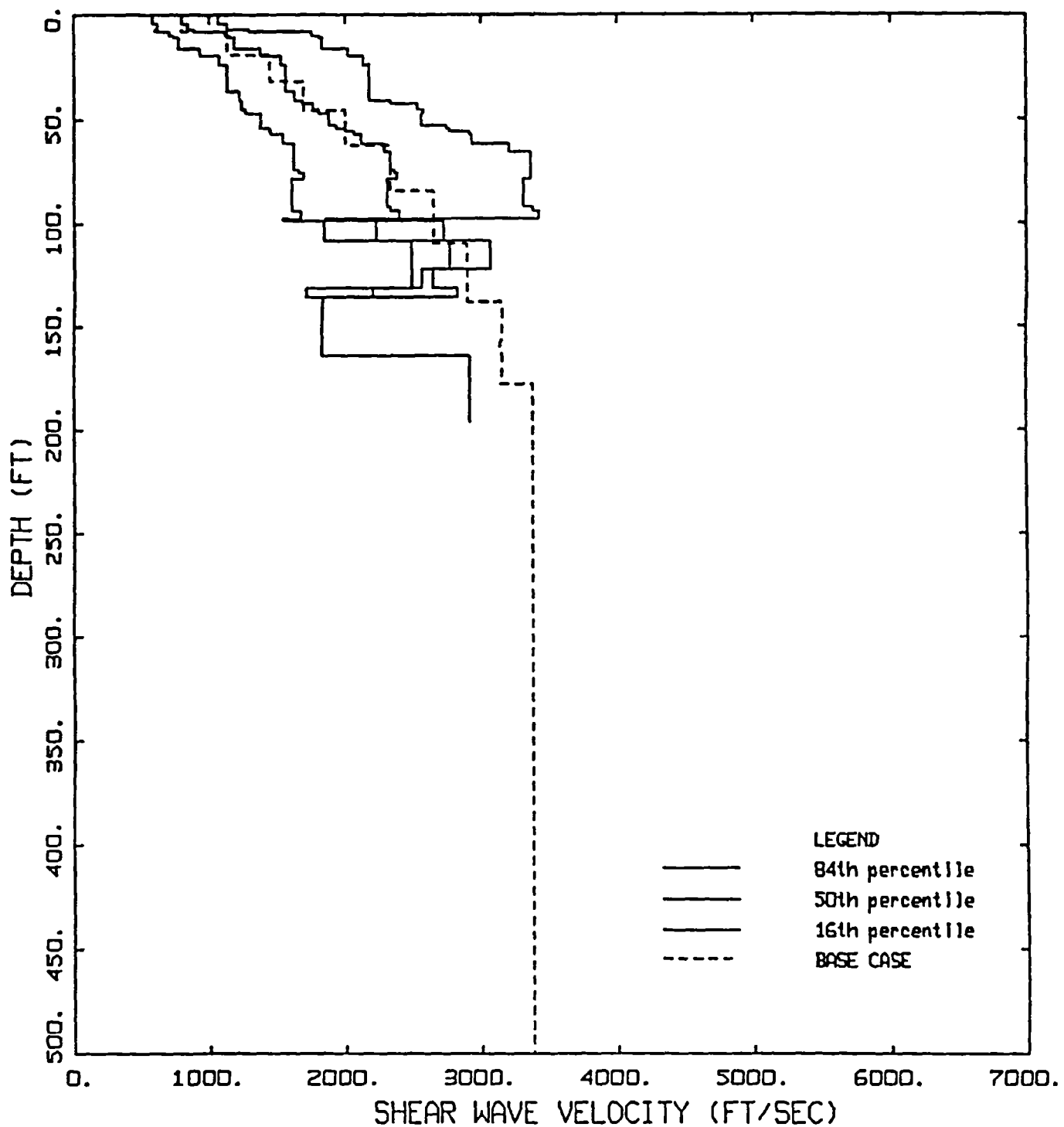
## SHEAR WAVE VELOCITY PROFILES SF, LA ALLUVIUM COMPARISON

Figure 8. Comparison of median Alluvium shear-wave velocity profiles for San Francisco (Figure 4) and Los Angeles (Figure 5) areas.



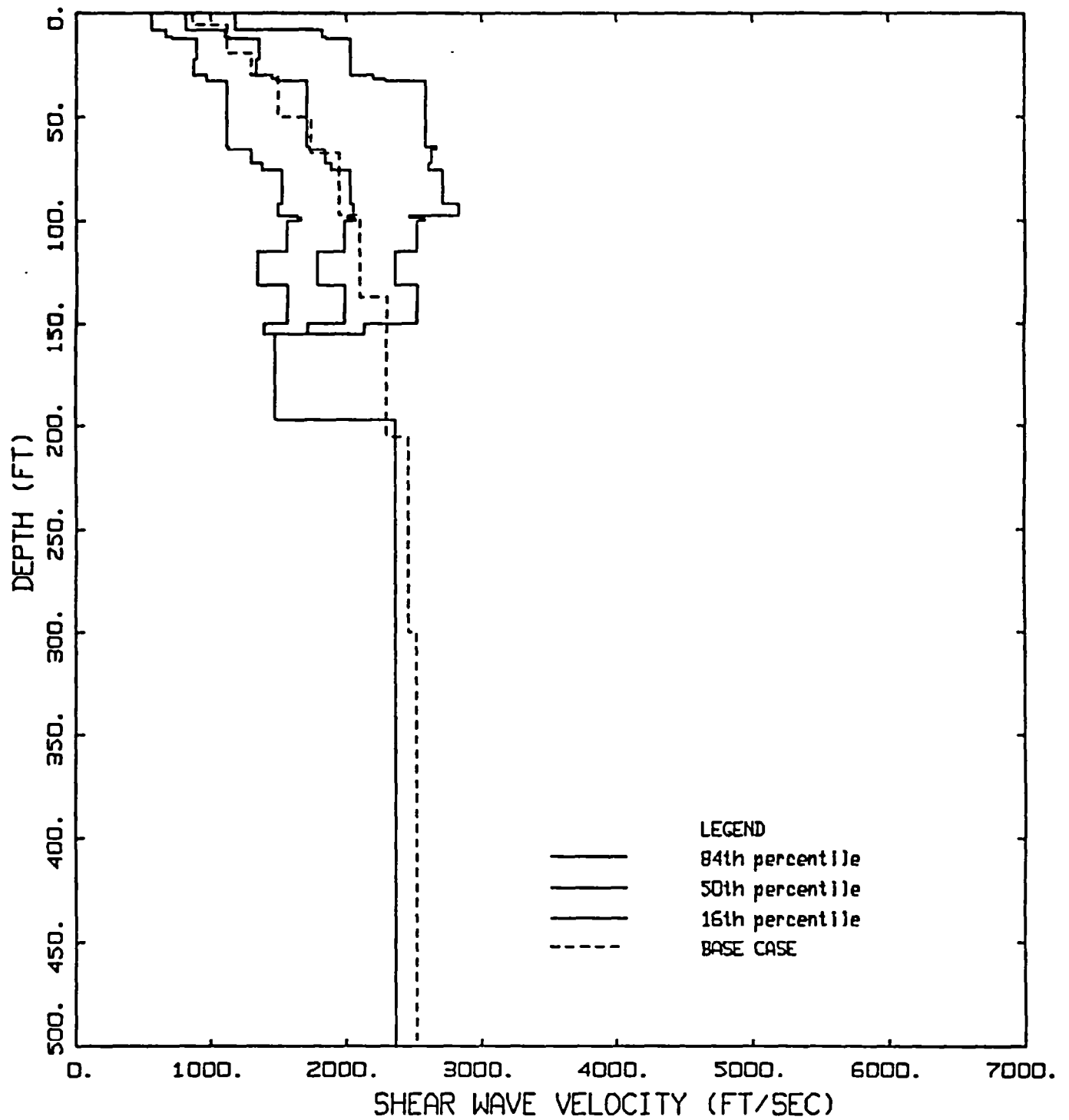
## SHEAR WAVE VELOCITY PROFILES KJf NORTH CALIFORNIA

Figure 9. Median and  $\pm 1 \sigma$  shear-wave velocity profiles for the San Francisco Bay area surface geologic unit  $K_{j6}$  Franciscan (Table 1).



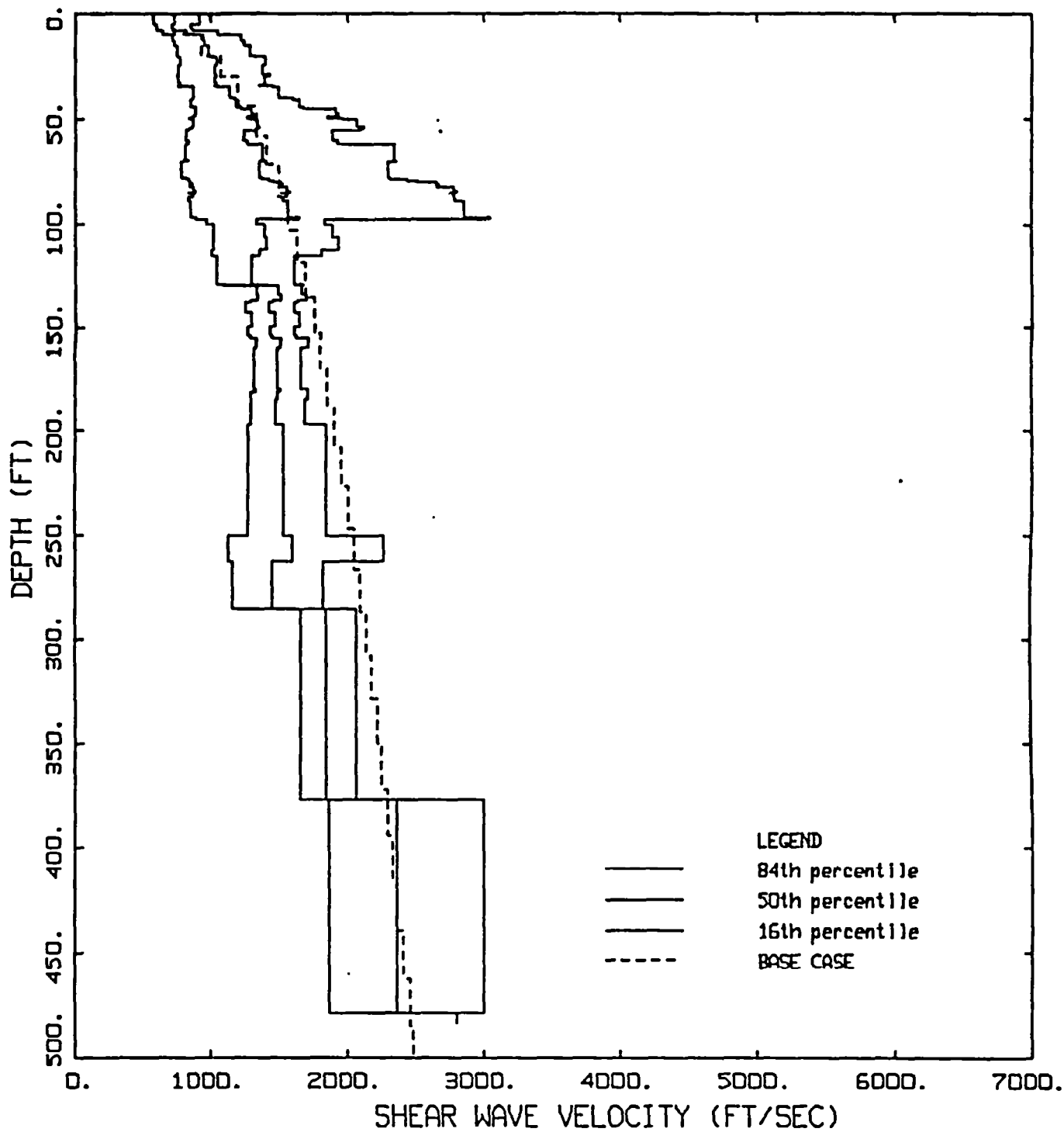
## SHEAR WAVE VELOCITY PROFILES TMzs NORTH CALIFORNIA

Figure 10. Median and  $\pm 1 \sigma$  shear-wave velocity profiles for the San Francisco Bay area surface geologic unit TM<sub>zs</sub>, Tertiary Bedrock (Table 1).



## SHEAR WAVE VELOCITY PROFILES QTs NORTH CALIFORNIA

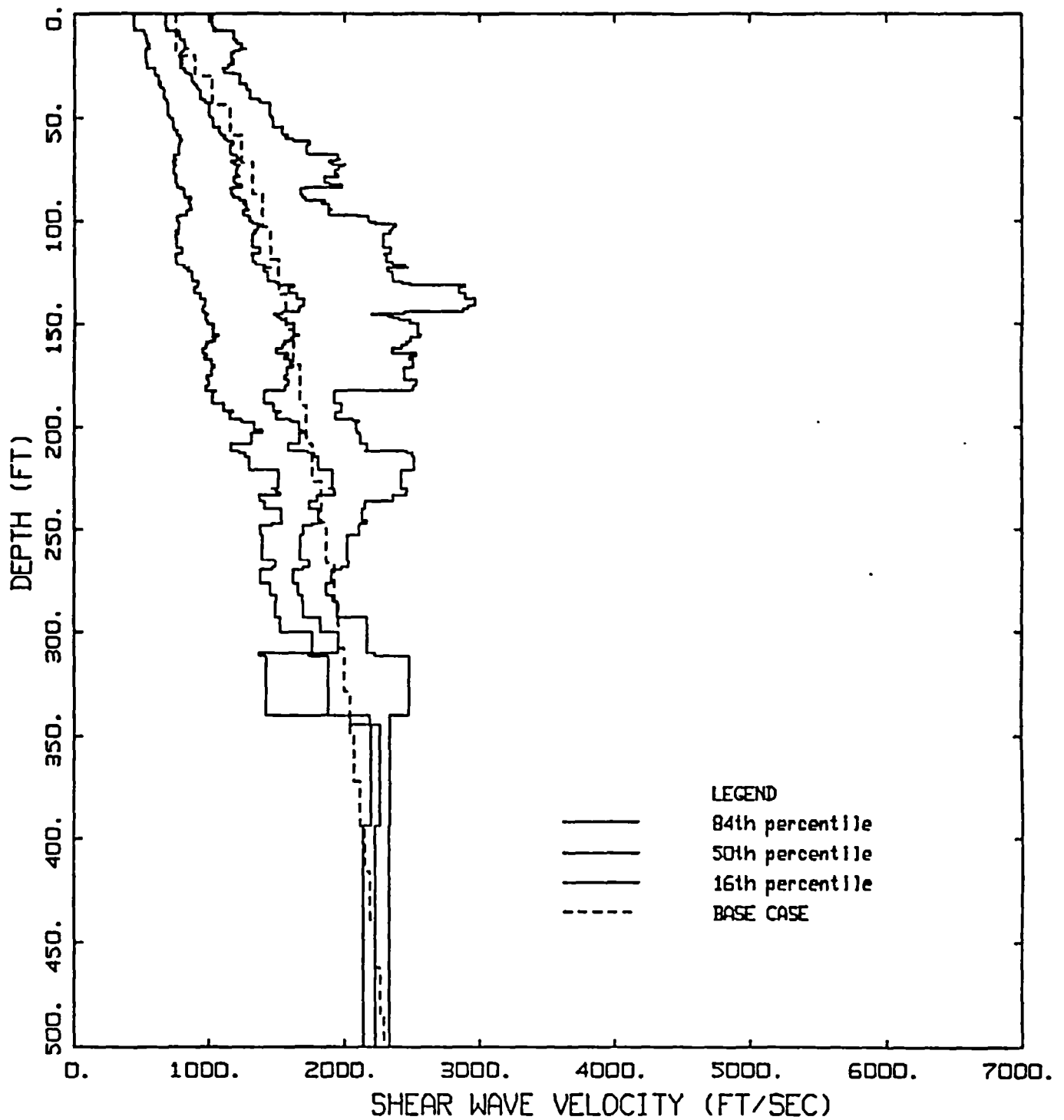
Figure 11. Median and  $\pm 1 \sigma$  shear-wave velocity profiles for the San Francisco Bay area surface geologic unit QTs, Quaternary/Tertiary (Table 1).



## SHEAR WAVE VELOCITY PROFILES Q<sub>oa</sub> NORTH CALIFORNIA

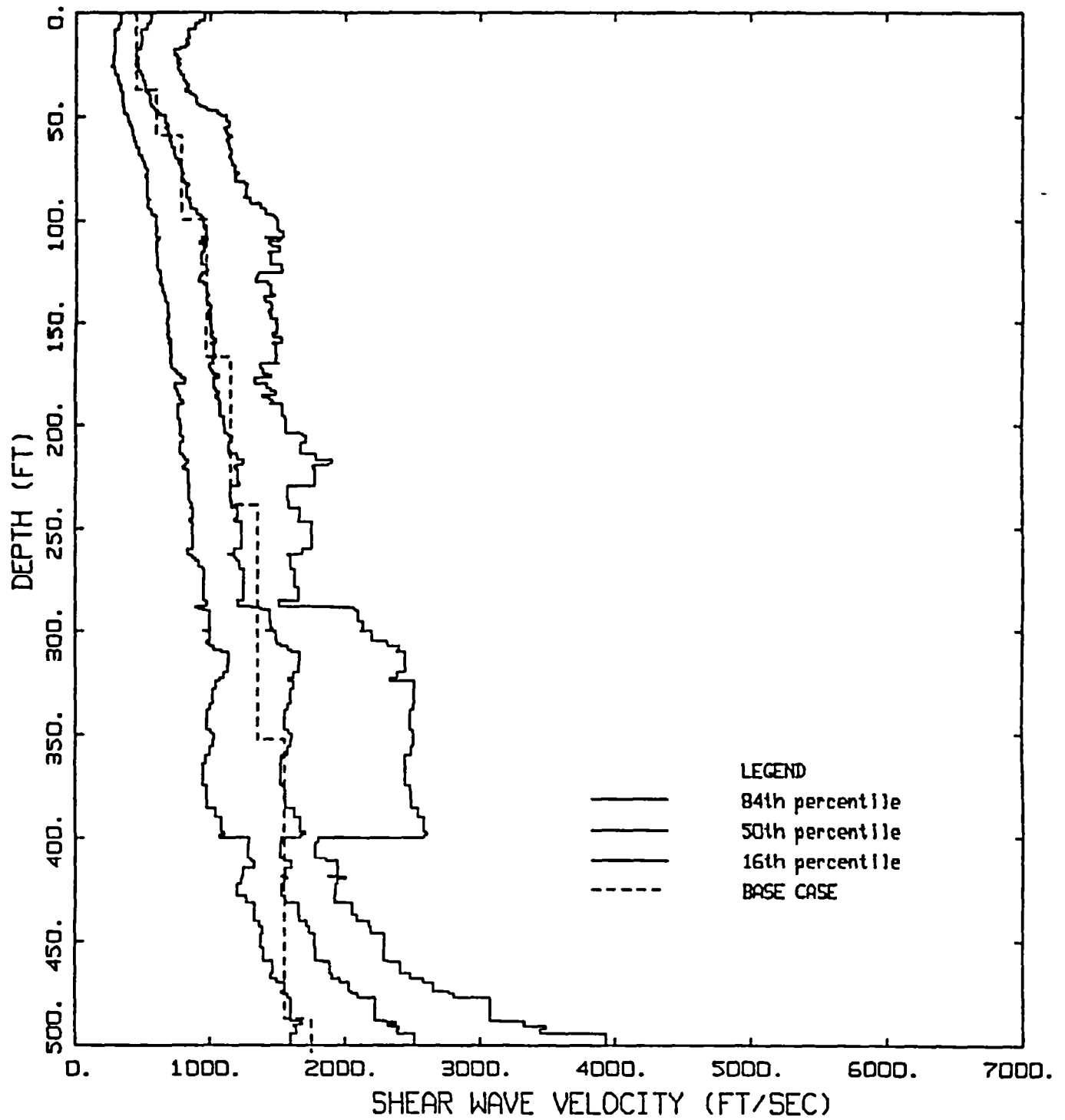
Figure 12. Median and  $\pm 1 \sigma$  shear-wave velocity profiles for the San Francisco Bay area surface geologic unit Q<sub>oa</sub>, Older Alluvium (Table 1).





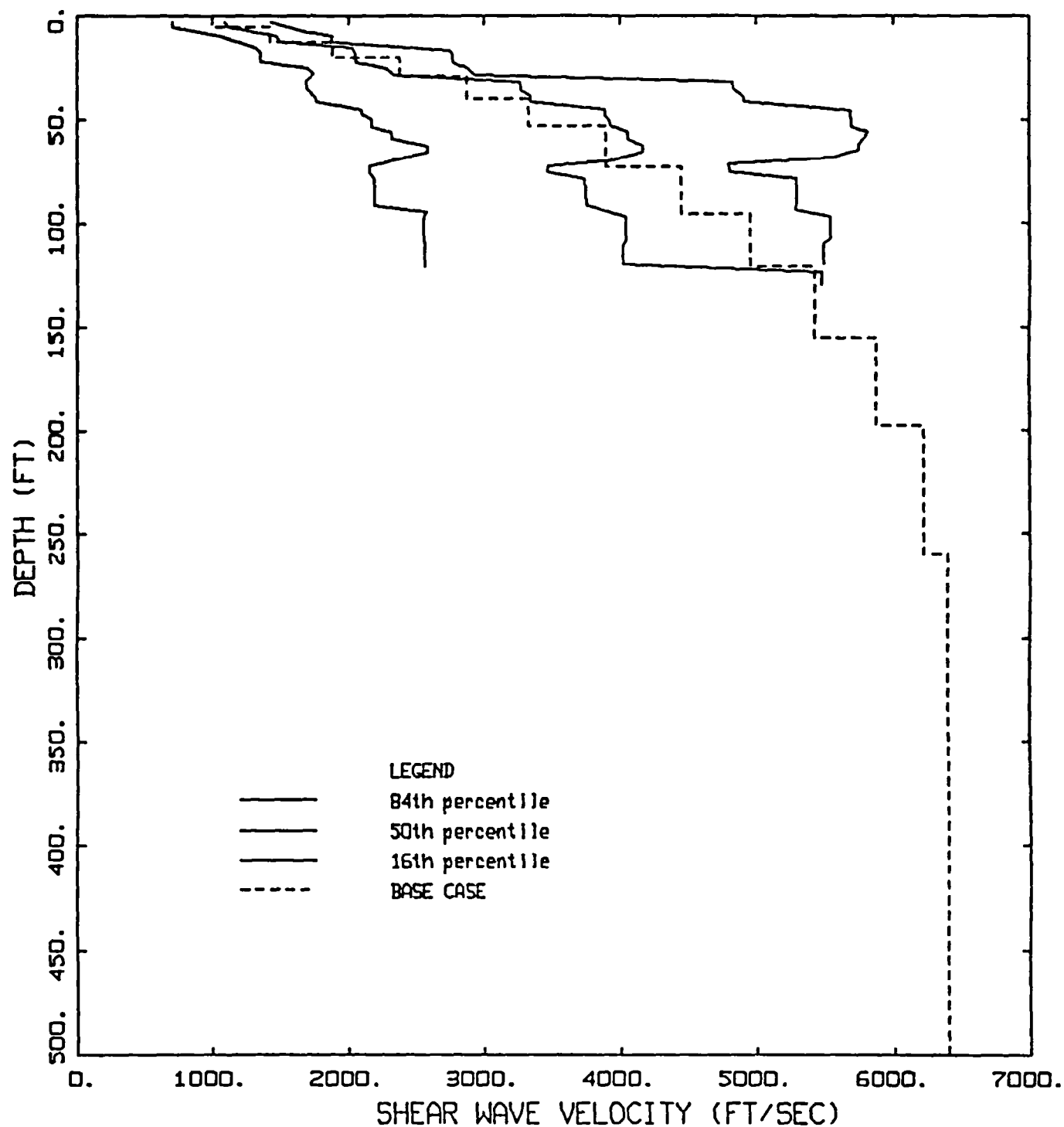
## SHEAR WAVE VELOCITY PROFILES Qa1 NORTH CALIFORNIA

Figure 13. Median and  $\pm 1 \sigma$  shear-wave velocity profiles for the San Francisco Bay area surface geologic unit Qa1, Quaternary Alluvium (Table 1).



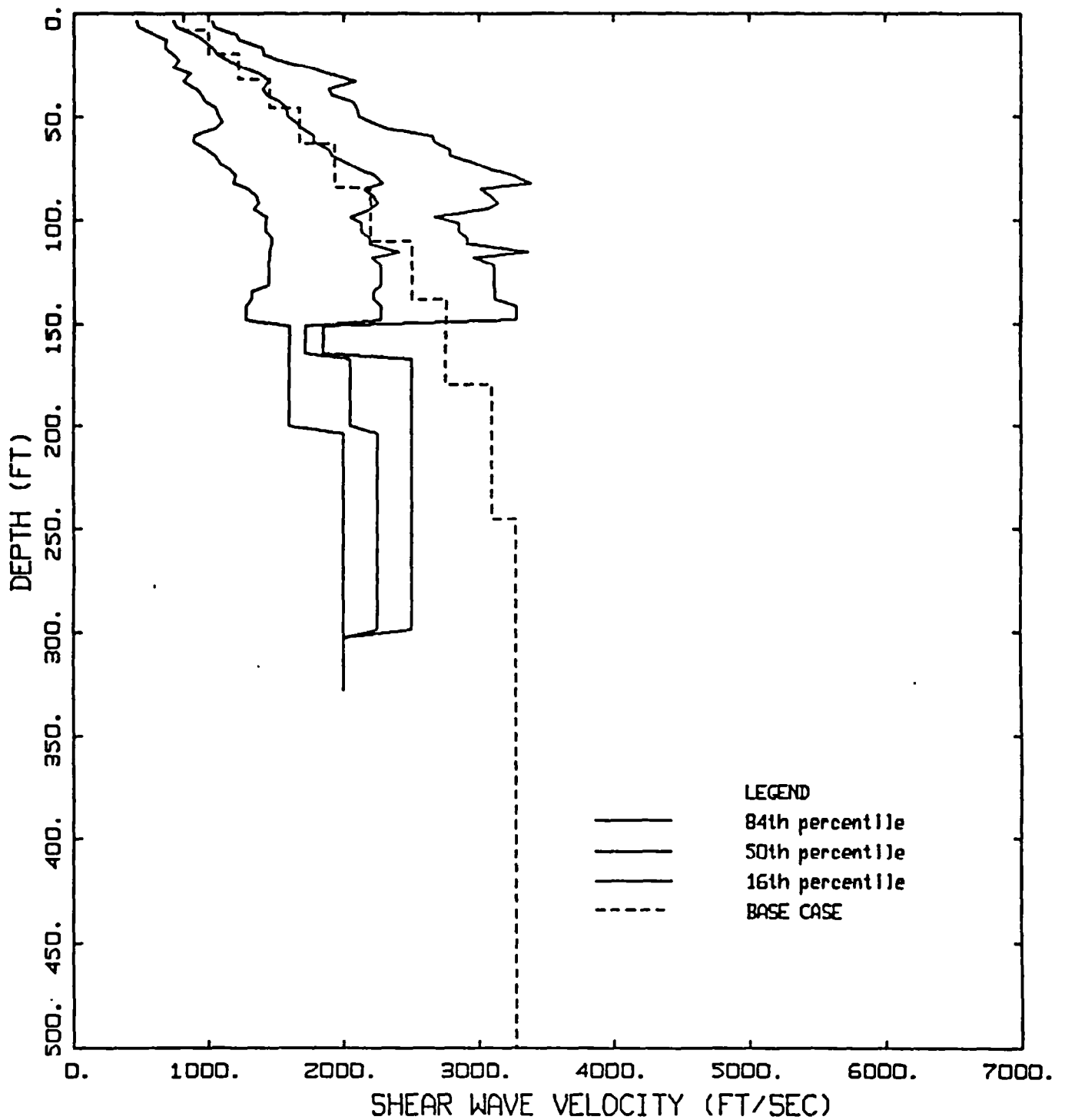
## SHEAR WAVE VELOCITY PROFILES Q<sub>m</sub> NORTH CALIFORNIA

Figure 14. Median and  $\pm 1 \sigma$  shear-wave velocity profiles for the San Francisco Bay area surface geologic unit Q<sub>m</sub>, Bay Mud (Table 1).



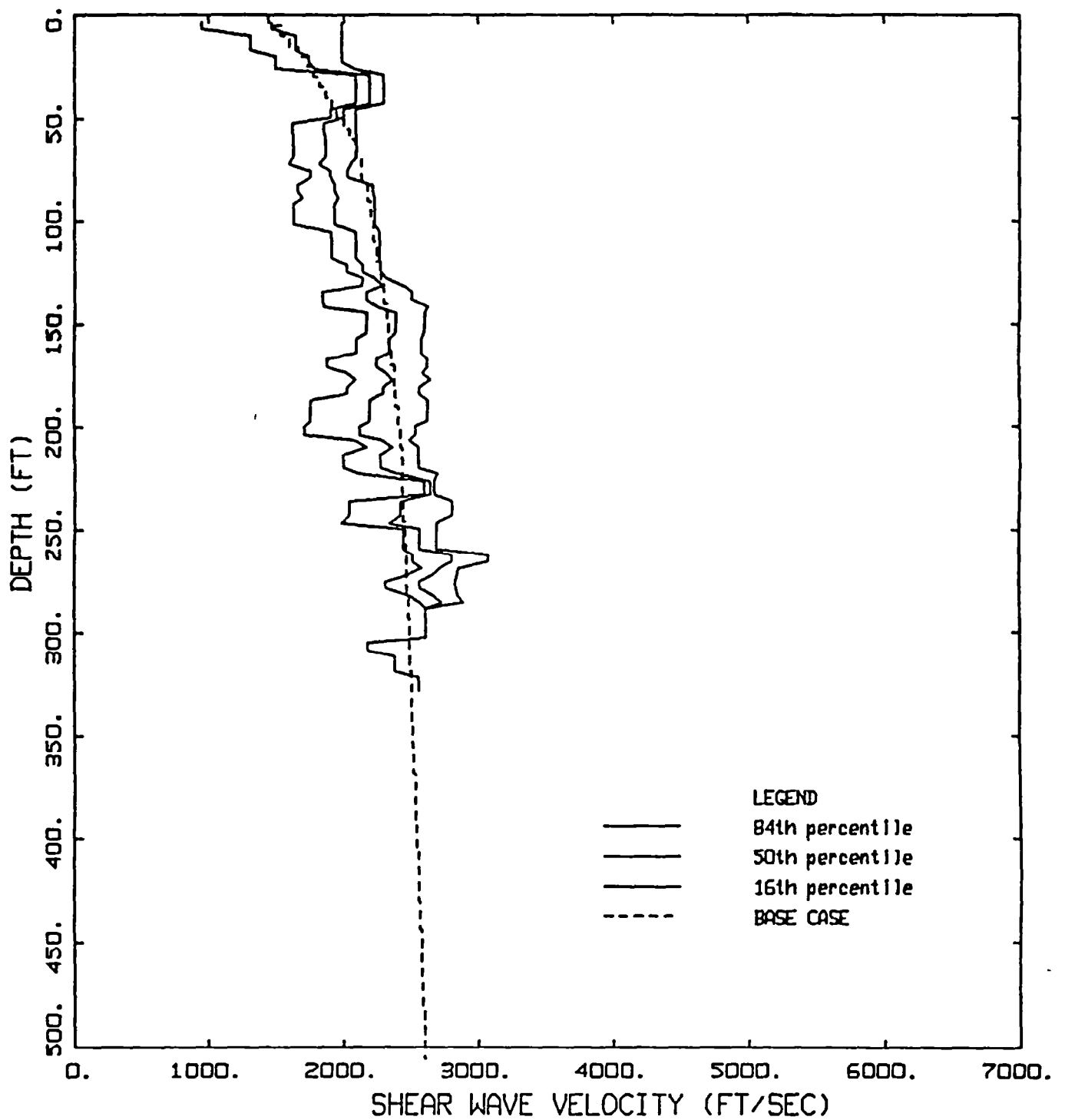
## SHEAR WAVE VELOCITY PROFILES Mxb (GRANITE) LOS ANGELES AREA

Figure 15. Median and  $\pm 1 \sigma$  shear-wave velocity profiles for the Los Angeles area surface geologic unit M<sub>xb</sub> Granite (Table 1).



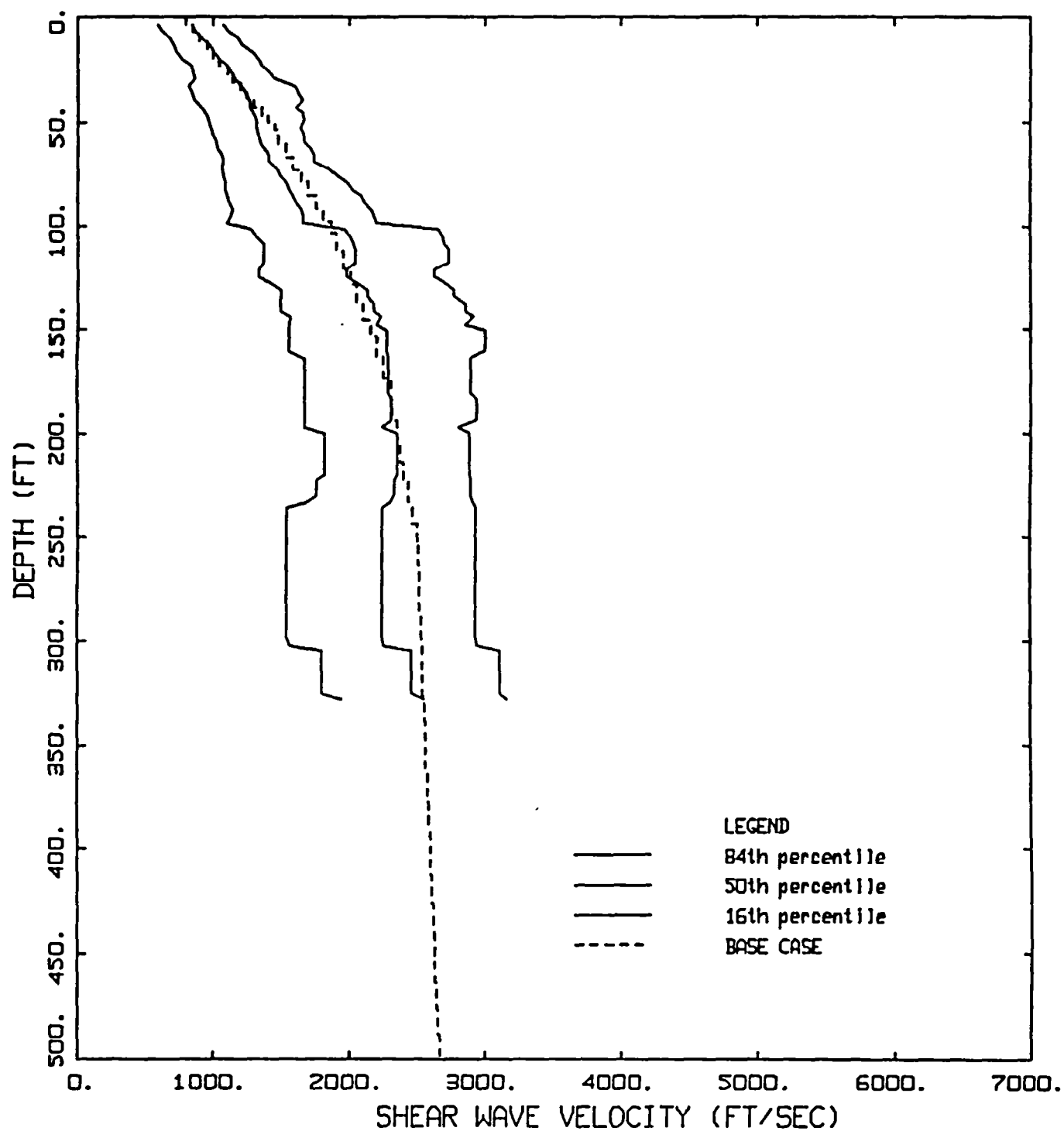
## SHEAR WAVE VELOCITY PROFILES T<sub>s</sub> (TERTIARY) LOS ANGELES AREA

Figure 16. Median and  $\pm 1 \sigma$  shear-wave velocity profiles for the Los Angeles area surface geologic unit T<sub>s</sub>, Tertiary (Table 1).



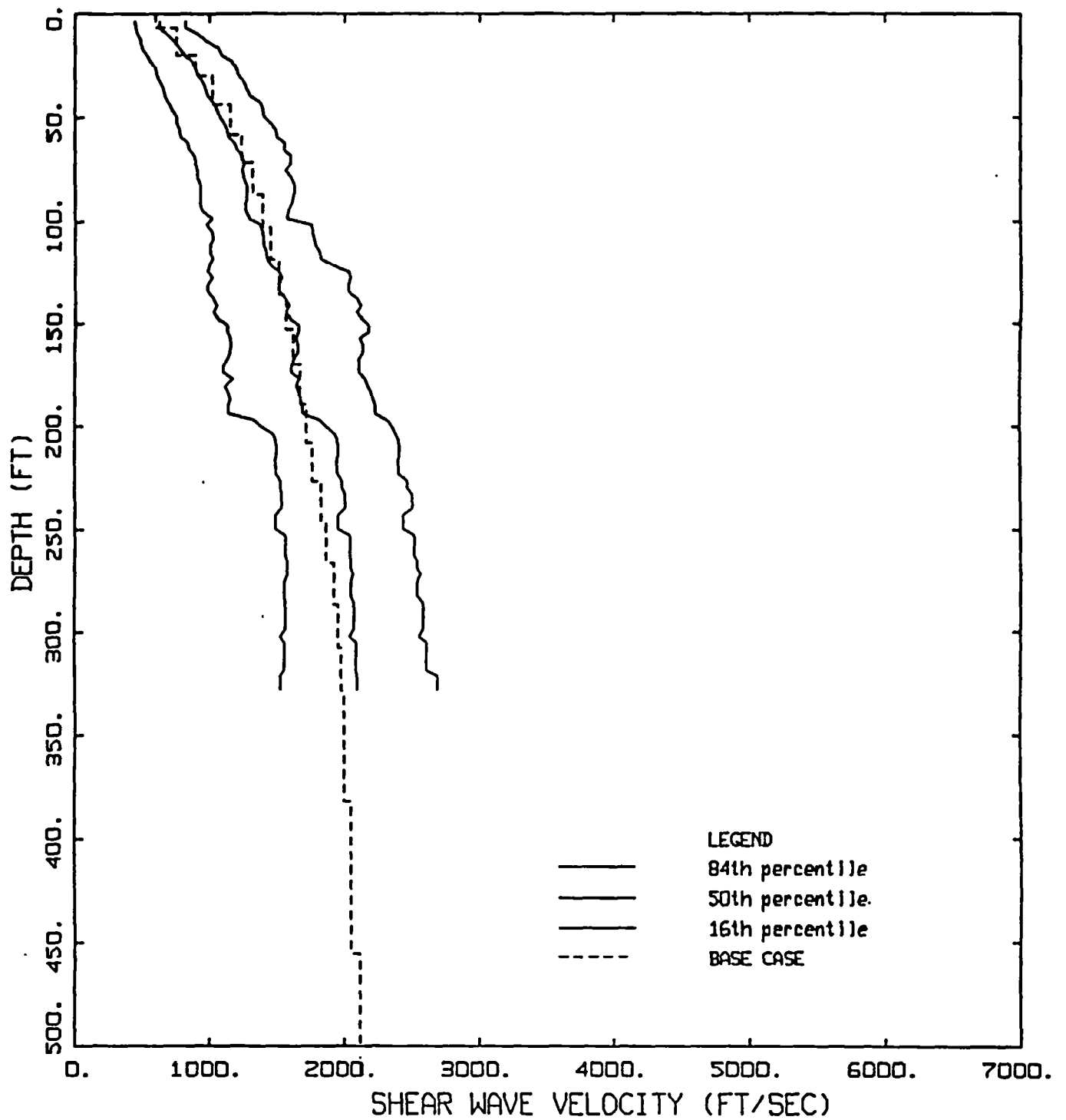
## SHEAR WAVE VELOCITY PROFILES T<sub>s</sub> (SAUGUS) LOS ANGELES AREA

Figure 17. Median and  $\pm 1 \sigma$  shear-wave velocity profiles for the San Francisco Bay area surface geologic unit T<sub>s</sub>, Saugus (Table 1).



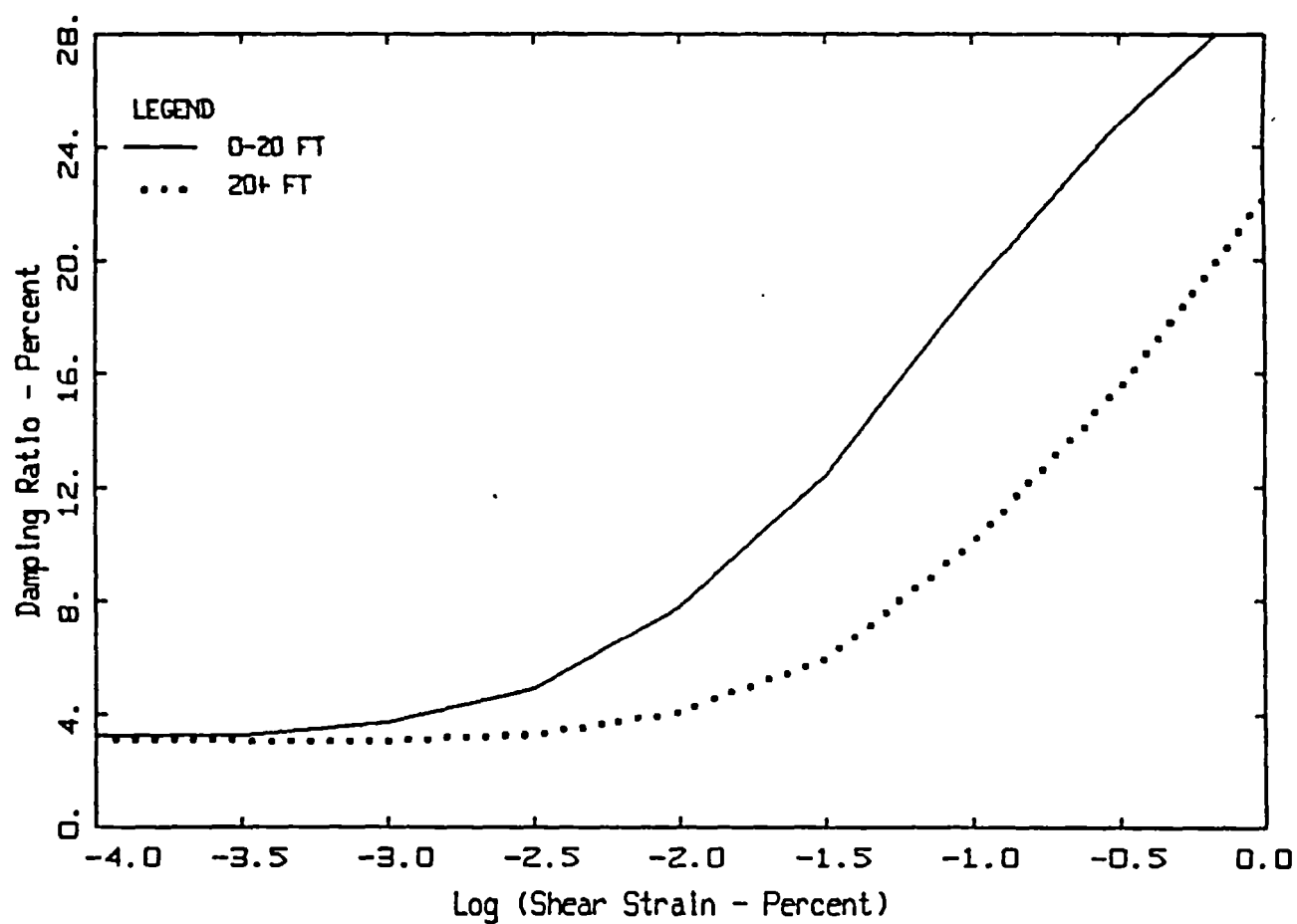
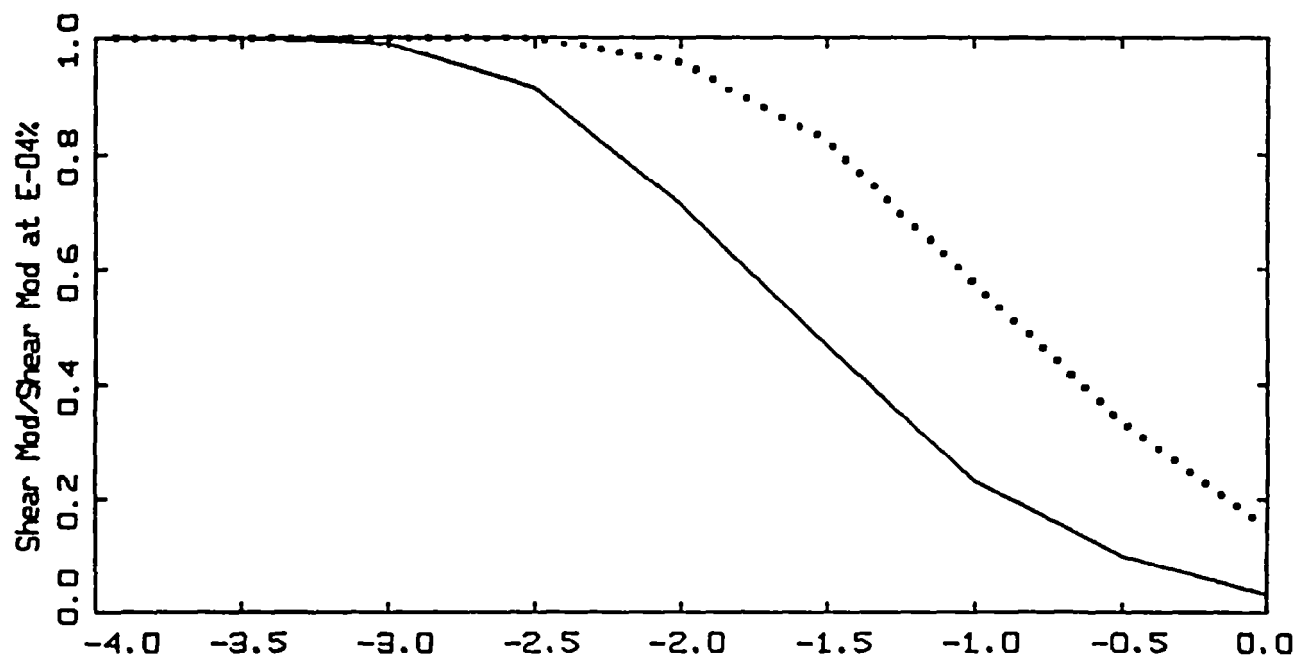
## SHEAR WAVE VELOCITY PROFILES Q<sub>0</sub> LOS ANGELES AREA

Figure 18. Median and  $\pm 1 \sigma$  shear-wave velocity profiles for the Los Angeles area surface geologic unit Q<sub>0</sub>, Older Alluvium (Table 1).



## SHEAR WAVE VELOCITY PROFILES Q<sub>y</sub> LOS ANGELES AREA

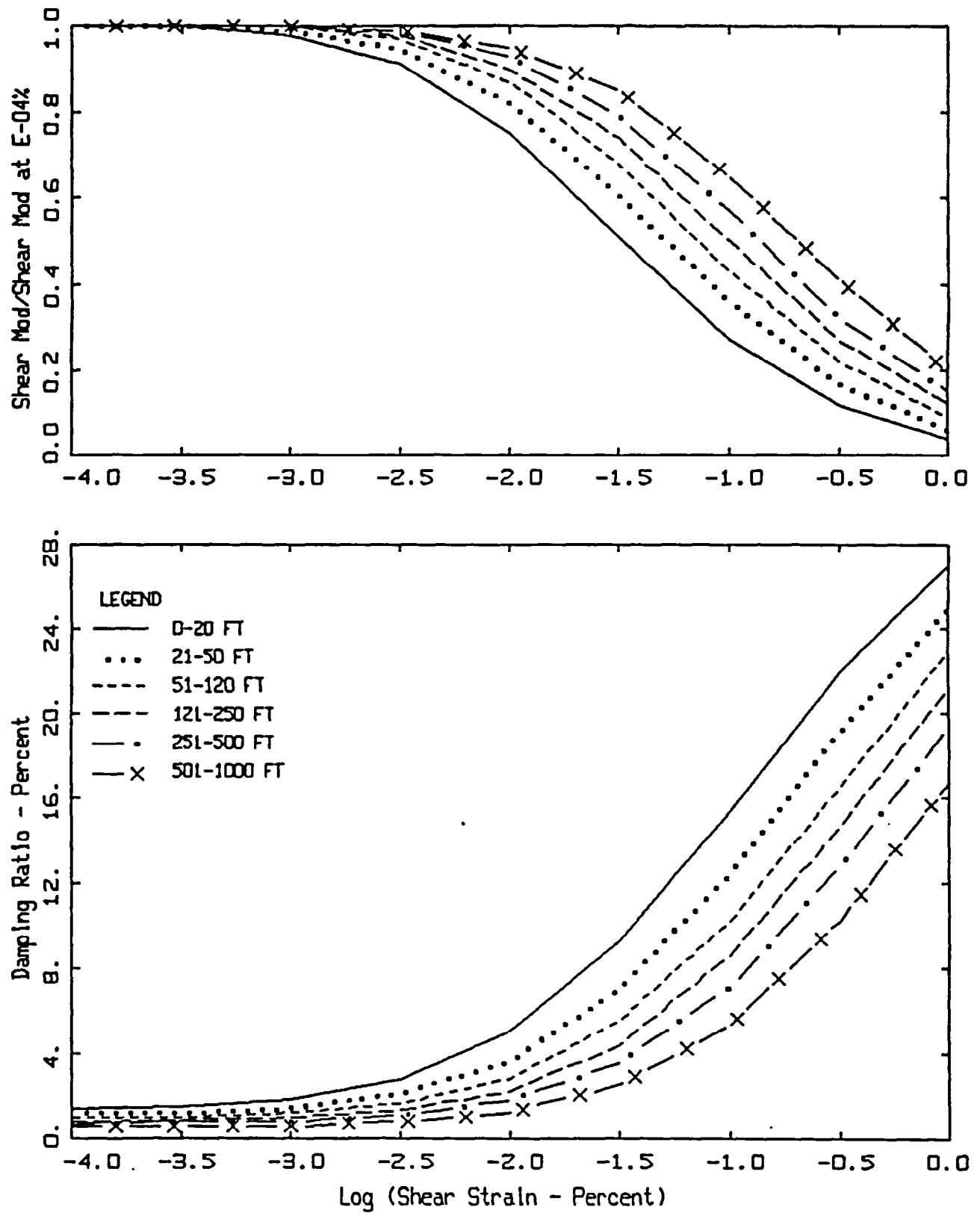
Figure 19. Median and  $\pm 1 \sigma$  shear-wave velocity profiles for the Los Angeles area surface geologic unit Q<sub>y</sub>, Younger Alluvium (Table 1).



### MODULUS REDUCTION AND DAMPING CURVES FOR ROCK

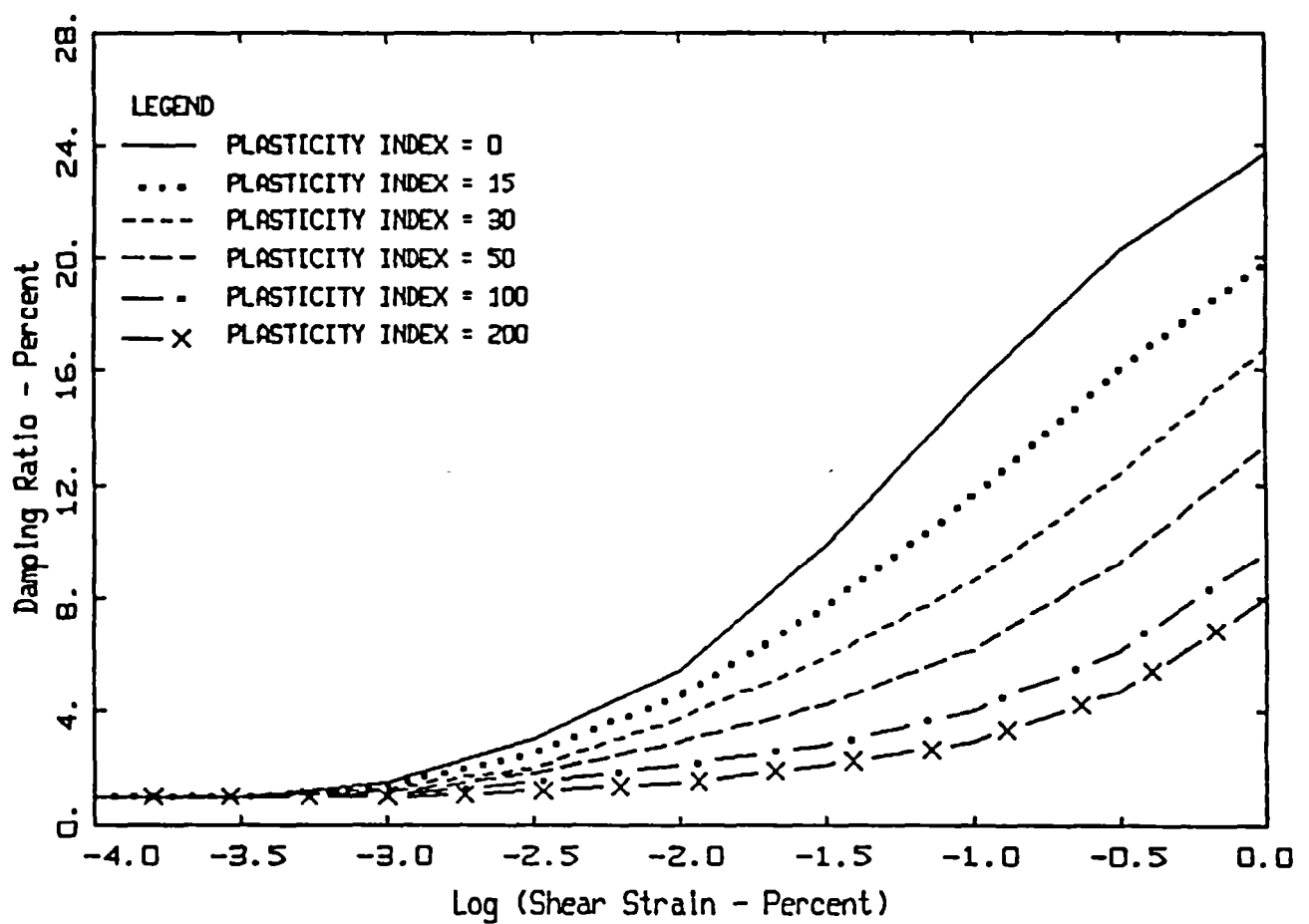
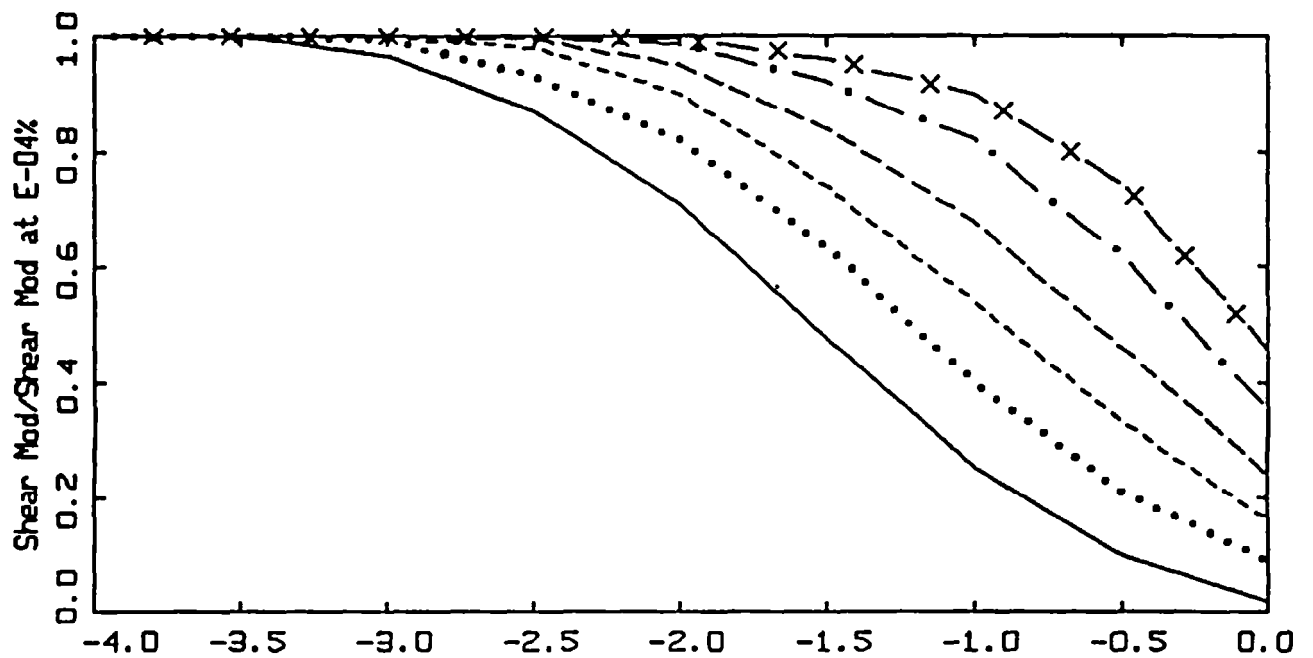
Figure 20. Generic  $G/G_{max}$  and hysteretic damping curves for rock site conditions.





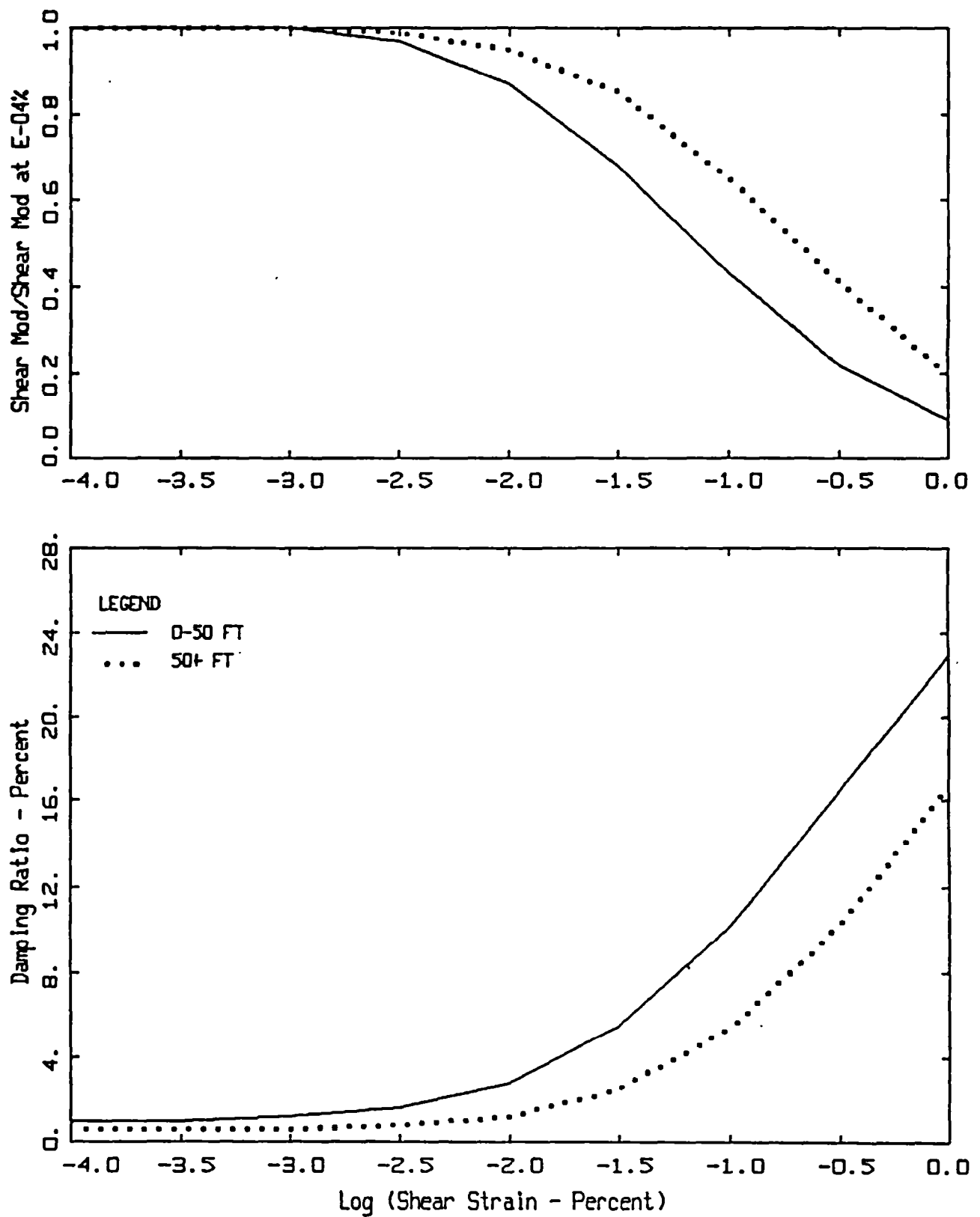
### MODULUS REDUCTION AND DAMPING CURVES FOR SAND

Figure 21. Generic  $G/G_{max}$  and hysteretic damping curves for North Coast cohesionless soil site conditions (EPRI, 1993).



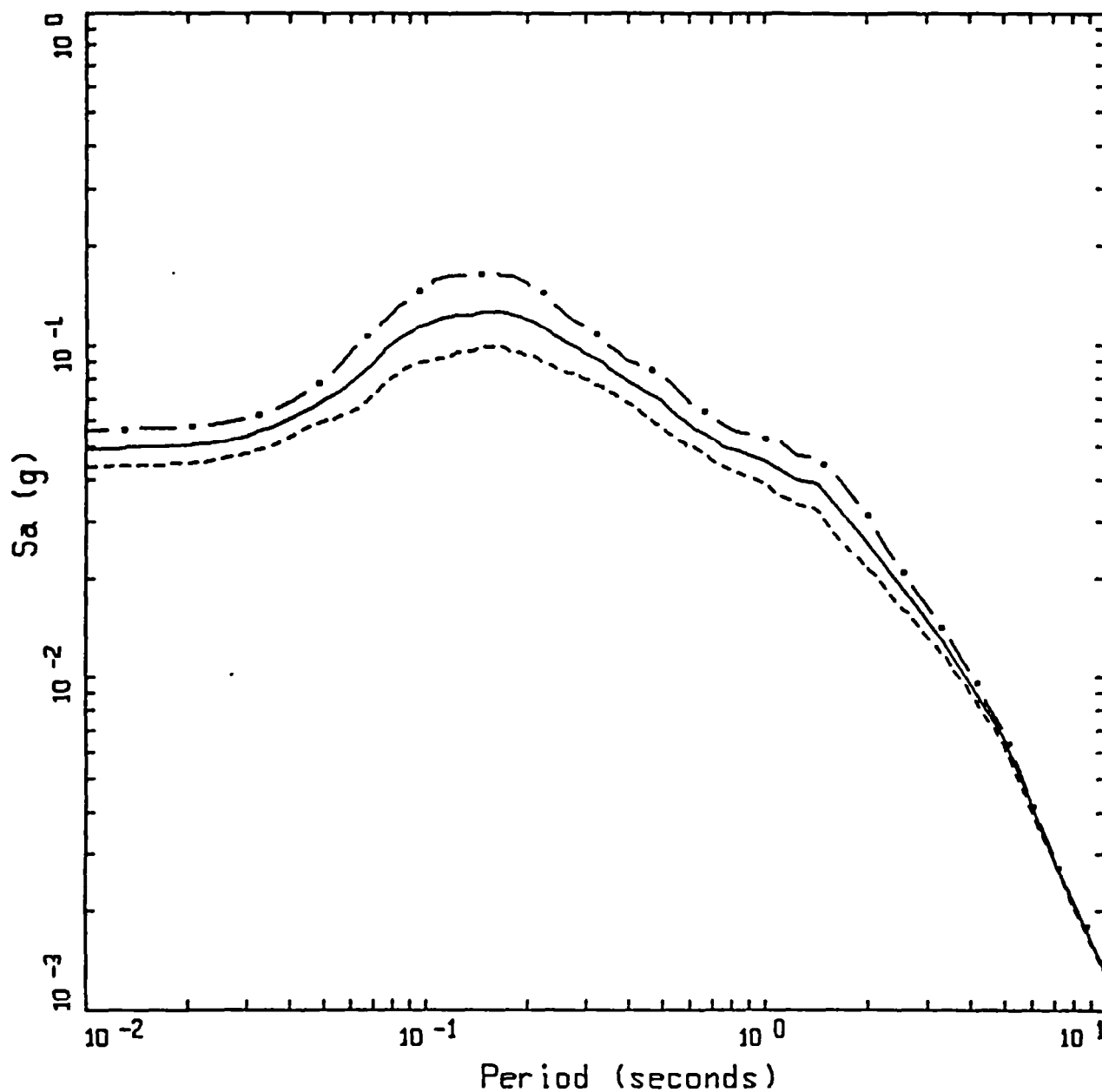
### VUCETIC/DOBRY MODULUS REDUCTION AND DAMPING CURVES

Figure 22. Generic  $G/G_{max}$  and hysteretic damping curves for cohesive soil site conditions (Vucetic and Dobry, 1991).



### MODULUS REDUCTION AND DAMPING CURVES FOR SAND

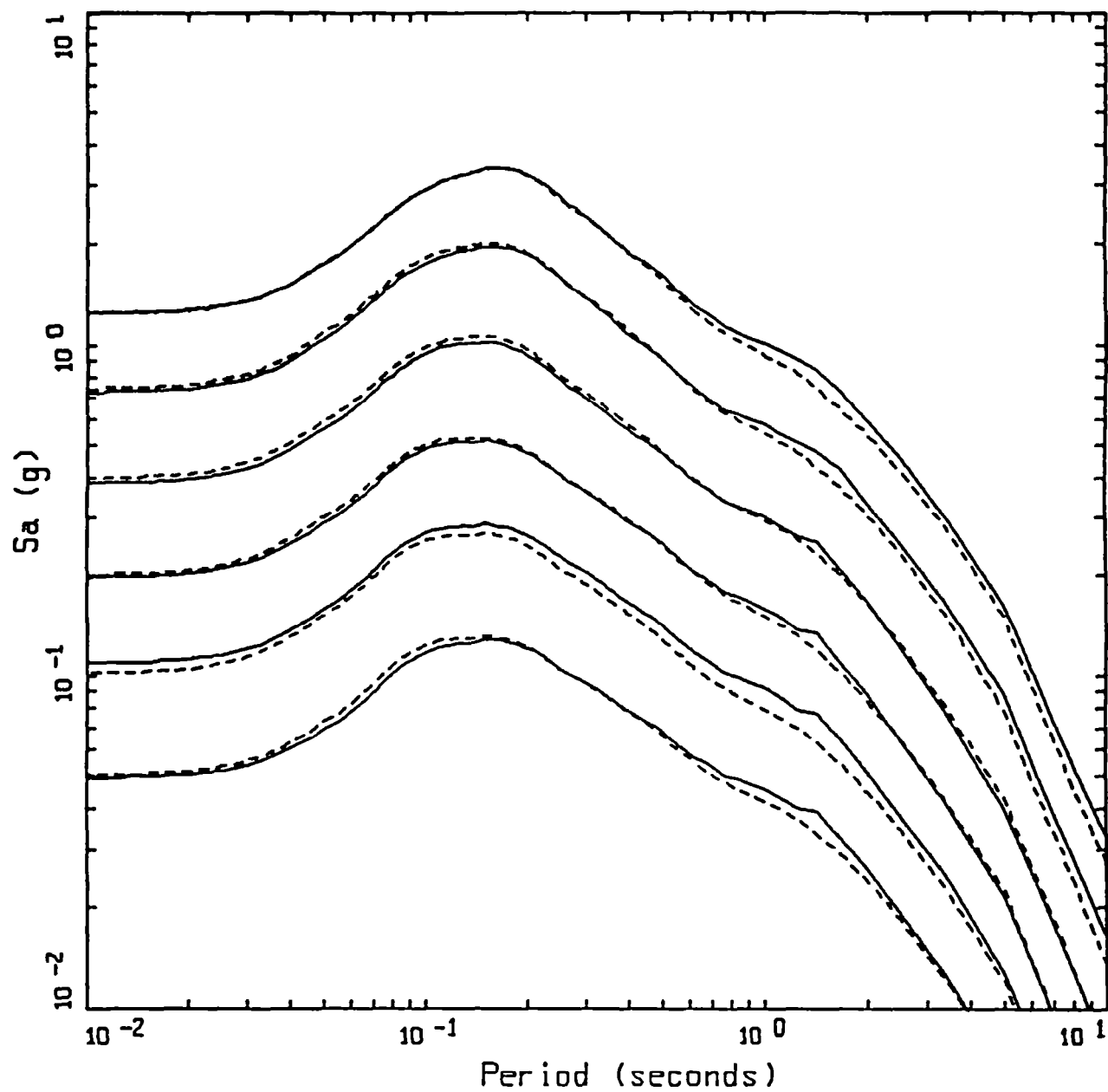
Figure 23. Generic  $G/G_{max}$  and hysteretic damping curves for Peninsular Range cohesionless soil site conditions (Silva et al., 1997).



FRANCISCAN OUTCROP, 0.05 G  
 M 6.5, STRESS DROP = 60 BARS

LEGEND  
 — • — 84TH PERCENTILE, PARAMETRIC UNCERTAINTY; PGA = 0.057 G  
 ——— 50TH PERCENTILE, PARAMETRIC UNCERTAINTY; PGA = 0.050 G  
 - - - - 16TH PERCENTILE, PARAMETRIC UNCERTAINTY; PGA = 0.044 G

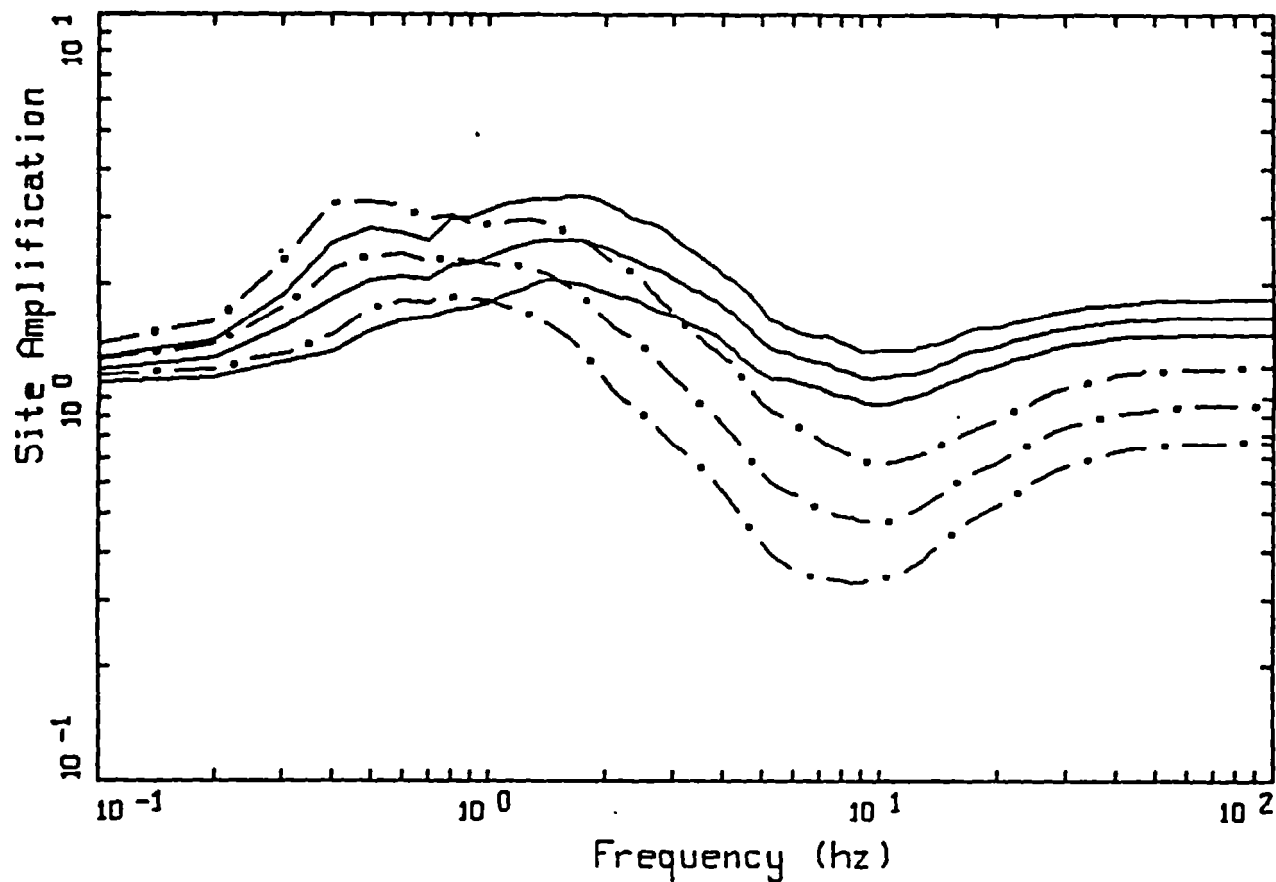
Figure 24. Median and  $\pm 1 \sigma$  5% damped baserock (Franciscan) motions for 5%g (Table 4): M = 6.5, stress drop = 60 bars. Parametric variation includes top 250 ft of the profile (Figure 15) and nonlinear properties (Figure 20).



REFERENCE ROCK OUTCROP  
M 6.5, STRESS DROP = 60 BARS

LEGEND  
— FRANCISCAN OUTCROP  
--- GRANITE OUTCROP

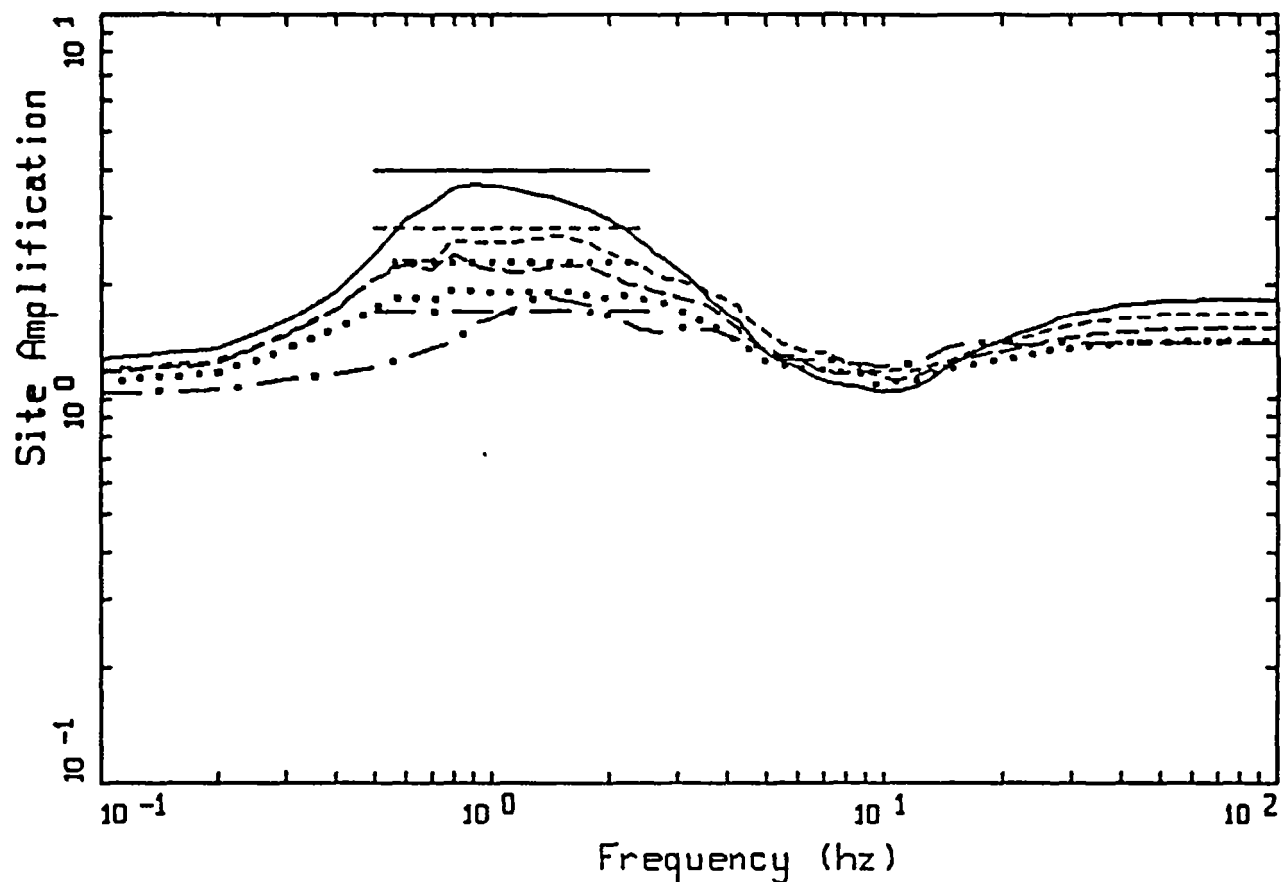
Figure 25. Comparison of median 5% damped response spectra computed for San Francisco (solid) and Los Angeles (dashed) area baserock site conditions for suite of outcrop peak acceleration values (Table 4):  $M=6.5$ , stress drop: 60 bars.



## QAL AMPLIFICATION (D), SF DEPTH RANGE 30 - 1000 FEET

LEGEND	
—	84TH PERCENTILE, REFERENCE FRANCISCAN, 0.05 G
—	50TH PERCENTILE, REFERENCE FRANCISCAN, 0.05 G
—	16TH PERCENTILE, REFERENCE FRANCISCAN, 0.05 G
- - -	84TH PERCENTILE, REFERENCE FRANCISCAN, 0.40 G
- - -	50TH PERCENTILE, REFERENCE FRANCISCAN, 0.40 G
- - -	16TH PERCENTILE, REFERENCE FRANCISCAN, 0.40 G

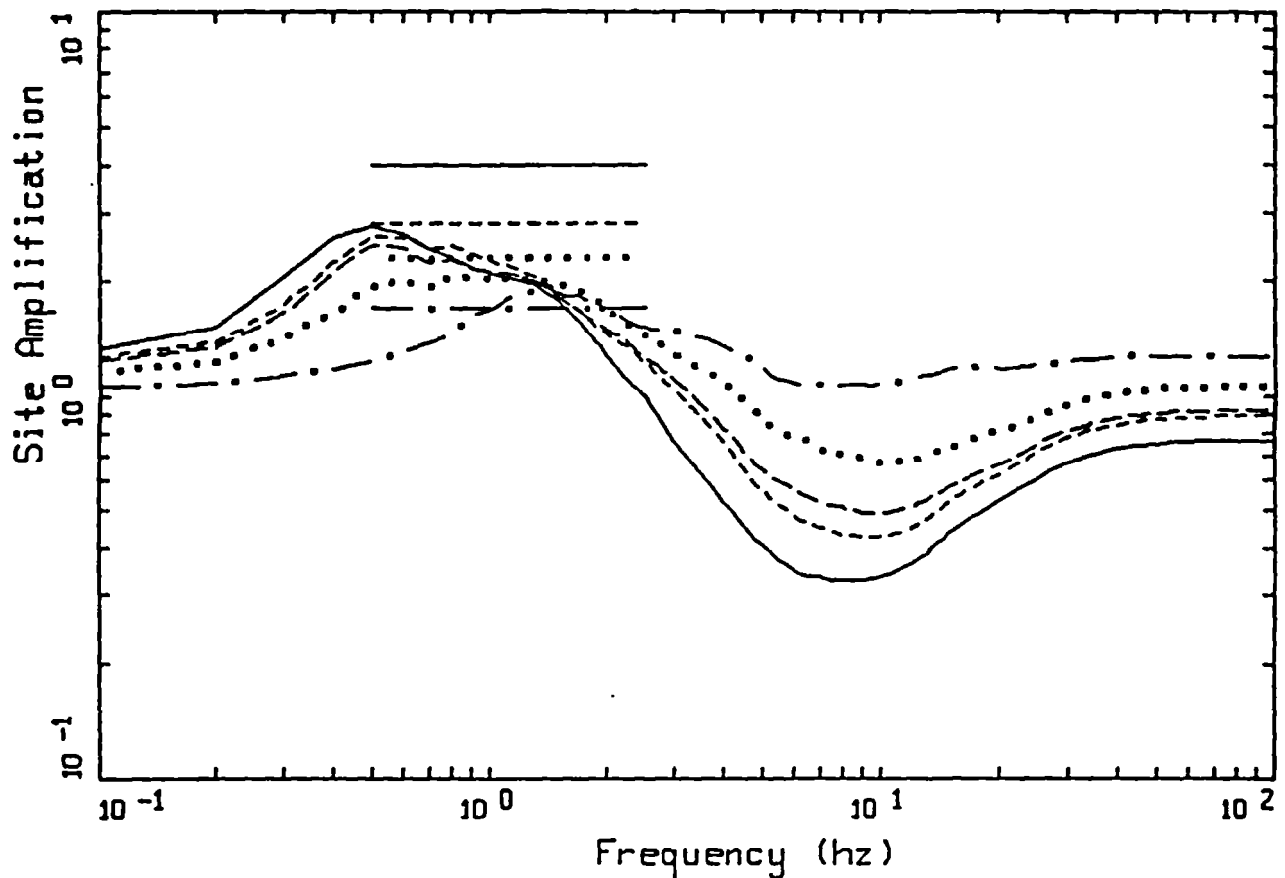
Figure 26. Comparison of median and  $\pm 1 \sigma$  amplification factors (5% damped response spectra) for San Francisco area Quaternary Alluvium ( $Q_u$ ) depth category 4 (30 to 1,000 ft) for reference Franciscan rock outcrop median peak acceleration values of 0.05g and 0.40g.



## AMPLIFICATION: 5% DAMPED RESPONSE SPECTRA REFERENCE FRANCISCAN 0.05 G

LEGEND	
————	BAY MUD, 150-350ft (5% Damped Response Spectra, median)
-----	OAL, 350-650ft (5% Damped Response Spectra, median)
-----	QQA, 350-650ft (5% Damped Response Spectra, median)
.....	QUATERNARY/TERTIARY, 350-650ft (5% Damped Response Spectra, median)
- . - .	TERTIARY (5% Damped Response Spectra, median)
————	BAY MUD (Borcherdt (1992) Empirical Fourier Amplitude Spectra, average)
-----	OAL (Borcherdt (1992) Empirical Fourier Amplitude Spectra, average)
.....	QUATERNARY/TERTIARY (Borcherdt (1992) Empirical Fourier Amplitude Spectra, average)
- . - .	TERTIARY (Borcherdt (1992) Empirical Fourier Amplitude Spectra, average)

Figure 27. Comparison of median amplification factors (5% damped response spectra) computed for reference Franciscan outcrop peak acceleration of 0.05g with empirical factors (smoothed Fourier amplitude spectra; Borcherdt and Glassmoyer, 1992). Empirical factors were computed using low levels of loading (generally  $\leq 0.10g$ ).

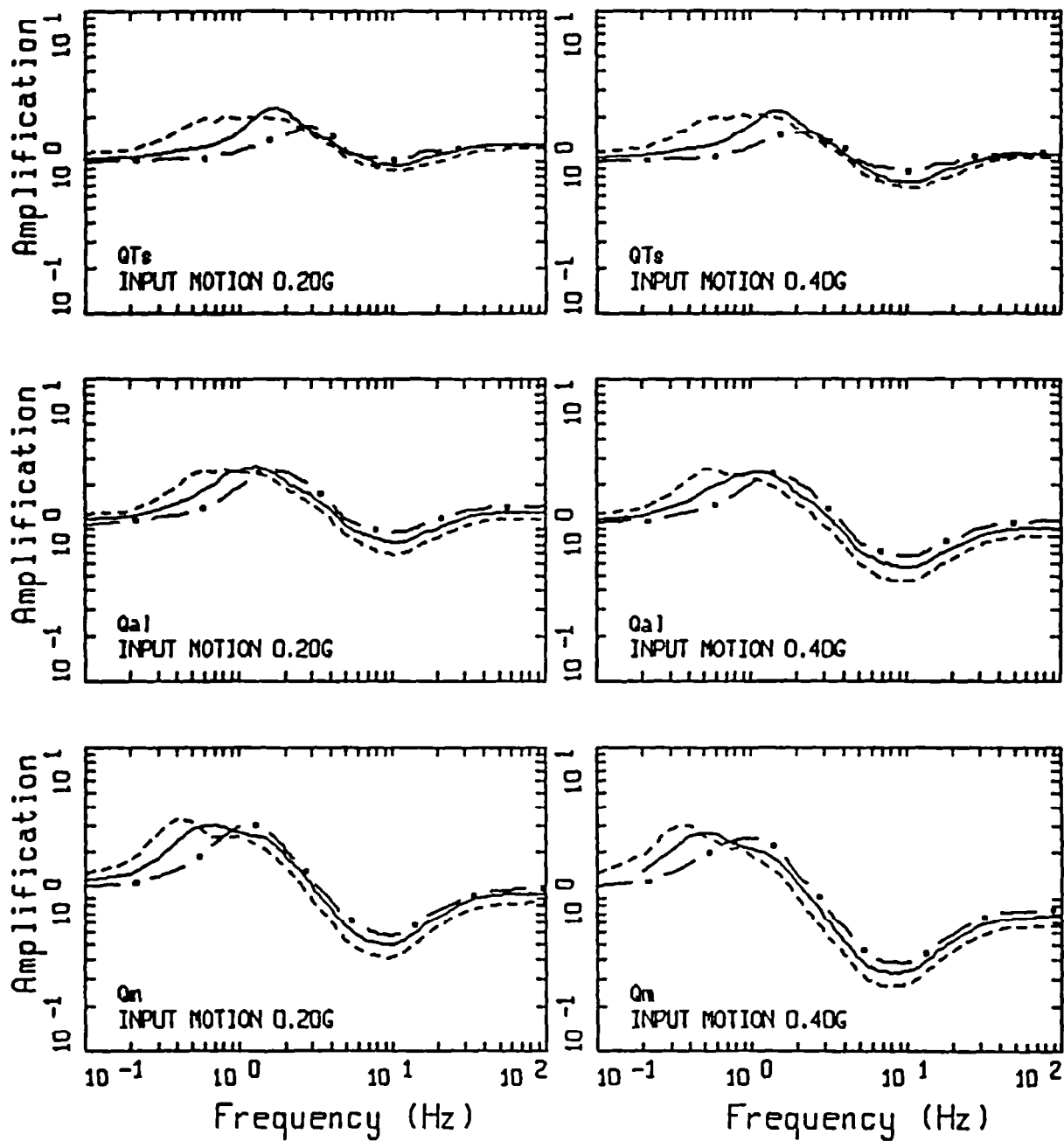


# AMPLIFICATION: 5% DAMPED RESPONSE SPECTRA REFERENCE FRANCISCAN 0.40 G

LEGEND	
————	BAY MUD, 150-350ft (5% Damped Response Spectra, median)
-----	QAL, 350-650ft (5% Damped Response Spectra, median)
-----	QOA, 350-650ft (5% Damped Response Spectra, median)
.....	QUATERNARY/TERTIARY, 350-650ft (5% Damped Response Spectra, median)
- . - .	TERTIARY (5% Damped Response Spectra, median)
————	BAY MUD (Empirical Fourier Amplitude Spectra, average)
-----	QAL (Empirical Fourier Amplitude Spectra, average)
.....	QUATERNARY/TERTIARY (Empirical Fourier Amplitude Spectra, average)
- . - .	TERTIARY (Empirical Fourier Amplitude Spectra, average)

Figure 28. Comparison of median amplification factors (5% damped response spectra) computed for reference Franciscan outcrop peak acceleration of 0.40g with empirical factors (smoothed Fourier amplitude spectra; Borchardt and Glassmoyer, 1992). Empirical factors were computed using low levels of loading (generally  $\leq 0.10g$ ).

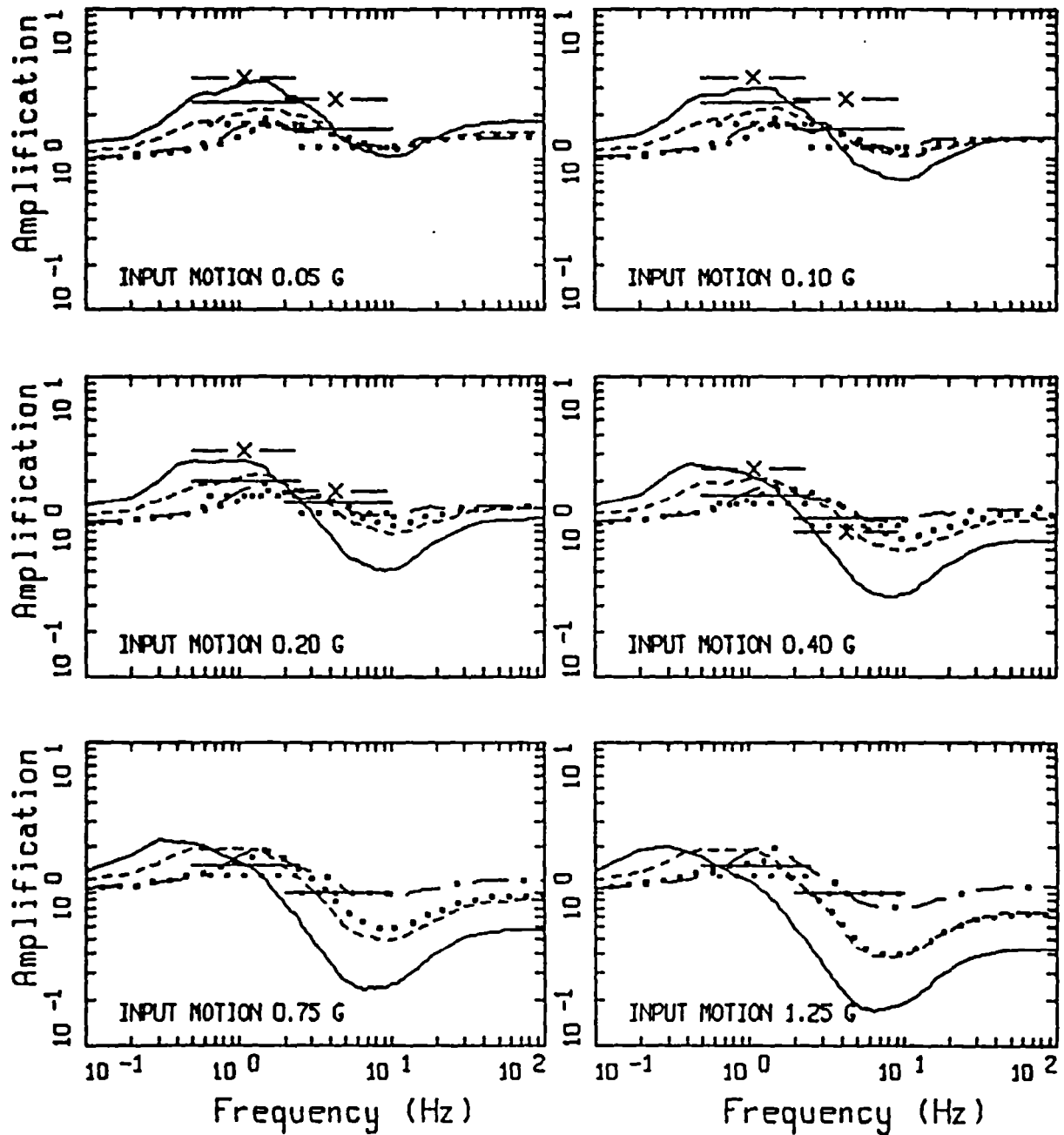




### SF AMPLIFICATION

Figure 29. Median amplification factors computed for  $QT_s$ ,  $Q_{a1}$ ,  $Q_m$  for different depth categories: 30 ft to 150 ft, dash dots; 150 ft to 350 ft, solid; 350 ft to 650 ft, dashes.

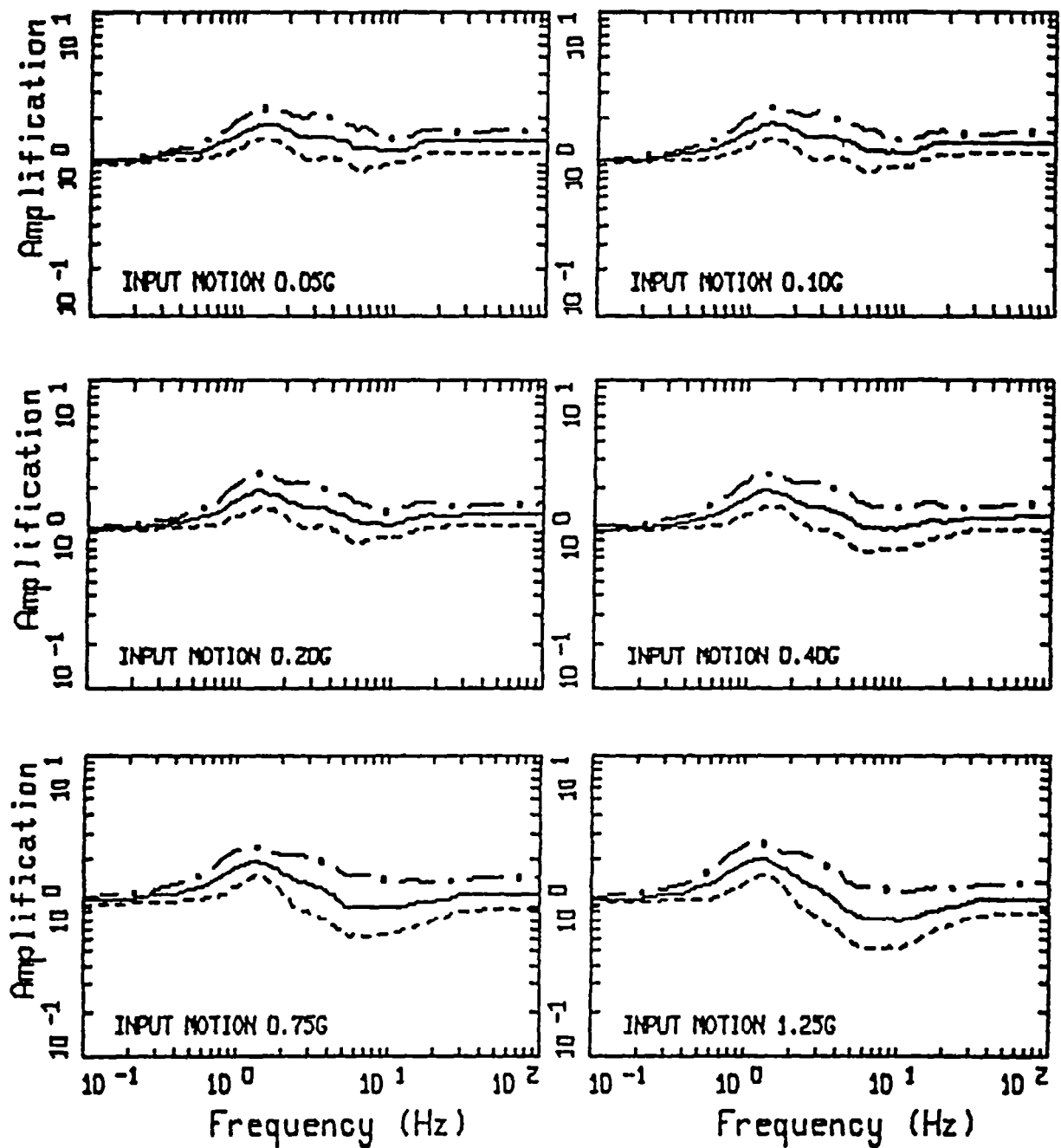
## SF AMPLIFICATION



### LEGEND

- BAY MUD (D), CATEGORY 6 (30-650ft)
- ALLUVIUM (D), CATEGORY 4 (30-1000ft)
- ..... QUATERNARY/TERTIARY (C), CATEGORY 5 (30-450ft)
- · — TERTIARY (C)
- X — E: 0.50-2.5 Hz, 2.0-10.00 Hz (NEHRP, 1994)
- D( $Q_{a1} + Q_{a2} + Q_n$ ): 0.50-2.5 Hz, 2.0-10.00 Hz (NEHRP, 1994)
- ..... C( $T_{Mz} + Q_{Ts}$ ): 0.50-2.5 Hz, 2.0-10.00 Hz (NEHRP, 1994)

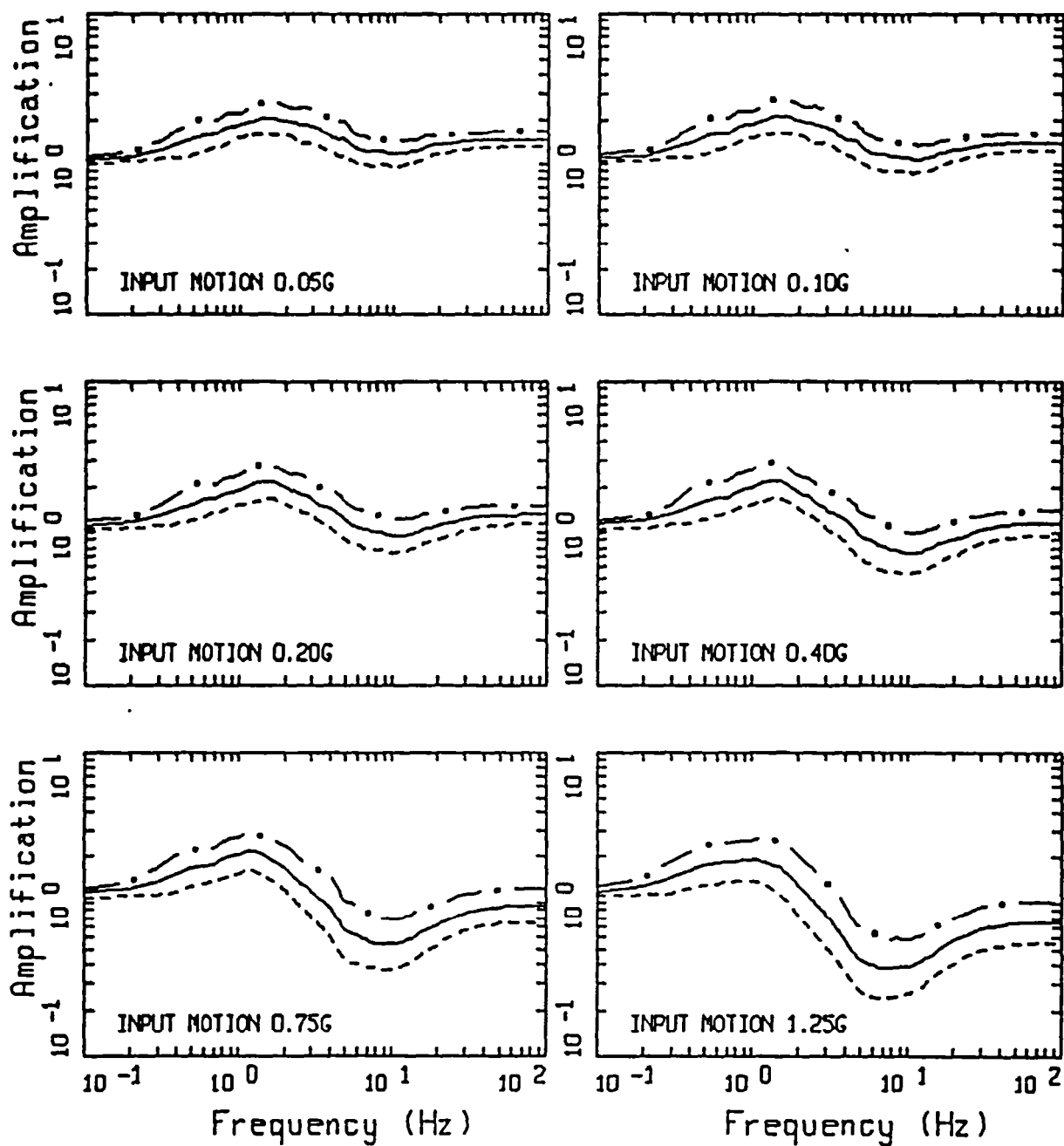
Figure 30. Comparison of median amplification factors with NEHRP provisions.



SF AMPLIFICATION

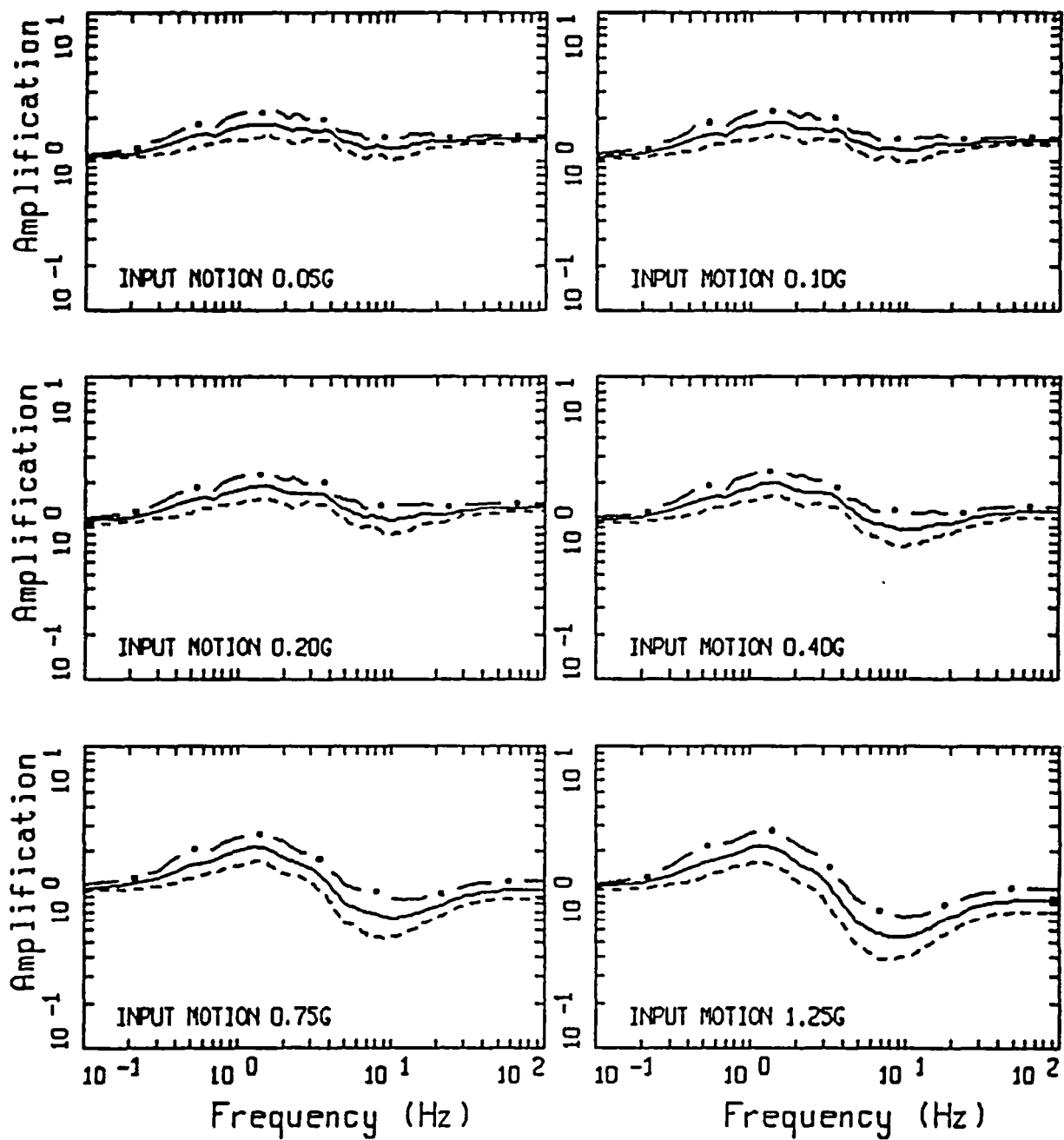
TMzs

Figure 31. Median and  $\pm 1 \sigma$  amplification factors computed for San Francisco area surficial geologic unit TM<sub>zs</sub> (Table 1).



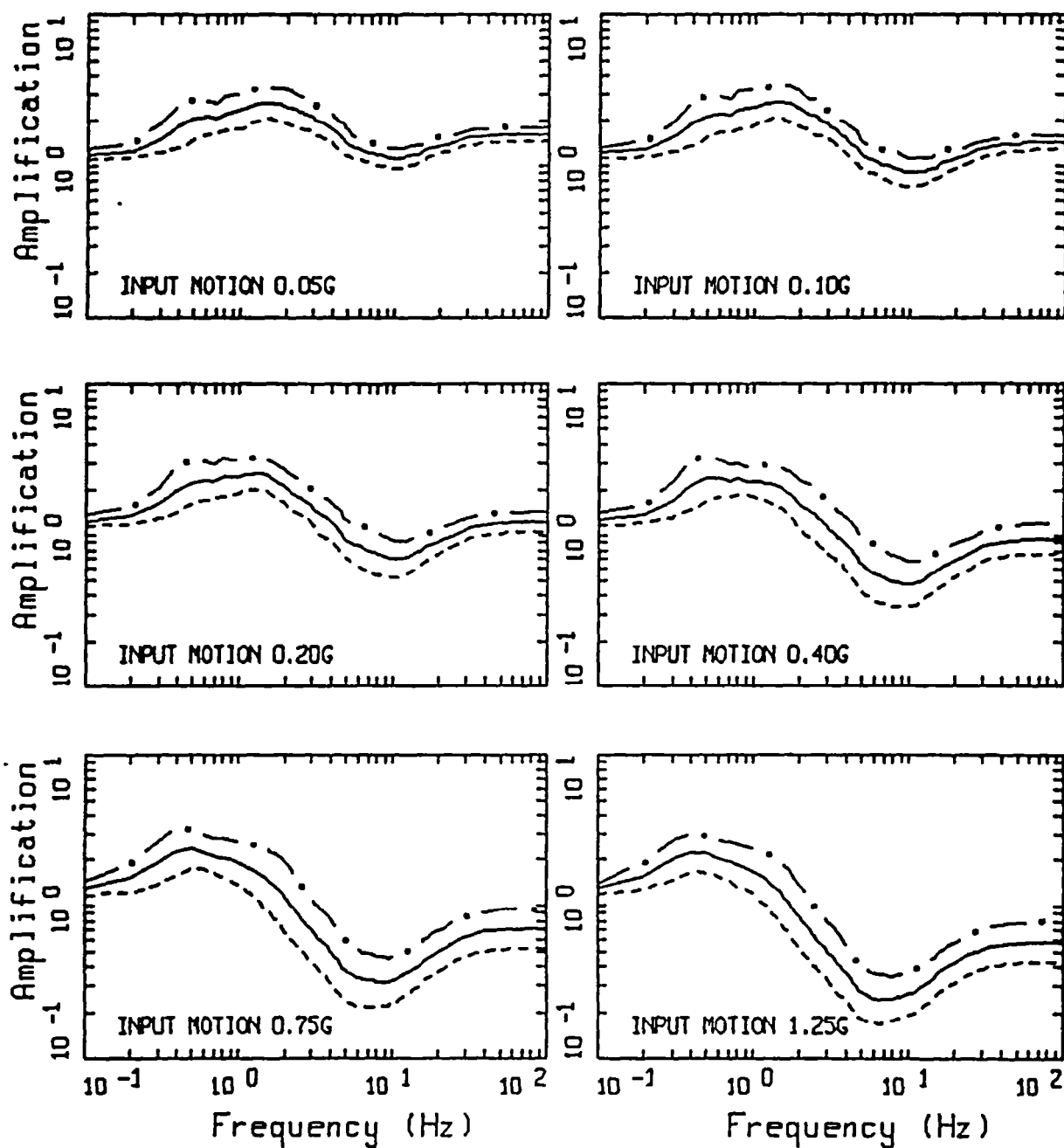
SF AMPLIFICATION  
 QT<sub>s</sub> (30 - 650 ft)

Figure 32. Median and  $\pm 1\sigma$  amplification factors computed for San Francisco area surficial geologic unit QT<sub>s</sub> (Table 1).



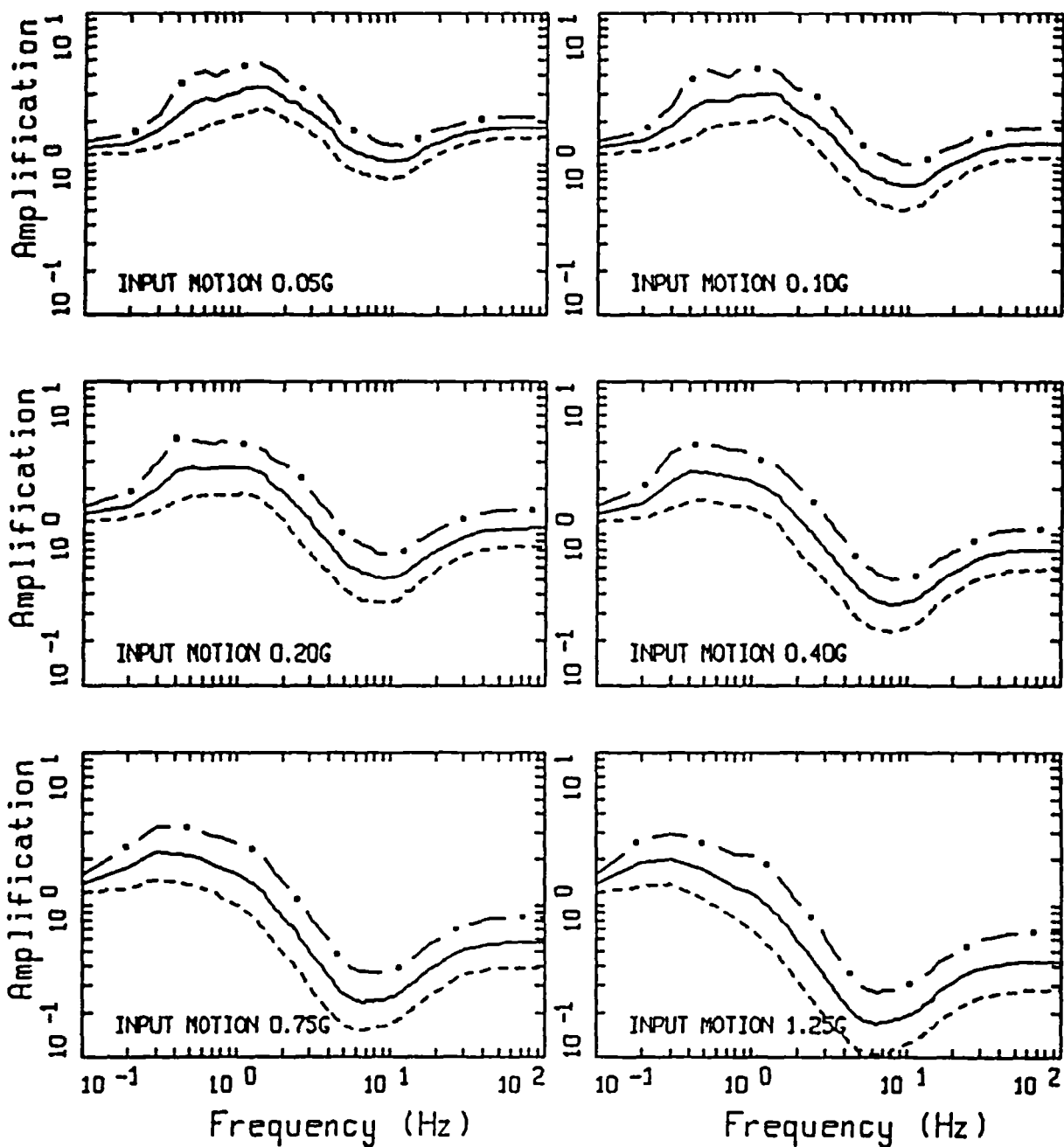
SF AMPLIFICATION  
QOA (30 - 1000 ft)

Figure 33. Median and  $\pm 1\sigma$  amplification factors computed for San Francisco area surficial geologic unit  $Q_{oa}$  (Table 1).



SF AMPLIFICATION  
QAL (30 - 1000 ft)

Figure 34. Median and  $\pm 1\sigma$  amplification factors computed for San Francisco area surficial geologic unit  $Q_{AL}$  (Table 1).

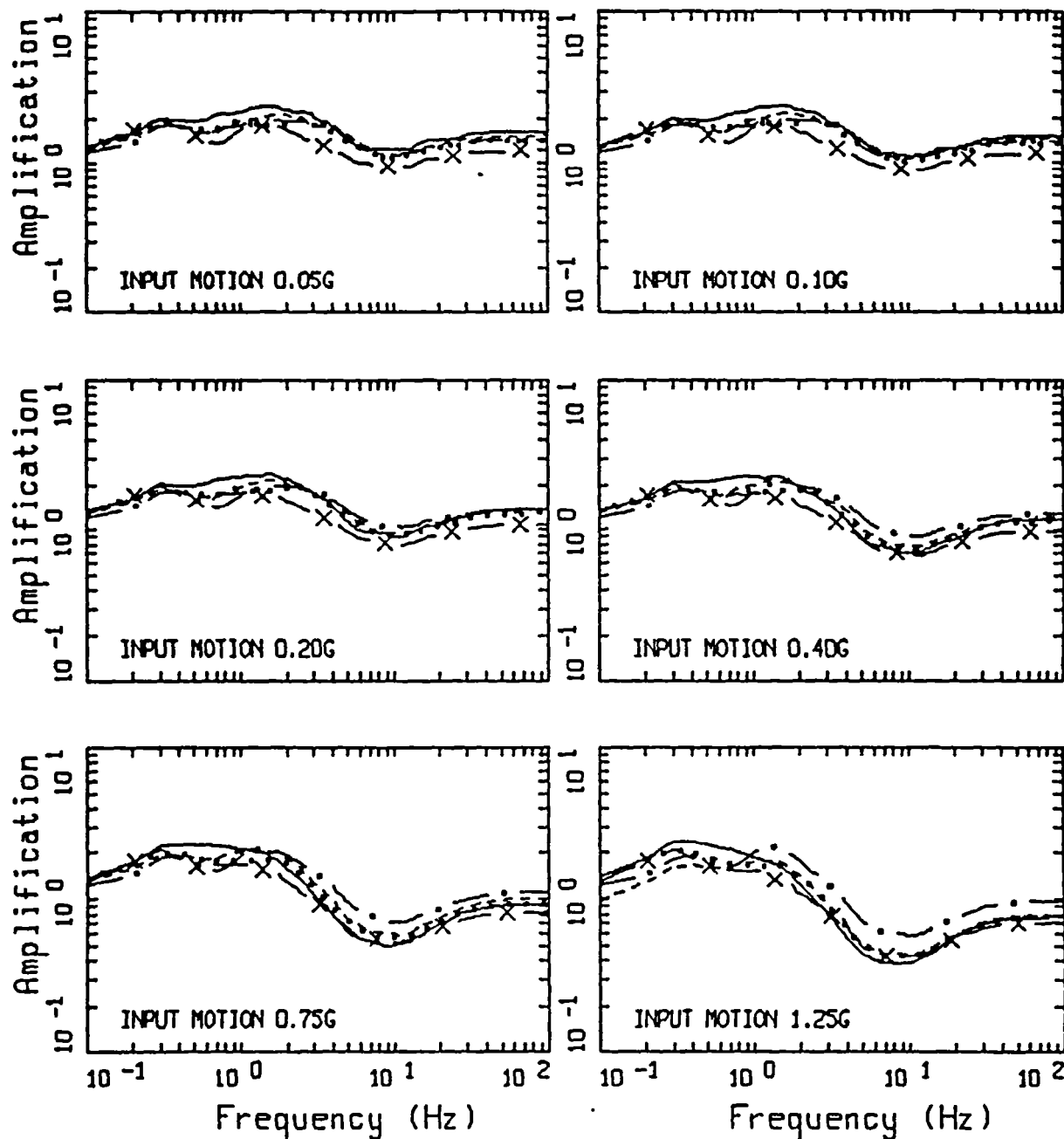


SF AMPLIFICATION

$Q_m$  (30 - 650 ft)

Figure 35. Median and  $\pm 1 \sigma$  amplification factors computed for San Francisco area surficial geologic unit  $Q_m$  (Table 1).

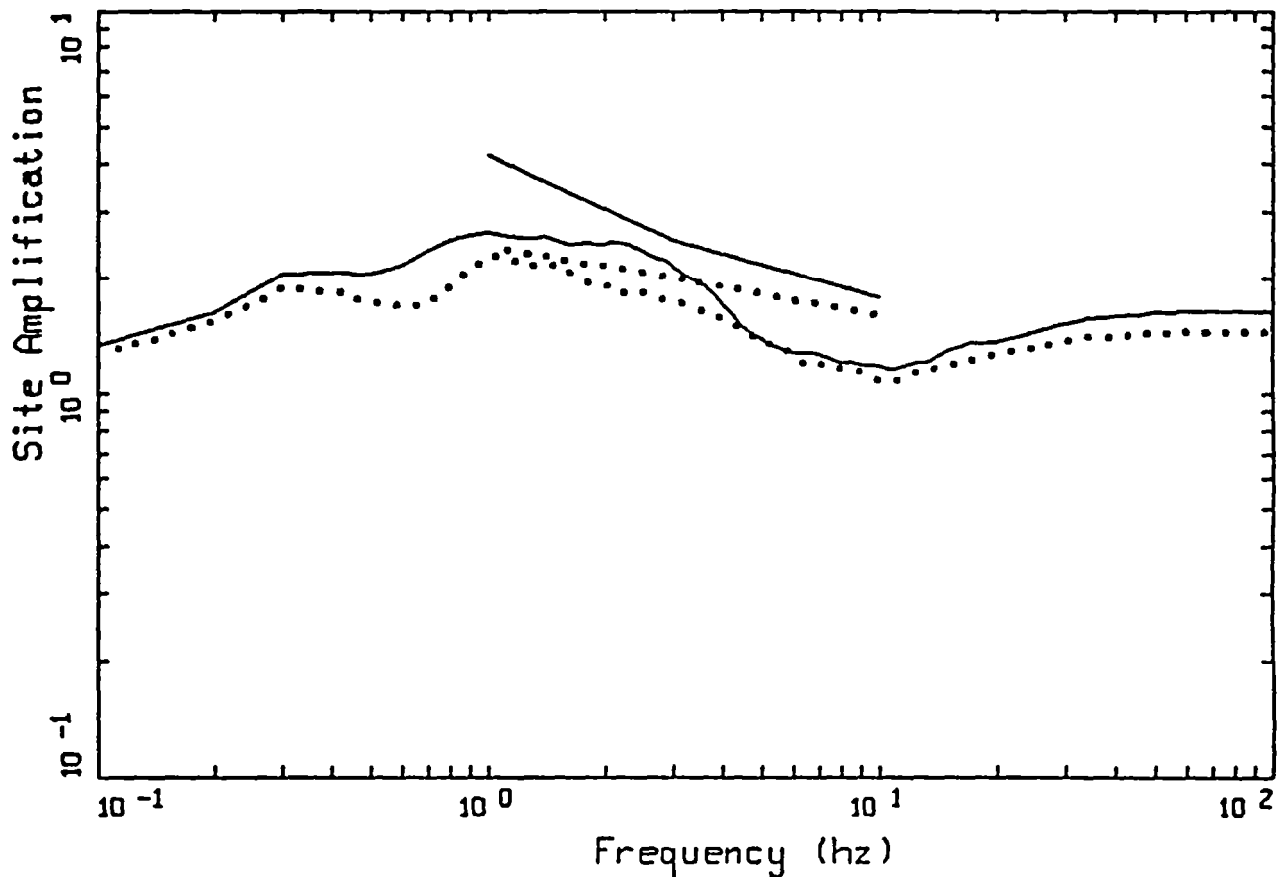
# LA AMPLIFICATION



- LEGEND
- QUATERNARY ALLUVIUM, CATEGORY 4 (30-1000ft)
  - OLD ALLUVIUM, CATEGORY 4 (30-1000ft)
  - X — SAUGUS, CATEGORY 4 (30-1000ft)
  - ..... OLD ALLUVIUM + TERTIARY, CATEGORY 4 (30-1000ft)
  - - - TERTIARY

Figure 36. Comparison of median amplification factors computed for units  $Q_u$ ,  $Q_o$ , Saugus ( $T_s$ ),  $T_s$ , and  $Q_o + T_s$  (Table 1) for the depth categories with the widest depth ranges (Table 5).

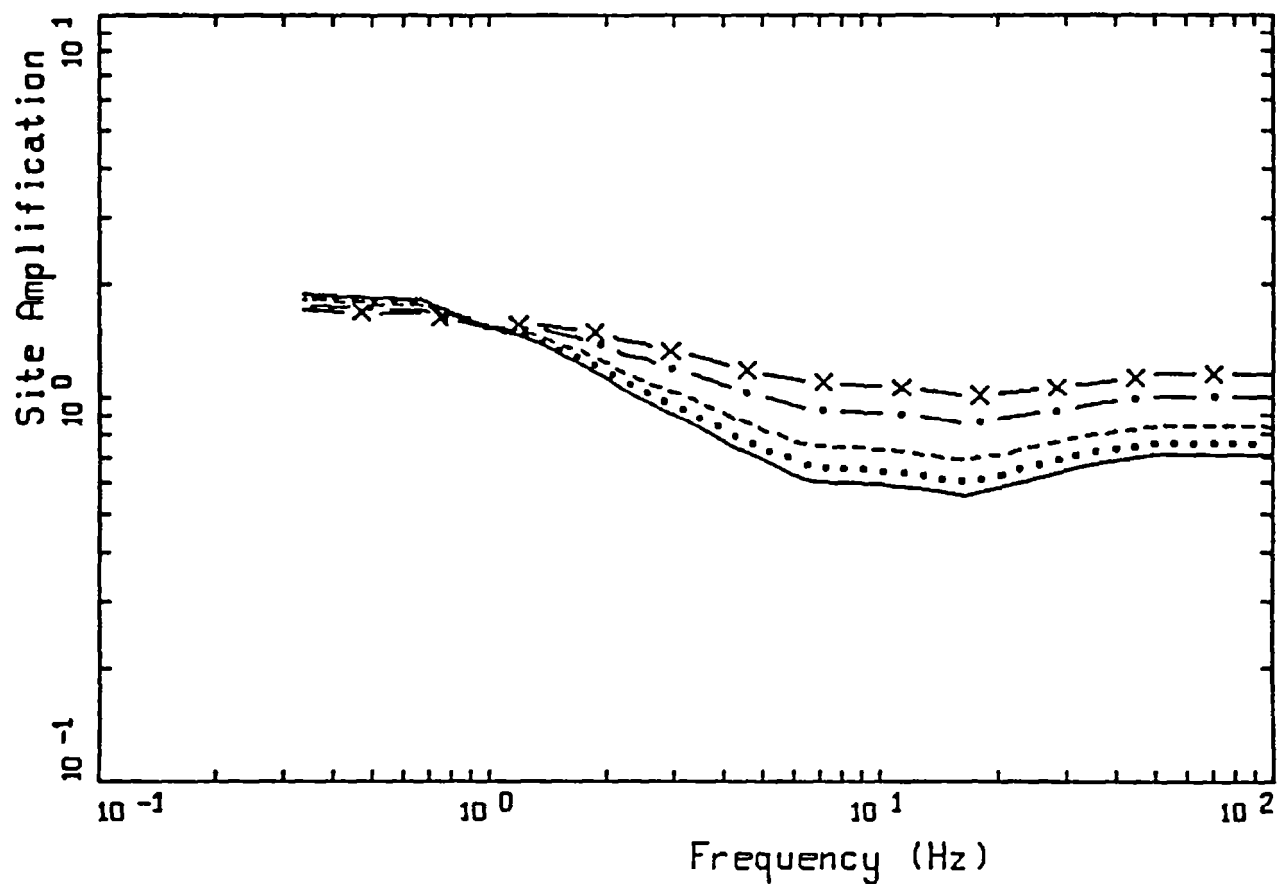




AMPLIFICATION: 5% DAMPED RESPONSE SPECTRA  
REFERENCE GRANITE 0.05 G

LEGEND	
————	Q <sub>y</sub> , 350-650ft (5% Damped Response Spectra, median)
.....	QUATERNARY(Q <sub>o</sub> )+TERTIARY(T <sub>s</sub> ) 350-650ft (5% Damped Response Spectra, median)
————	Q <sub>y</sub> (D) (Bonilla et al (1997) Empirical Fourier Amplitude Spectra, average)
.....	Q <sub>o</sub> +T <sub>s</sub> (C) (Bonilla et al (1997) Empirical Fourier Amplitude Spectra, average)

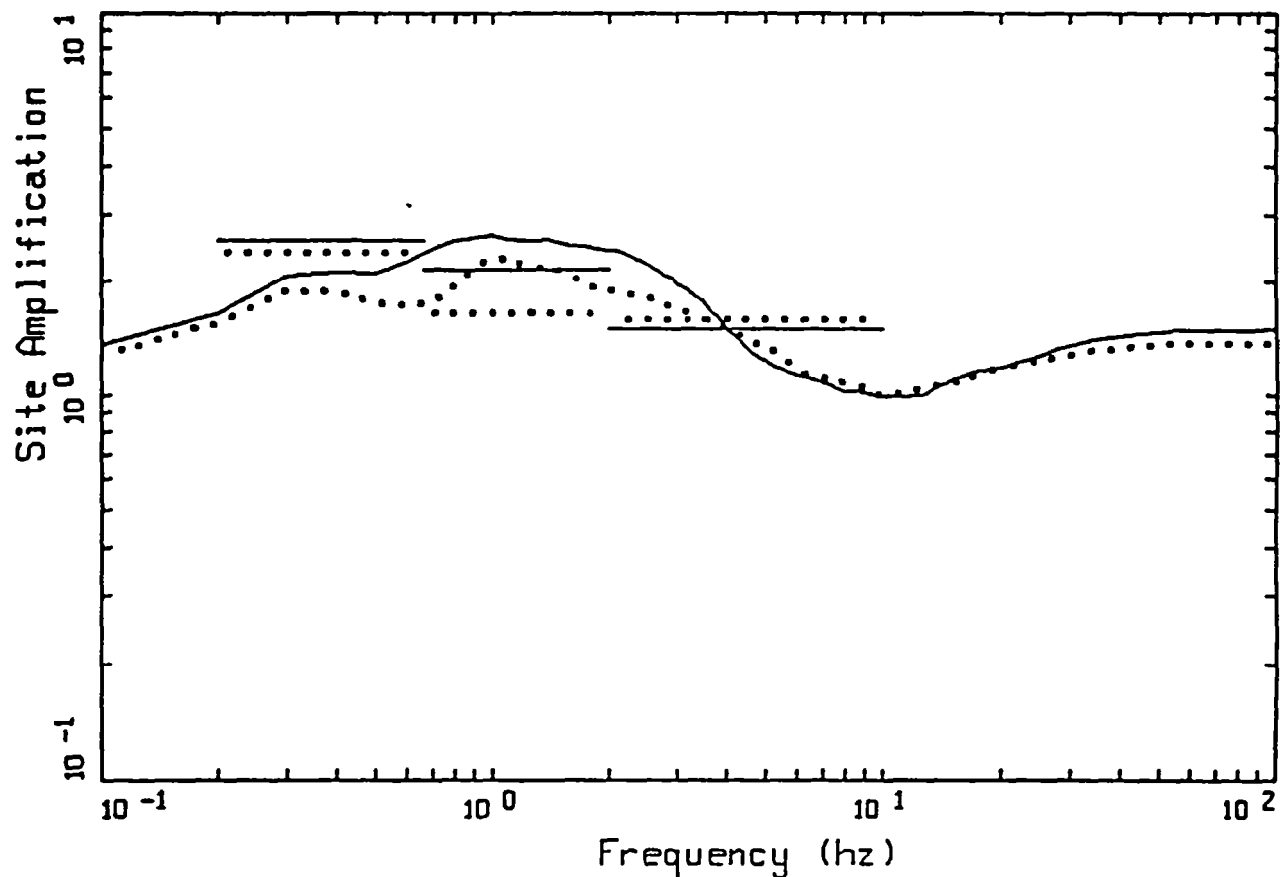
Figure 37. Comparison of median amplification factors (5% damped response spectra) computed for reference Granite outcrop peak acceleration of 0.05g with empirical factors (smoothed Fourier amplitude spectra; Bonilla et al., 1997). Empirical factors are based on small earthquakes.



### WNA EMPIRICAL M6.5 SOIL OVER ROCK

LEGEND	
————	D = 1.0 KM, ROCK PGA = 0.715 g
.....	D = 5.0 KM, ROCK PGA = 0.523 g
-----	D = 10.0 KM, ROCK PGA = 0.324 g
— • —	D = 25.0 KM, ROCK PGA = 0.131 g
— x —	D = 50.0 KM, ROCK PGA = 0.061 g

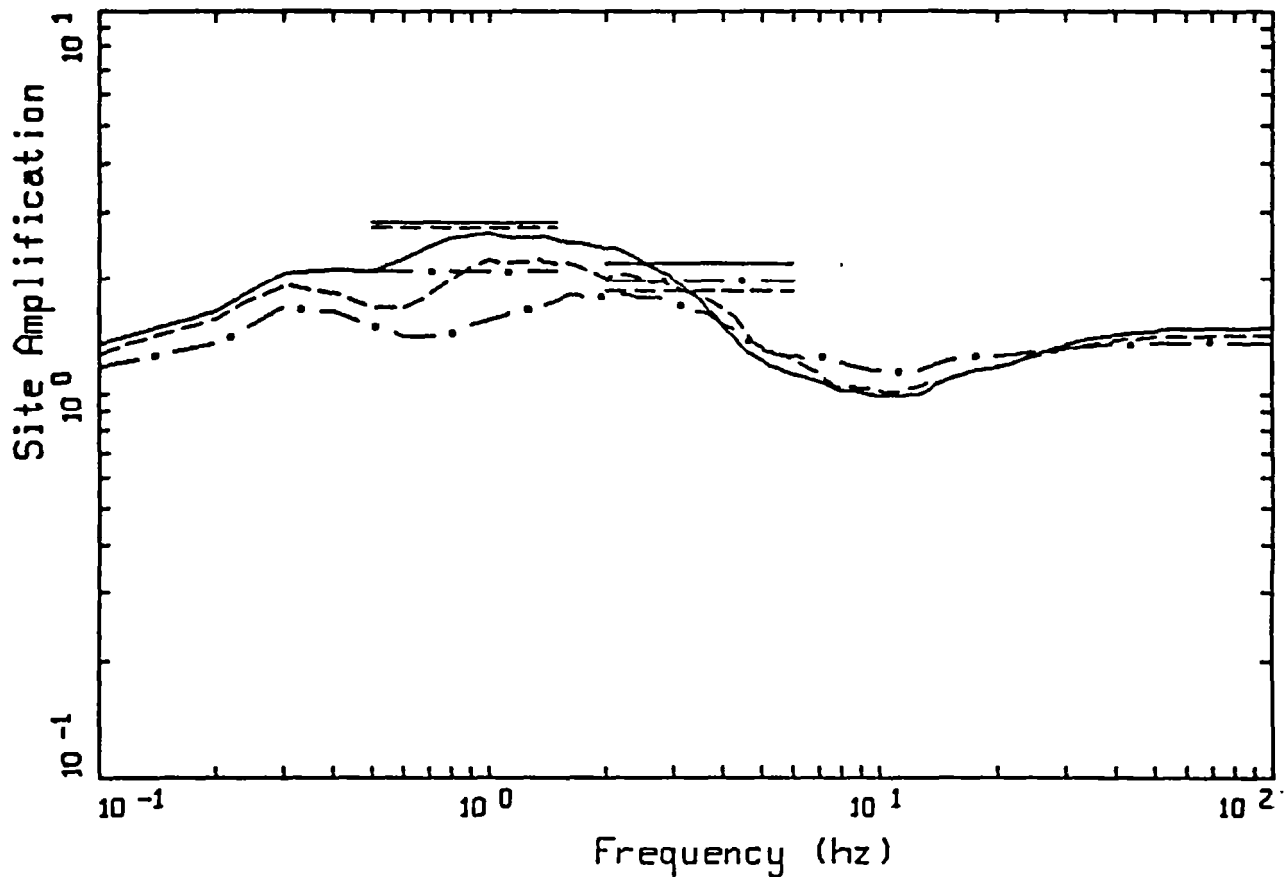
Figure 38. Deep firm to stiff soil (Geomatrix C + D, Table 2) amplification of 5% damped response spectra relative to soft rock (Geomatrix A + B) from an empirical attenuation relation (Abrahamson and Silva, 1997).



AMPLIFICATION: 5% DAMPED RESPONSE SPECTRA  
REFERENCE GRANITE 0.10 G

LEGEND	
————	Q <sub>y</sub> , Category 3 (350-650 ft)
.....	Q <sub>0</sub> +T <sub>s</sub> , Category 3 (350-650 ft)
————	Q <sub>y</sub> (D): 2-10 Hz (Borcherdt (1996) Empirical 5% Damped Response Spectra, average)
————	Q <sub>y</sub> (D): 0.67-2.0 Hz
————	Q <sub>y</sub> (D): 0.2-0.67 Hz
.....	Q <sub>0</sub> +T <sub>s</sub> (C): 2.0-10.0 Hz
.....	Q <sub>0</sub> +T <sub>s</sub> (C): 0.67-2.0 Hz
.....	Q <sub>0</sub> +T <sub>s</sub> (C): 0.2-0.67 Hz

Figure 39. Comparison of median amplification factors (5% damped response spectra) computed for reference Granite outcrop peak acceleration of 0.10g with empirical factors (5% damped response spectra; Borcherdt, 1996). Empirical factors are based on recordings of the 1994 M 6.7 Northridge.



# AMPLIFICATION: 5% DAMPED RESPONSE SPECTRA REFERENCE GRANITE 0.10 G

LEGEND	
————	Q <sub>y</sub> , Category 3 (350-650ft) (5% Damped Response Spectra, median)
-----	Q <sub>o</sub> , Category 3 (350-650ft) (5% Damped Response Spectra, median)
- . - -	T <sub>s</sub> (5% Damped Response Spectra, median)
————	Q <sub>y</sub> (D): 0.5-1.5 Hz (Harmsen (1997): Empirical Fourier Amplitude Spectra, average)
-----	Q <sub>o</sub> (C): 0.5-1.5 Hz
- . - -	T <sub>s</sub> (C): 0.5 - 1.5 Hz
————	Q <sub>y</sub> (D): 2.0-6.0 Hz (Harmsen (1997): Empirical Fourier Amplitude Spectra, average)
-----	Q <sub>o</sub> (C): 2.0-6.0 Hz
- . - -	T <sub>s</sub> (C): 2.0-6.0 Hz

Figure 40. Comparison of median amplification factors (5% damped response spectra) computed for reference Granite outcrop peak acceleration of 0.10g with empirical factors (smoothed Fourier amplitude spectra; Harmsen, 1997). Empirical factors are based on the 1971 San Fernando, 1987 Whittier Narrows, 1991 Sierra Madre, and 1994 Northridge earthquakes.

## LA AMPLIFICATION

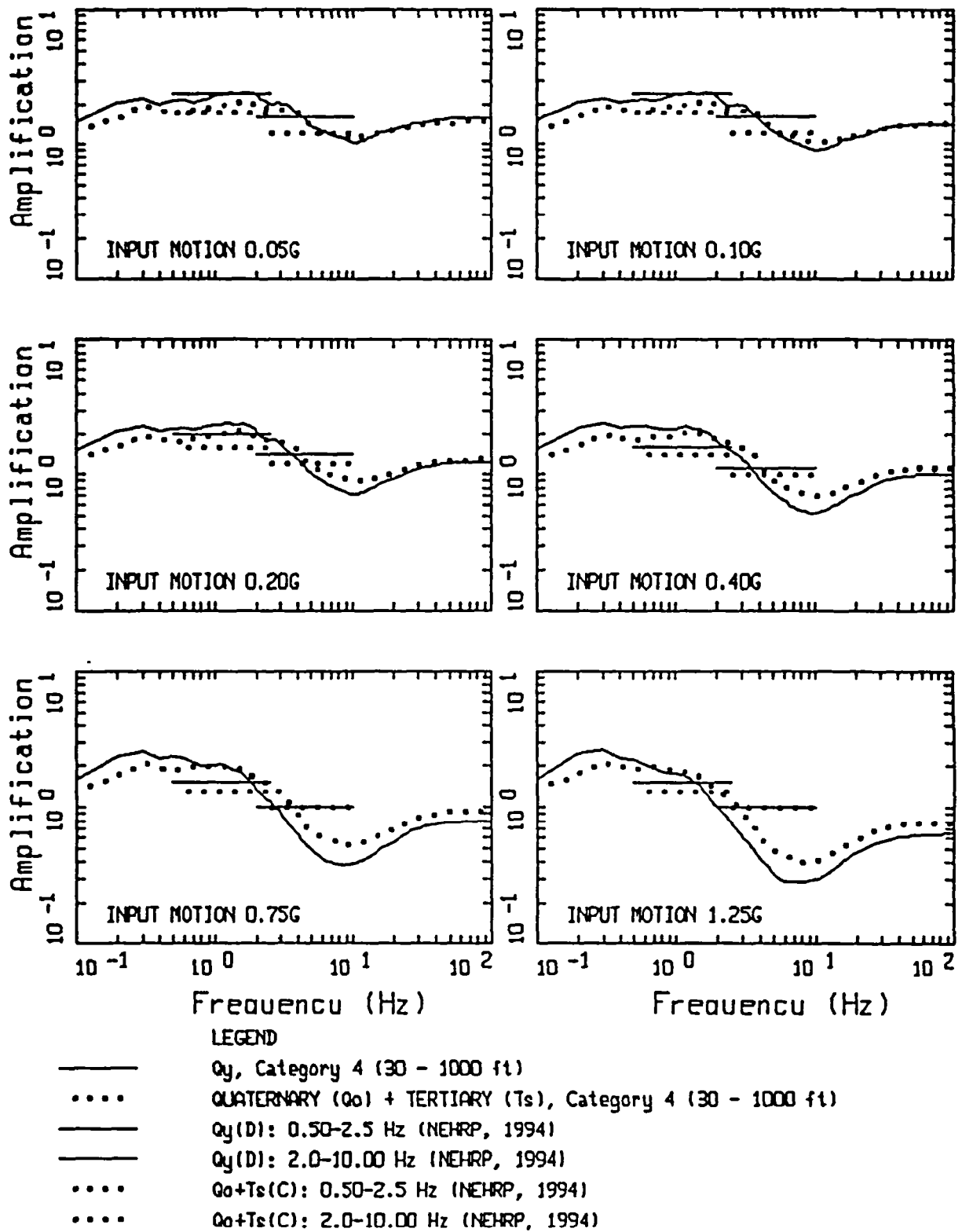
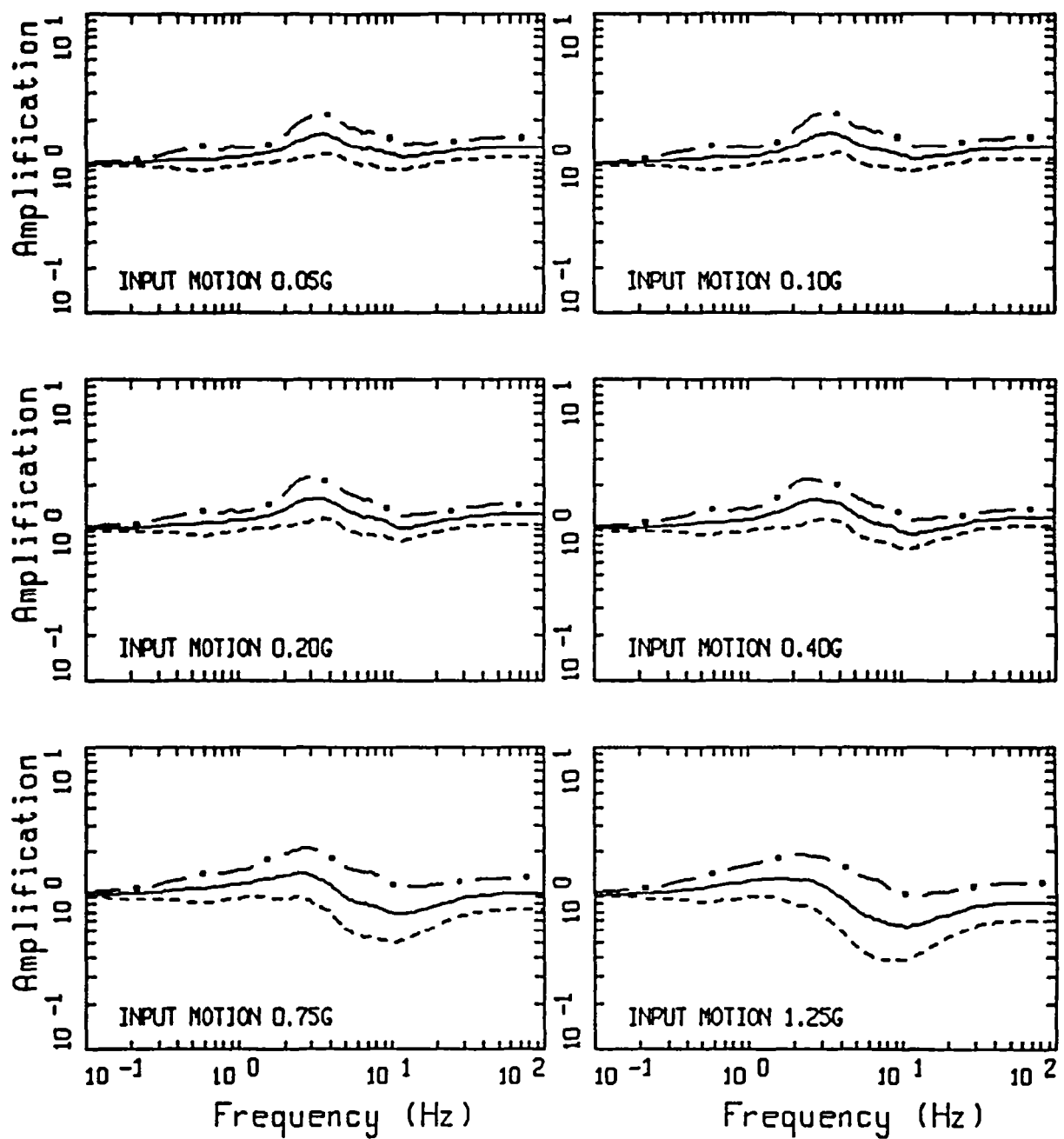
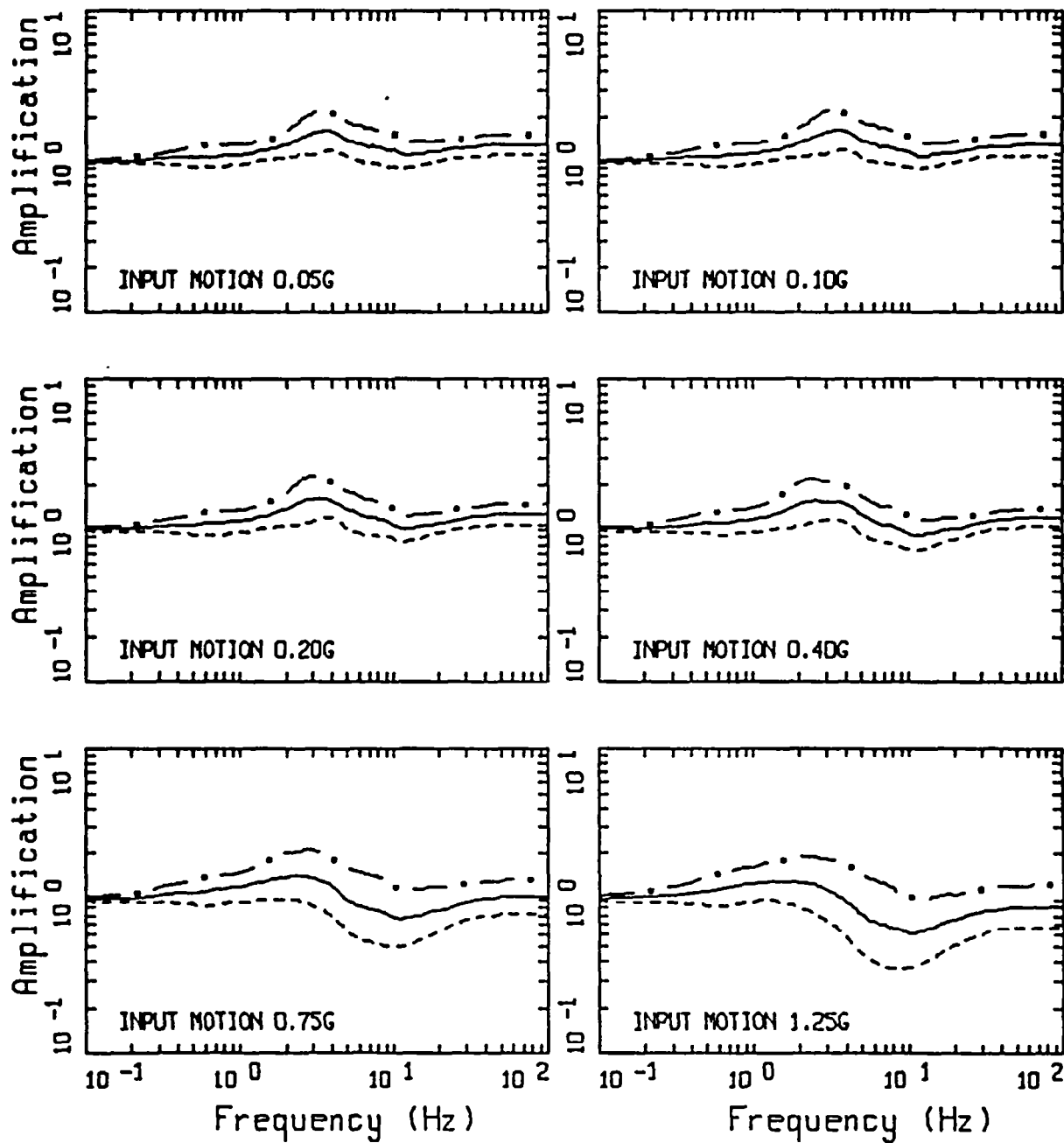


Figure 41. Comparison of median amplification factors with NEHRP provisions.



SF AMPLIFICATION  
GEOMATRIX CLASS A & B

Figure 42. Amplification factors computed for Geomatrix site categories A and B (Figure 6, Table 2) relative to San Francisco area reference rock outcrop Franciscan.



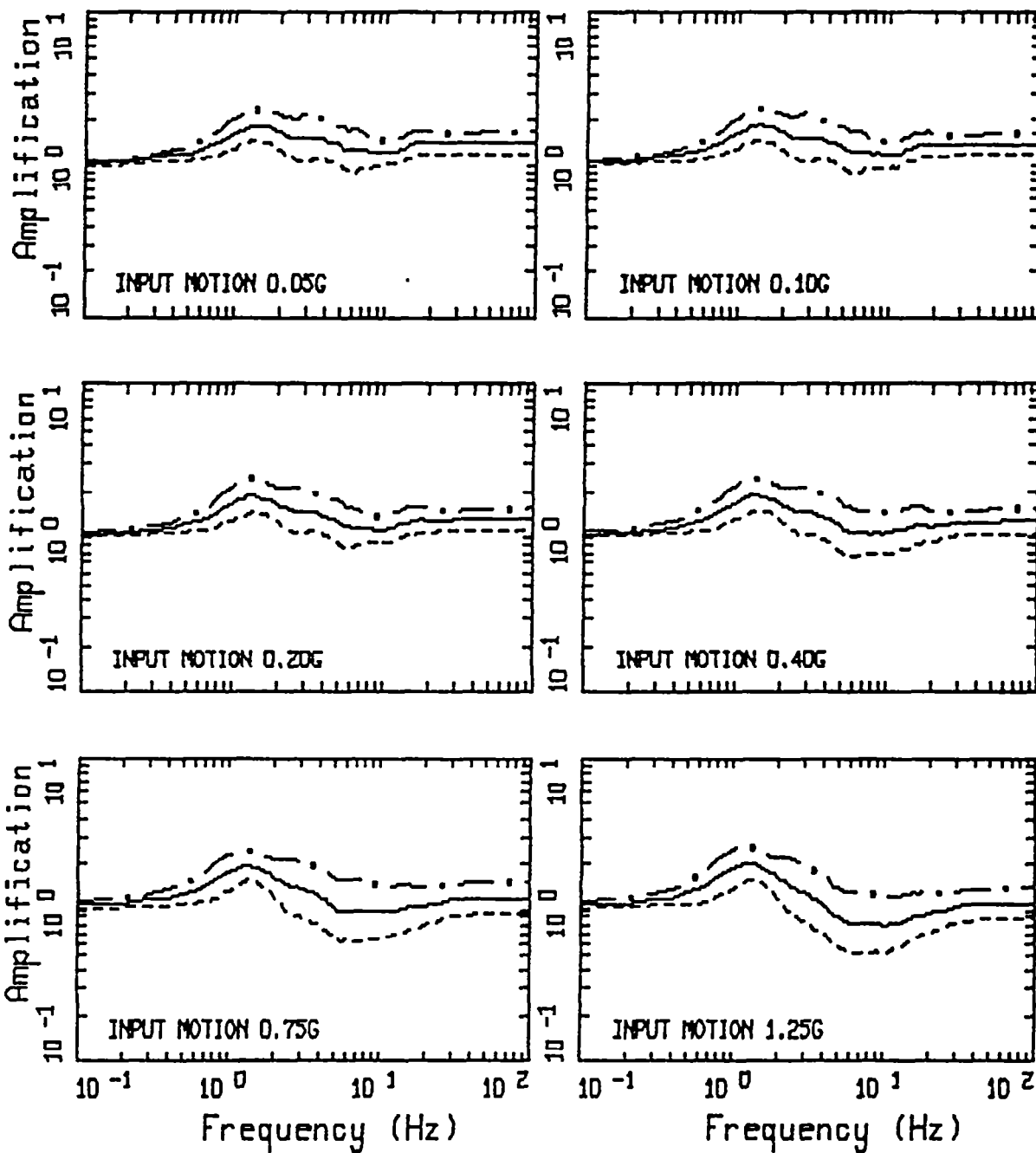
LA AMPLIFICATION  
GEOMATRIX CLASS A & B

Figure 43. Amplification factors computed for Geomatrix site categories A and B (Figure 6, Table 2) relative to Los Angeles area reference rock outcrop Granite.

## **APPENDIX A**

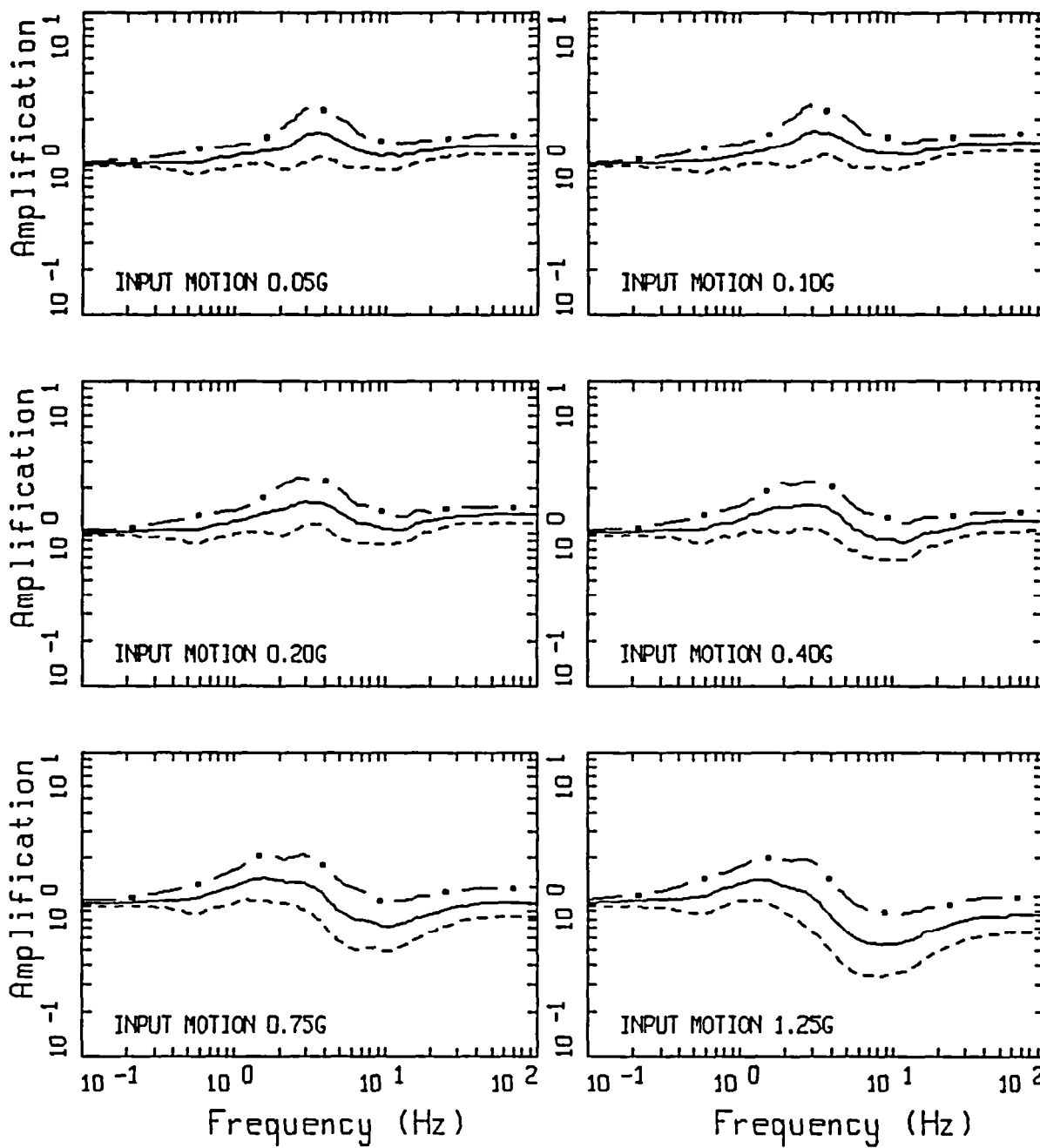
**Amplification Factors (5% damped response spectra) For  
The San Francisco Bay Area Based on Surface Geology:  $TM_{zs}$ ,  
 $QT_s$ ,  $Q_{oa}$ ,  $Q_{al}$ , and  $Q_m$  (Table 1).**



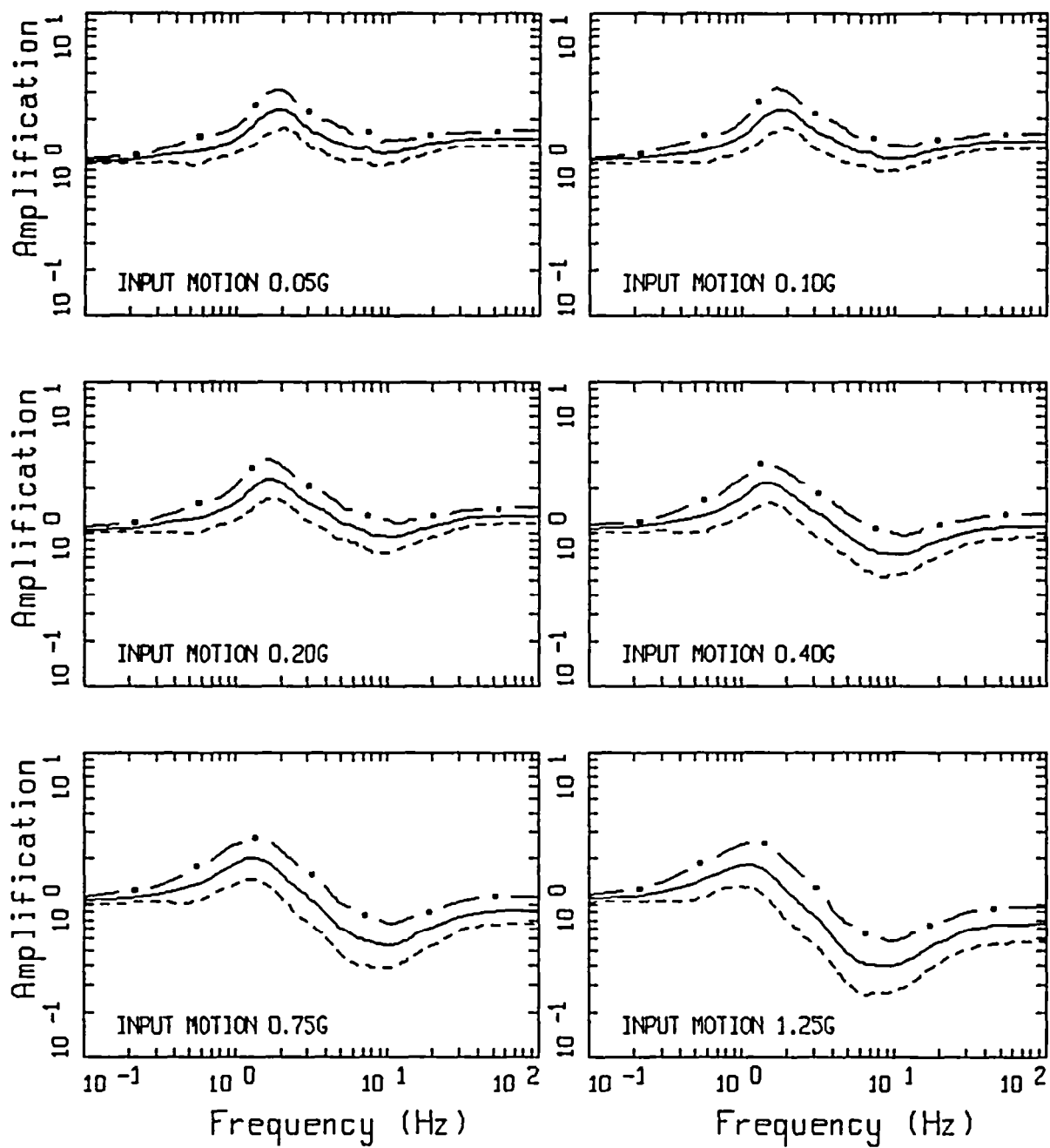


SF AMPLIFICATION

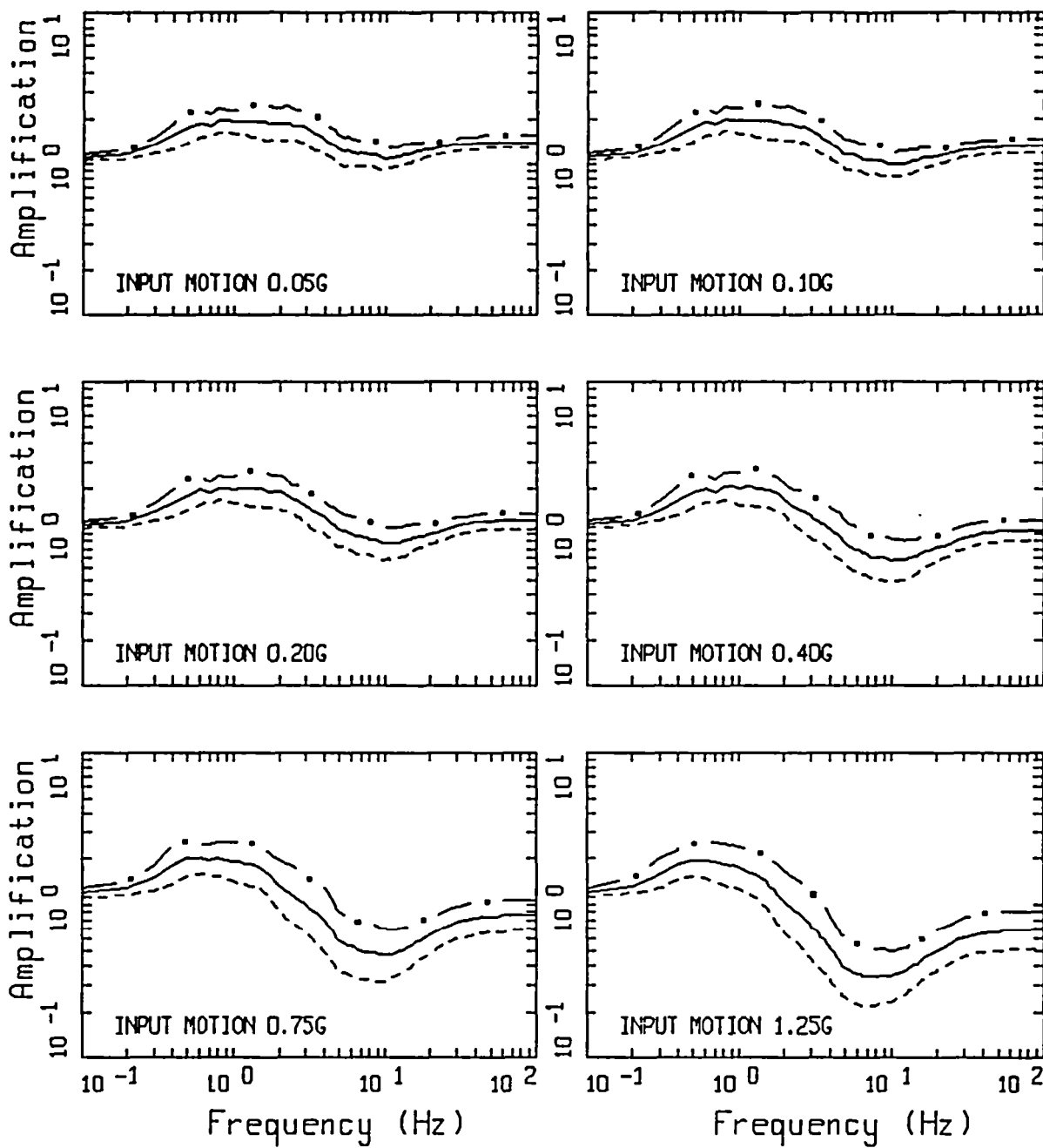
TMzs



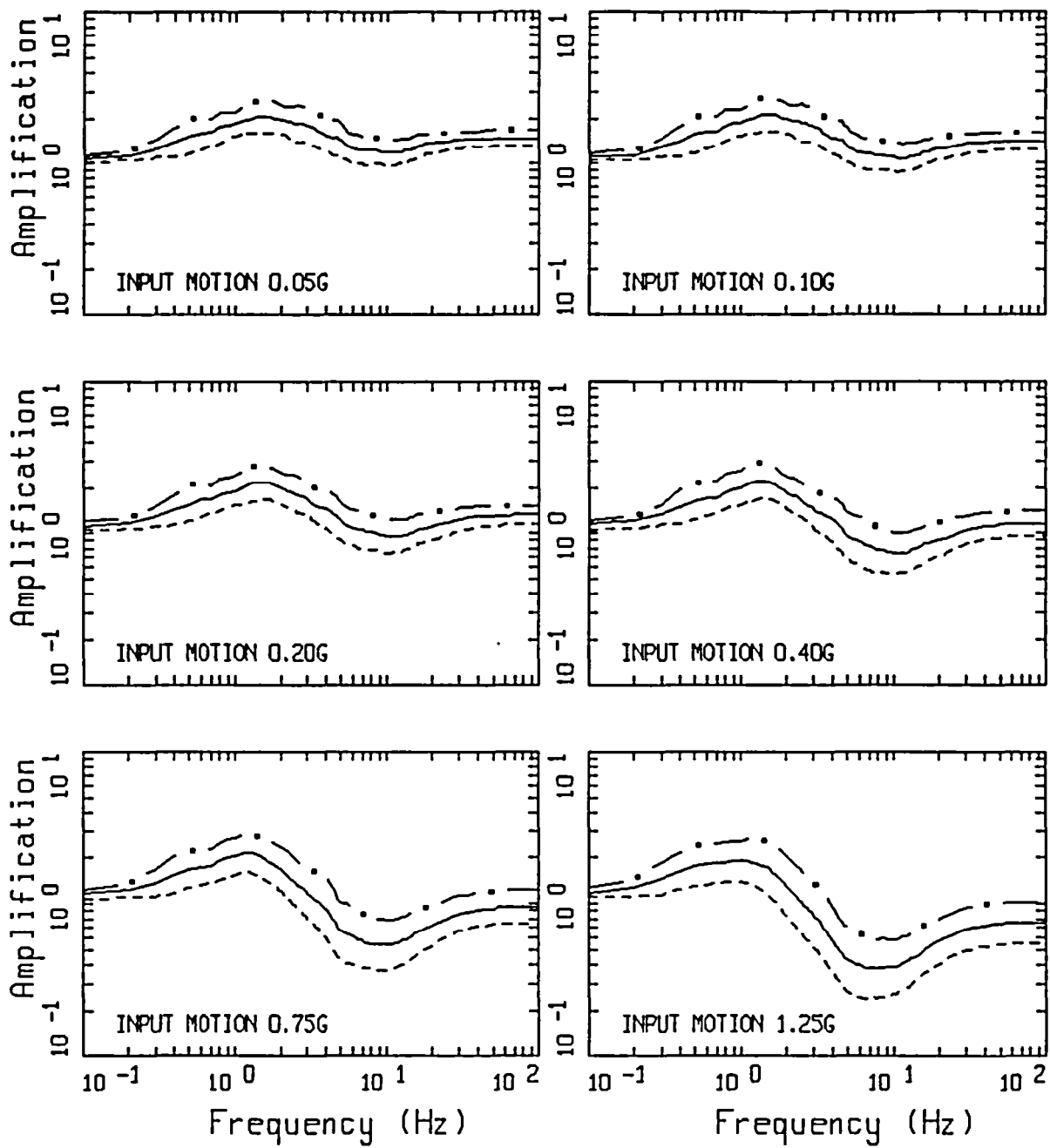
SF AMPLIFICATION  
 QTs (30 - 150 ft)



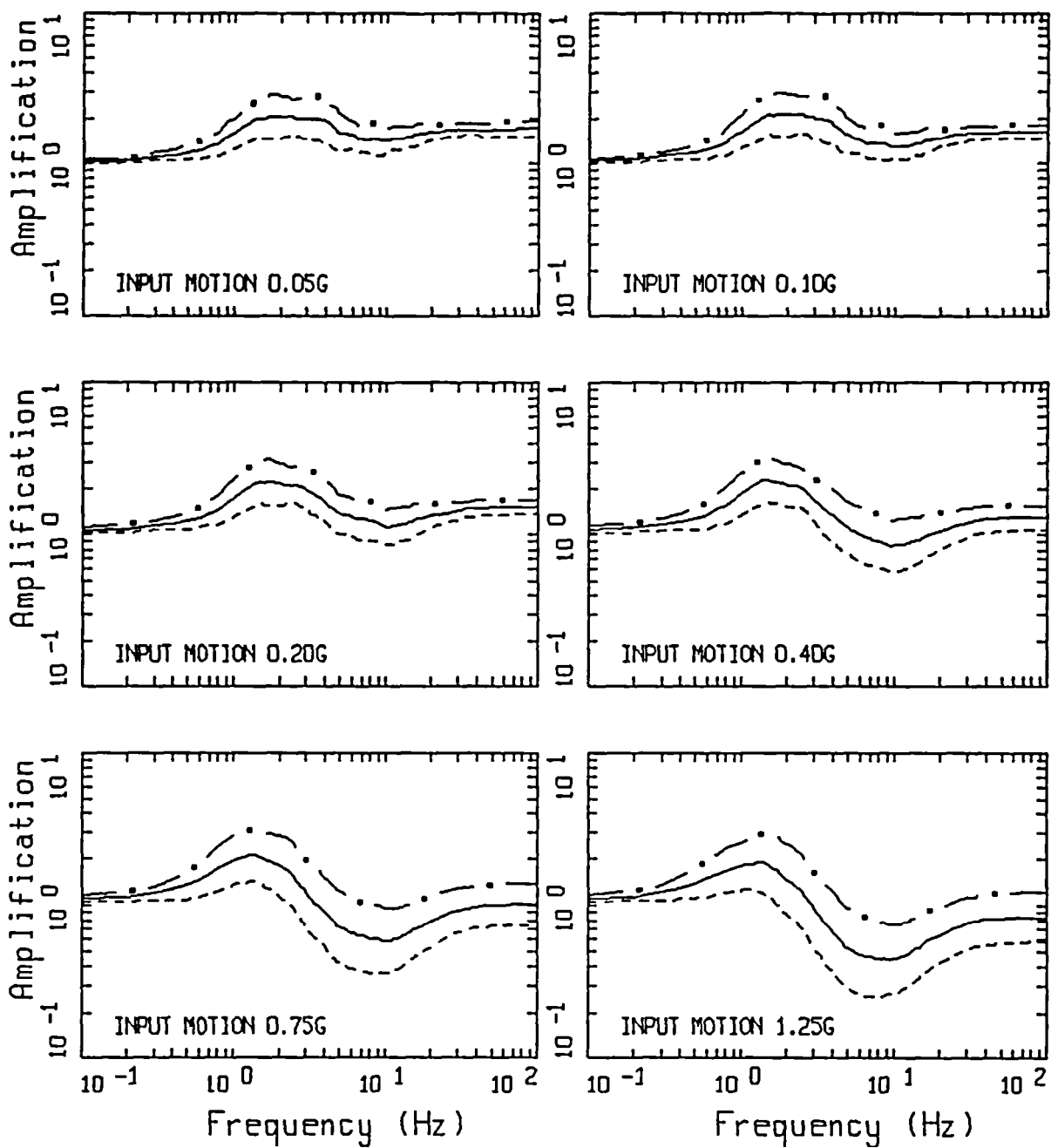
SF AMPLIFICATION  
 QTs (150 - 350 ft)



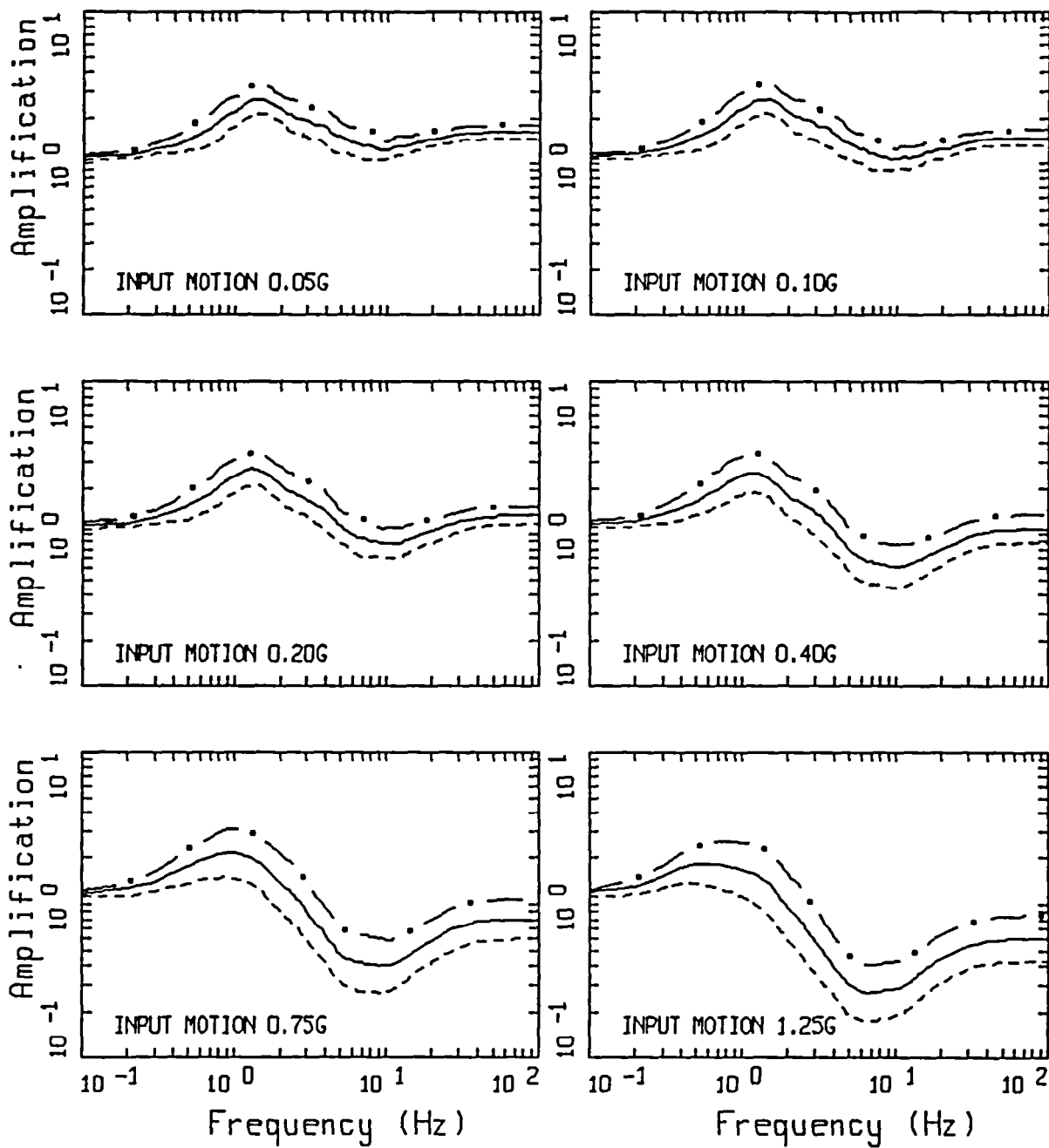
SF AMPLIFICATION  
 QTs (350 - 650 ft)



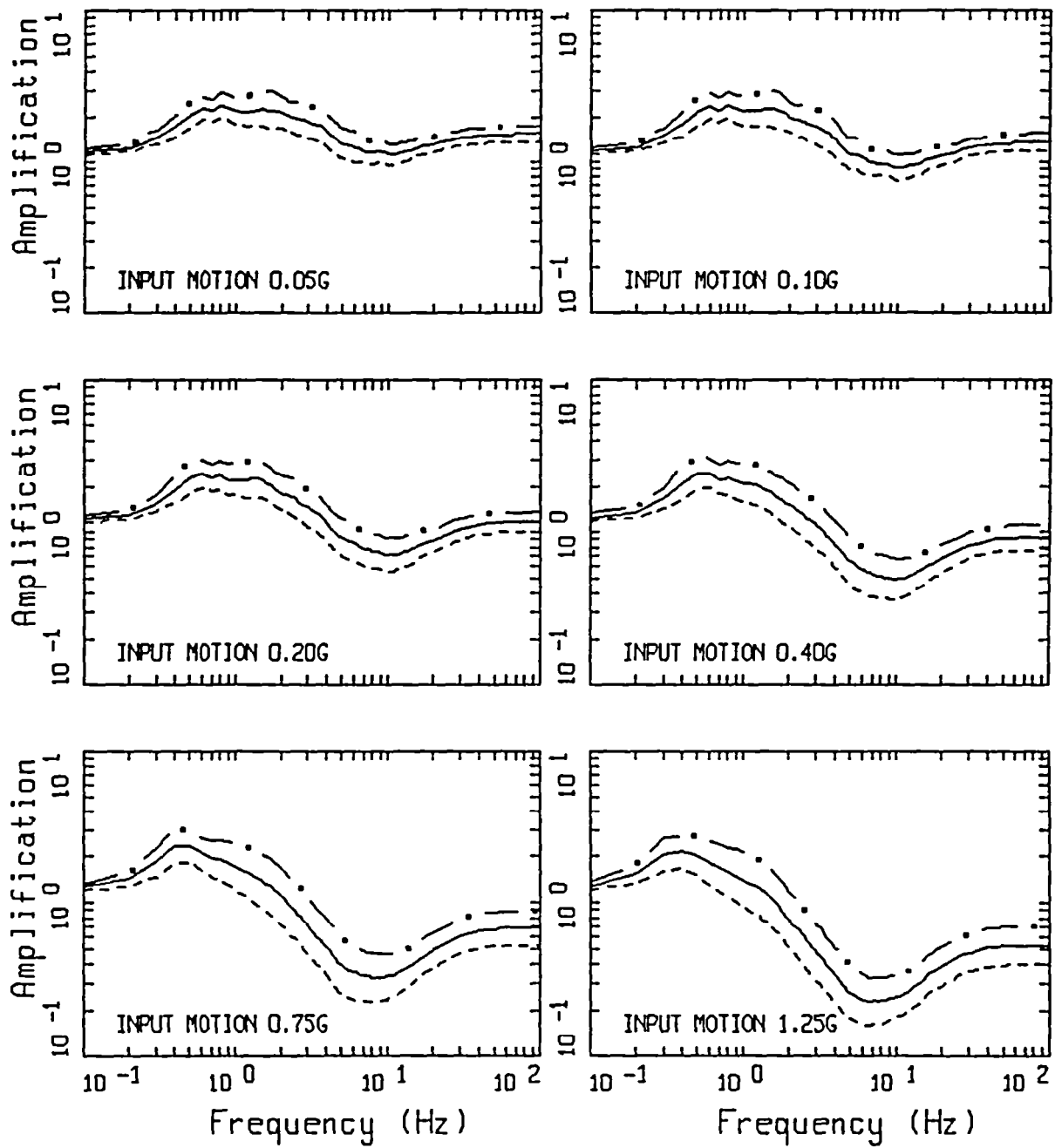
SF AMPLIFICATION  
 QTs (30 - 650 ft)



SF AMPLIFICATION  
QOA (30 - 150 ft)

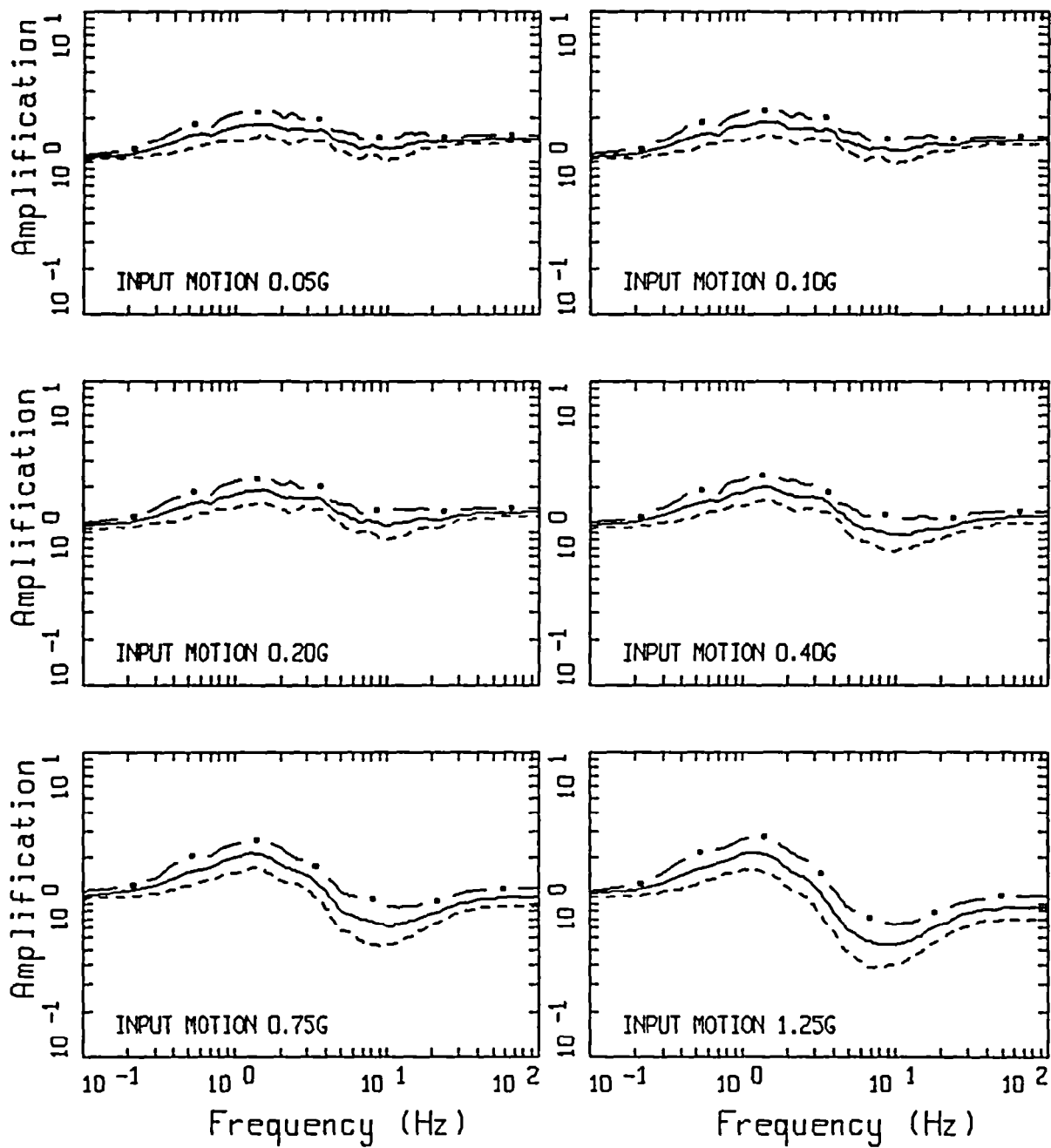


SF AMPLIFICATION  
Q0A (150 - 350 ft)

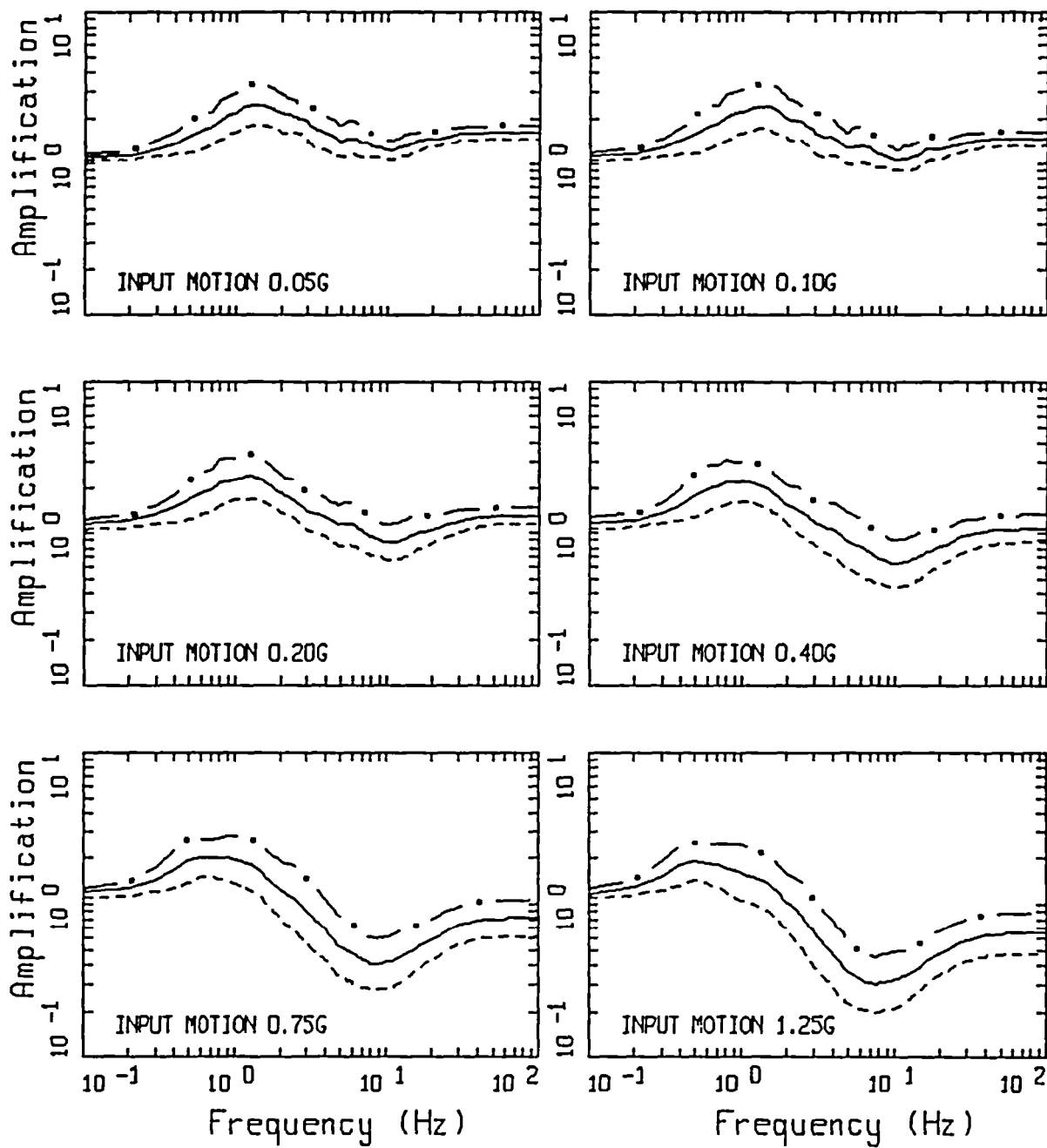


SF AMPLIFICATION  
Q0A (350 - 650 ft)

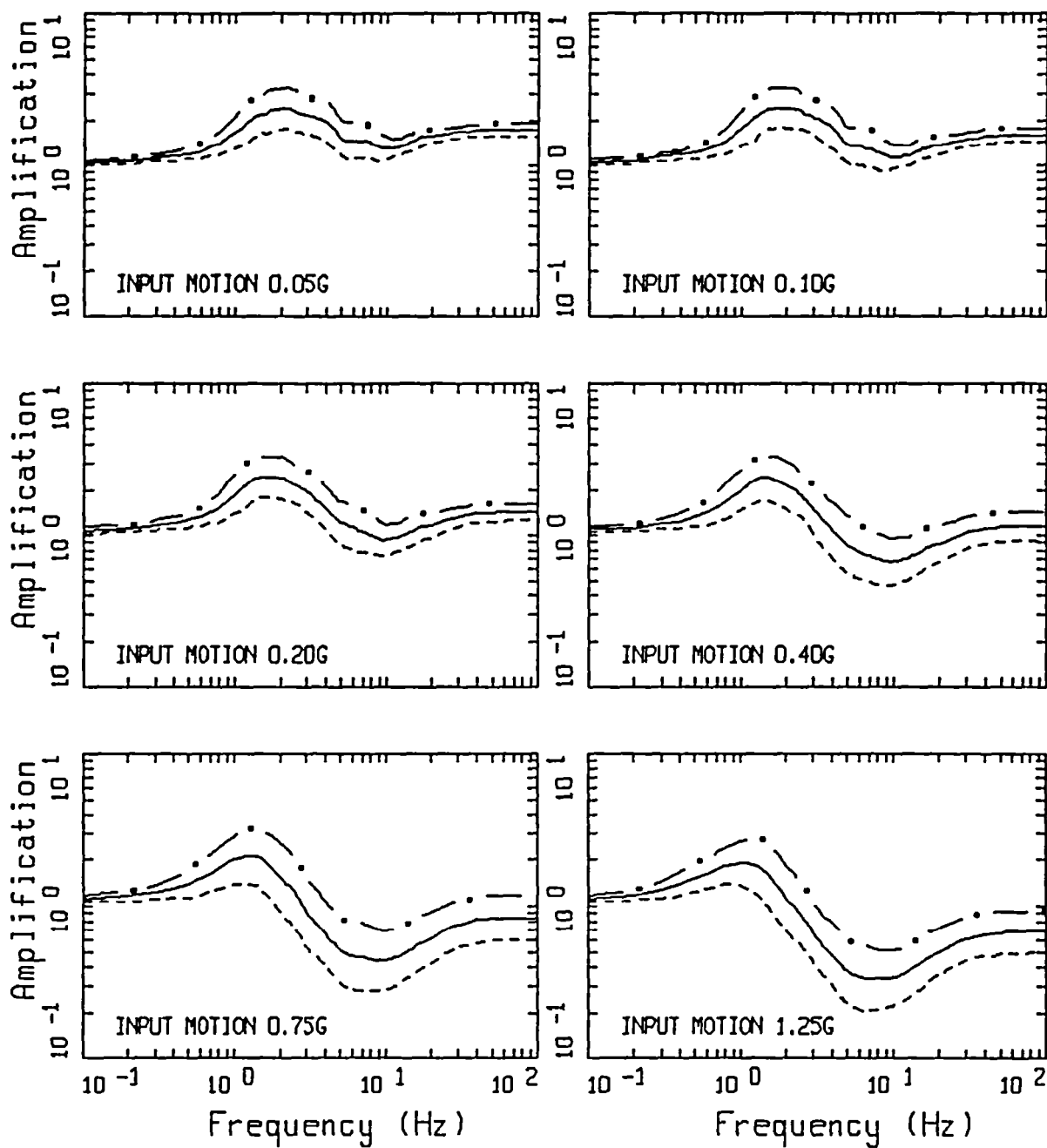




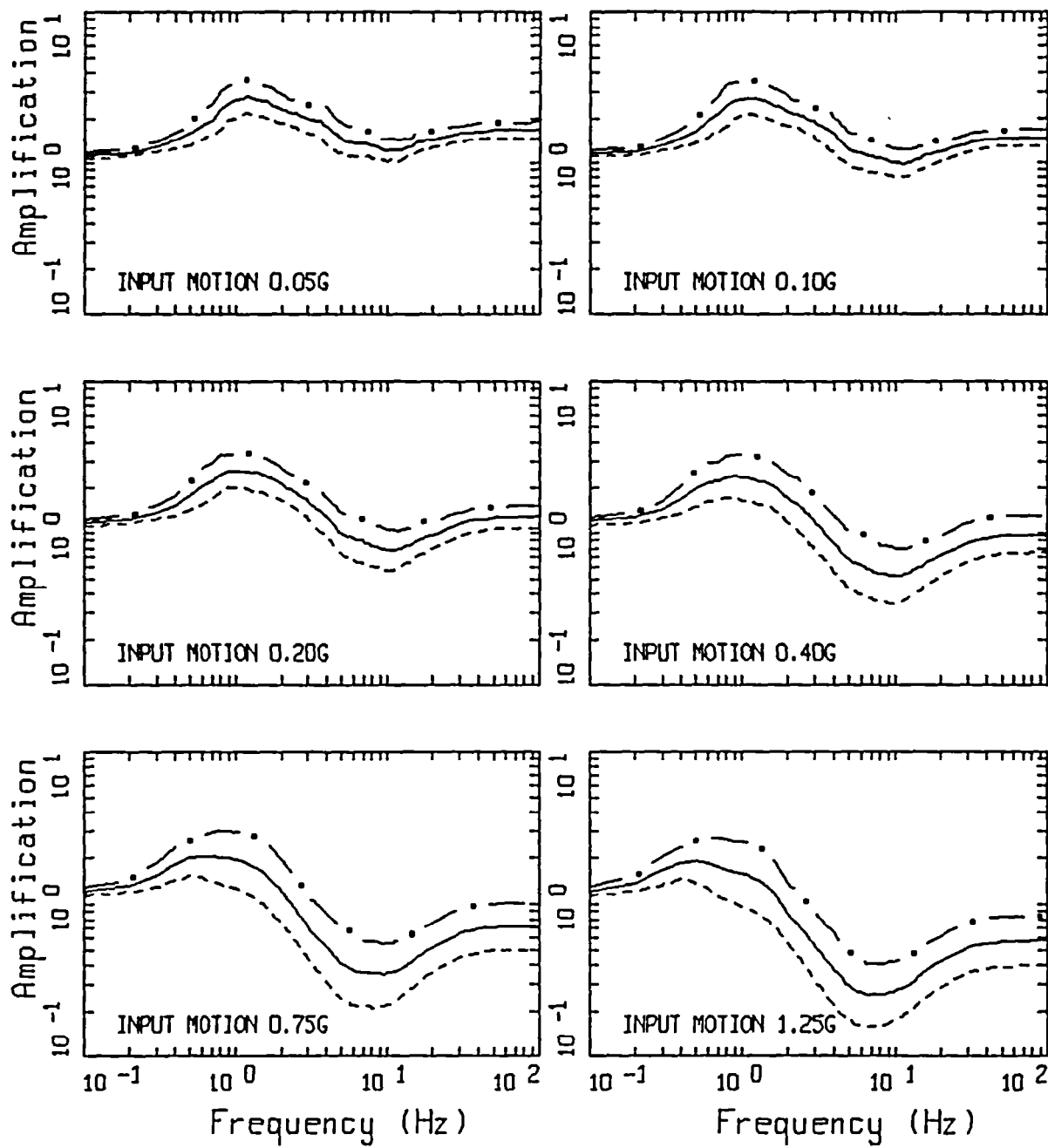
SF AMPLIFICATION  
QOA (30 - 1000 ft)



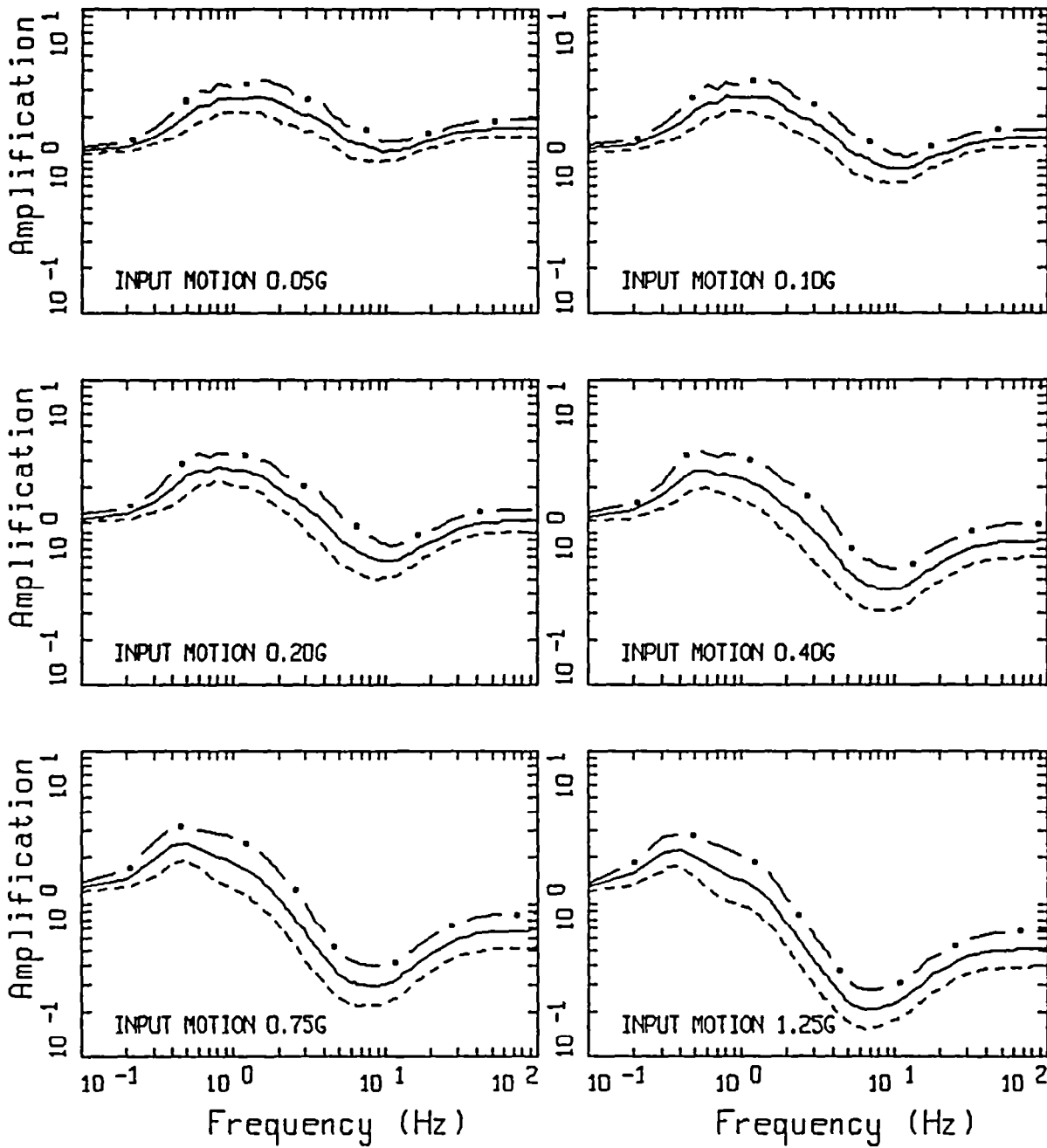
SF AMPLIFICATION  
Q0A (30 - 450 ft)



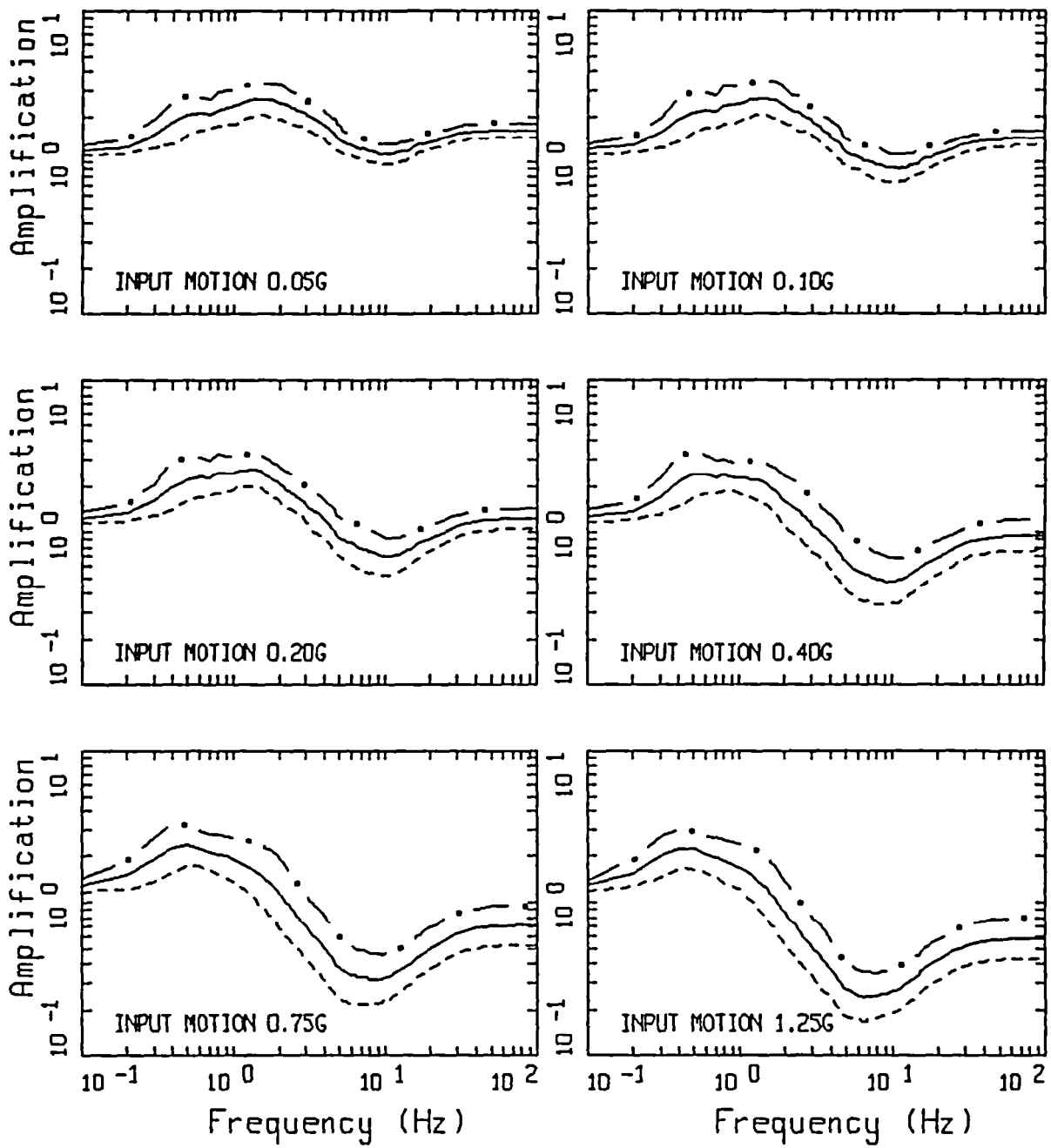
SF AMPLIFICATION  
QAL (30 - 150 ft)



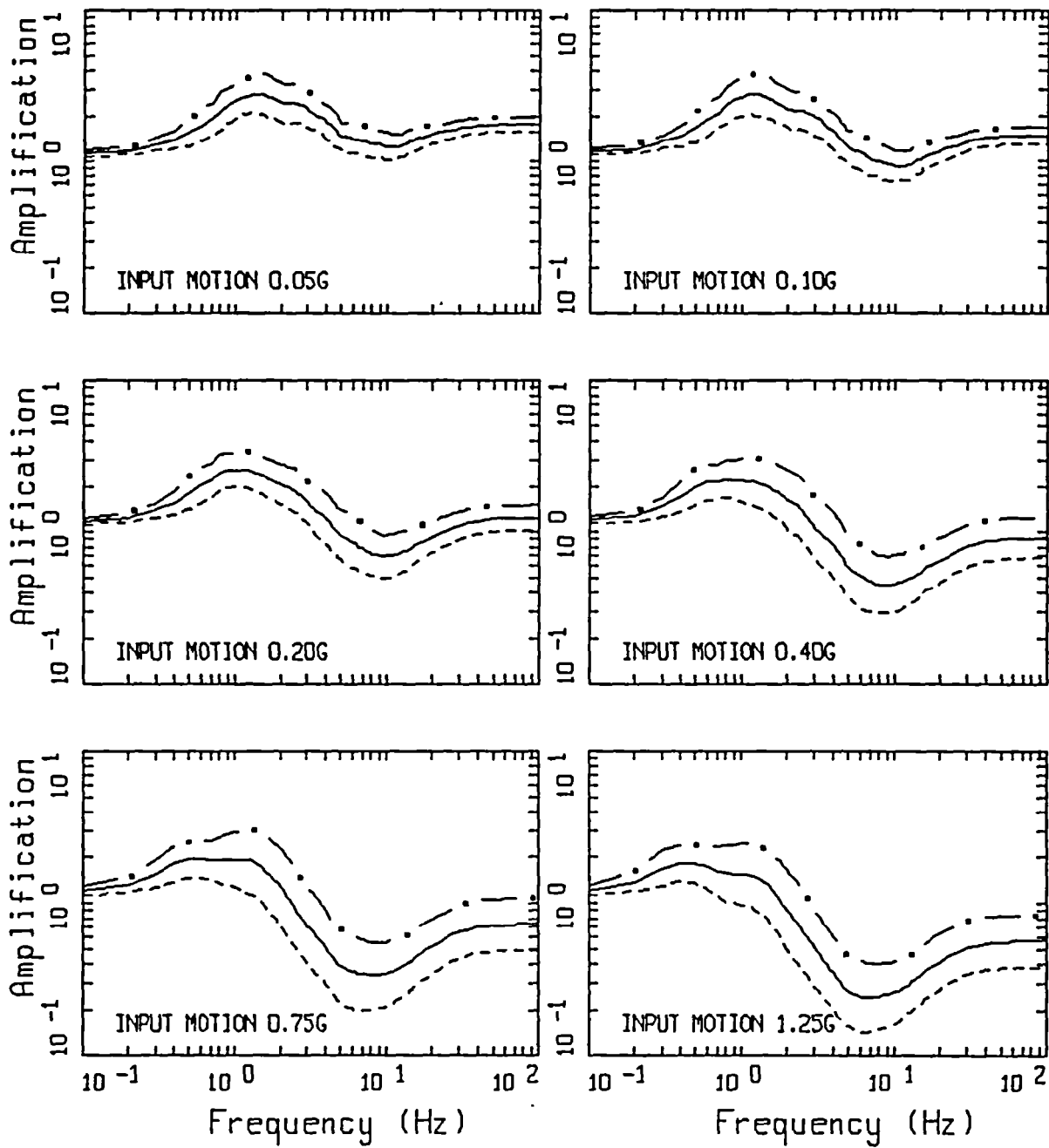
SF AMPLIFICATION  
QAL (150 - 350 ft)



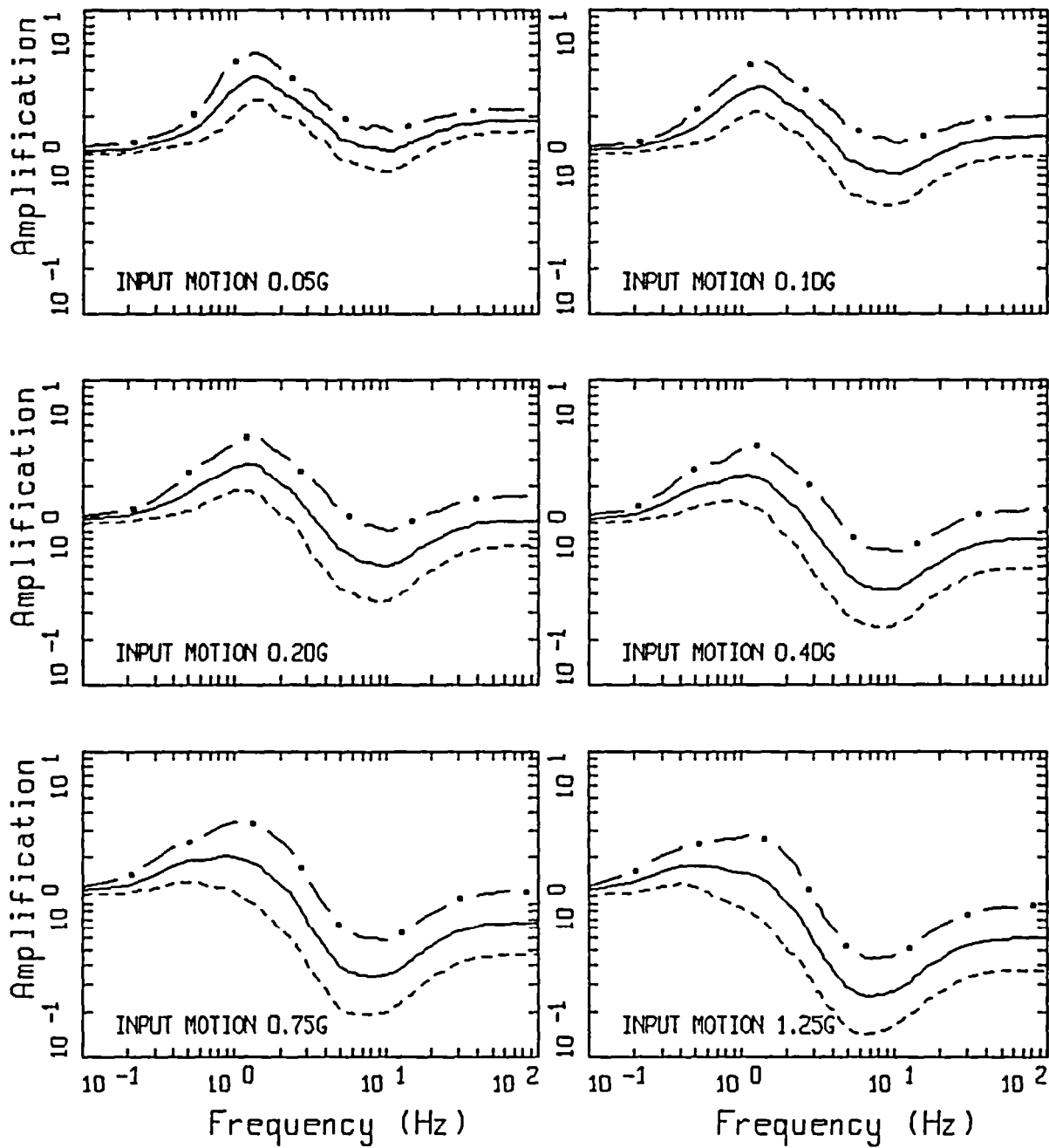
SF AMPLIFICATION  
QAL (350 - 650 ft)



SF AMPLIFICATION  
 QAL (30 - 1000 ft)

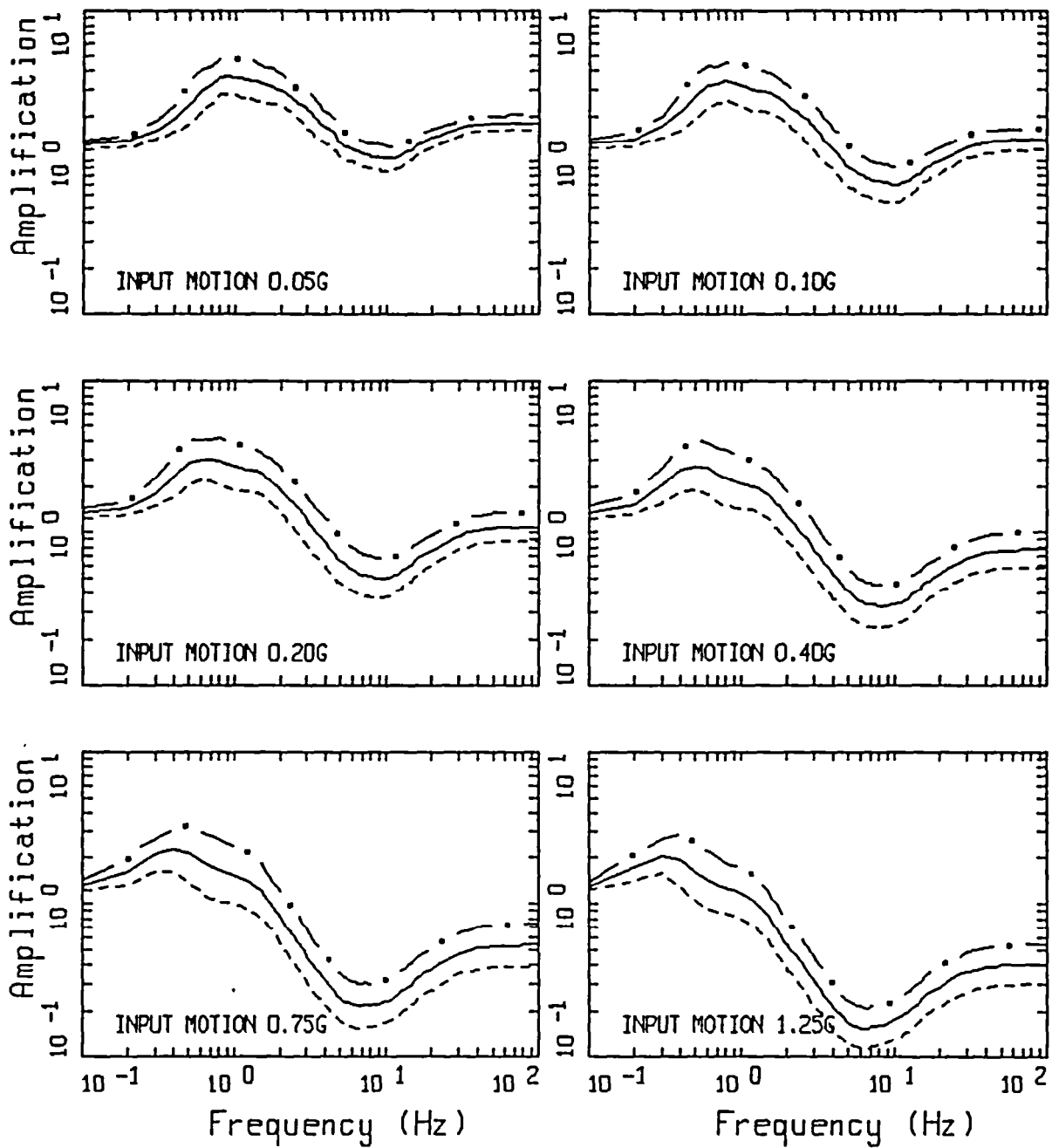


SF AMPLIFICATION  
QAL (30 - 450 ft)

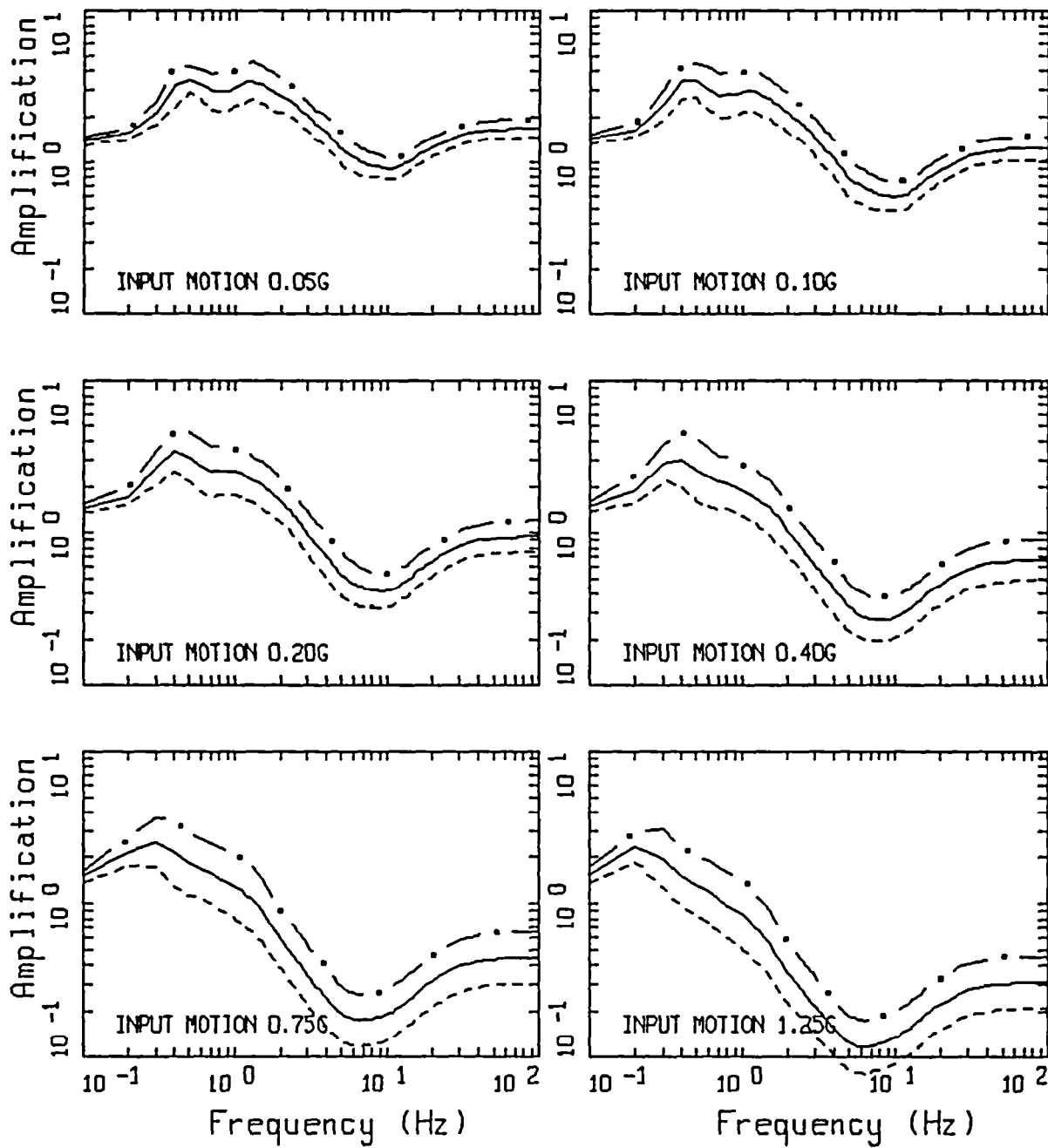


SF AMPLIFICATION  
 $Q_m$  (30 - 150 ft)

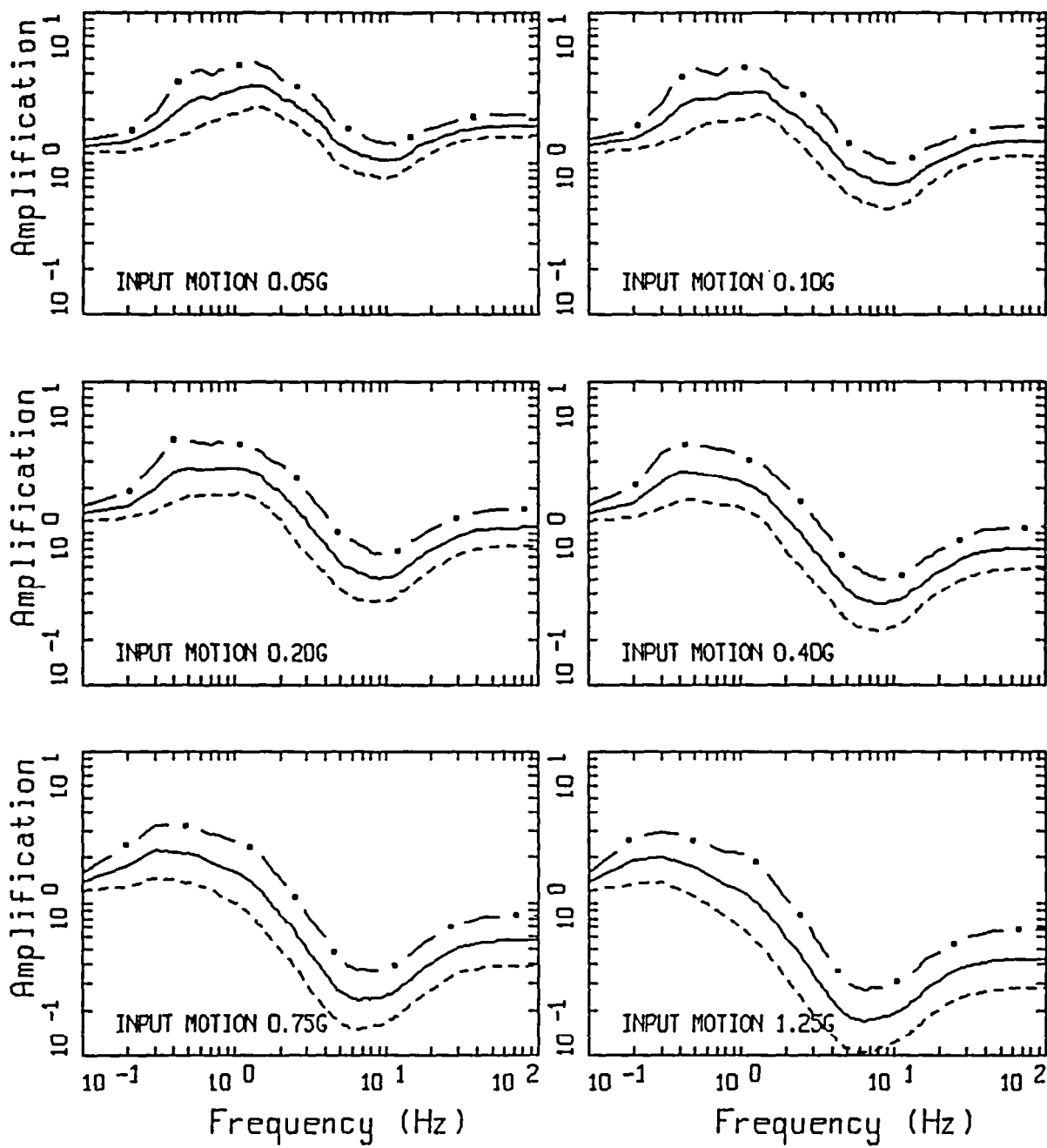




SF AMPLIFICATION  
 $Q_m$  (150 - 350 ft)



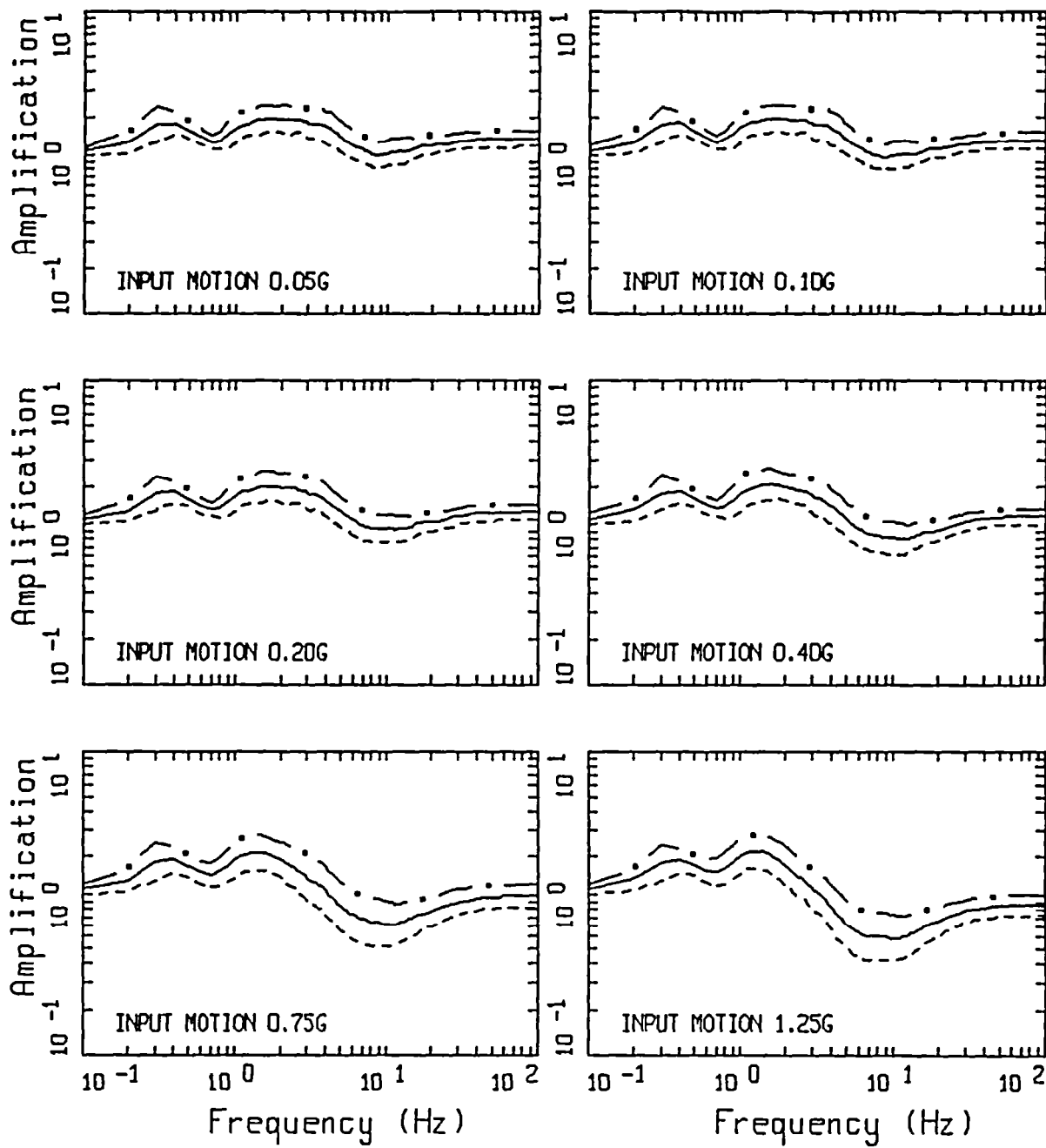
SF AMPLIFICATION  
 Qm (350 - 650 ft)



SF AMPLIFICATION  
 Qm (30 - 650 ft)

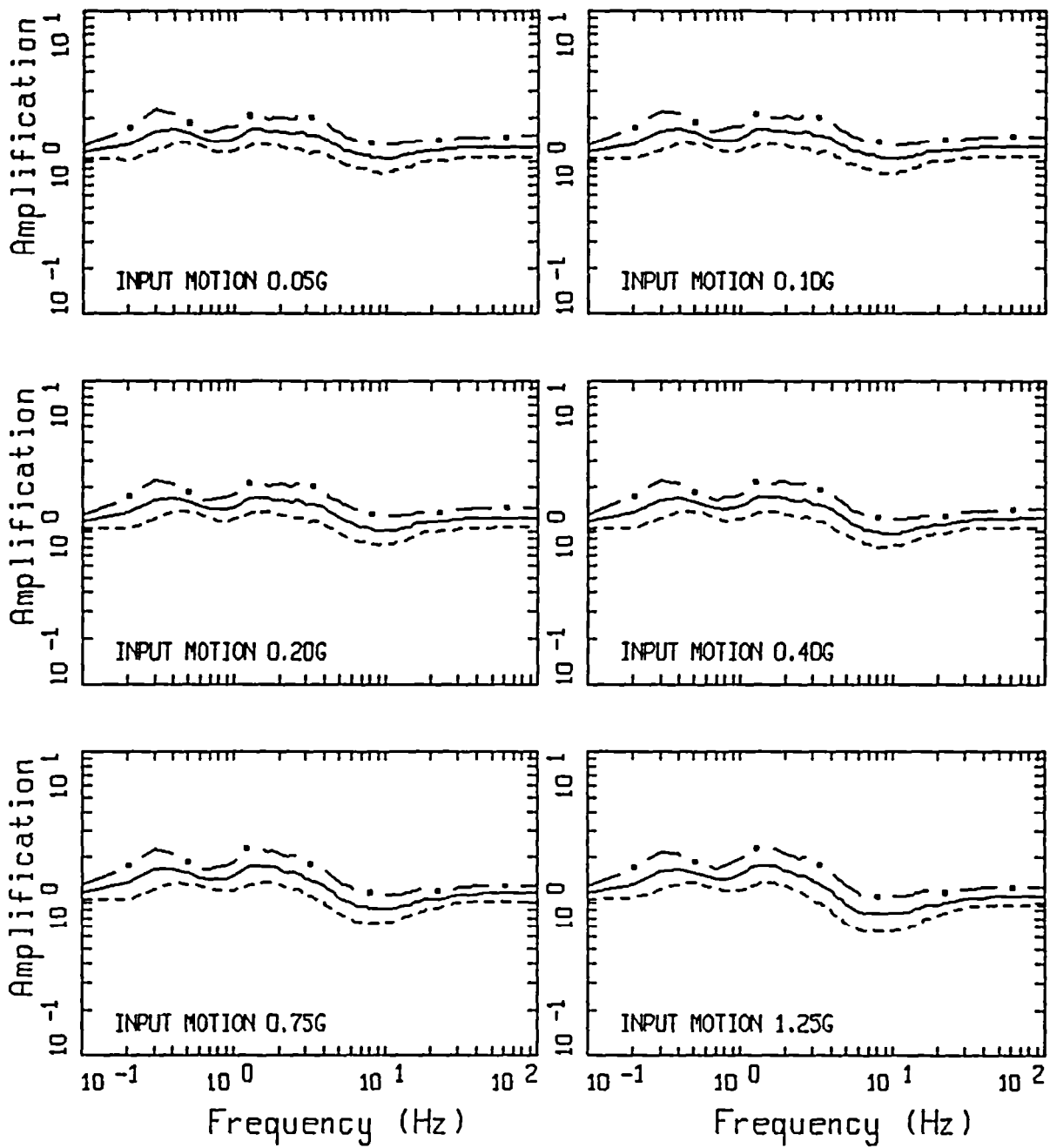
## **APPENDIX B**

**Amplification Factors (5% damped response spectra) For  
The Los Angeles Area Based on Surface Geology:  $TM_{zs}$ ,  $QT_s$ ,  
 $Q_{oa}$ ,  $Q_{al}$ , and  $Q_m$  (Table 1).**



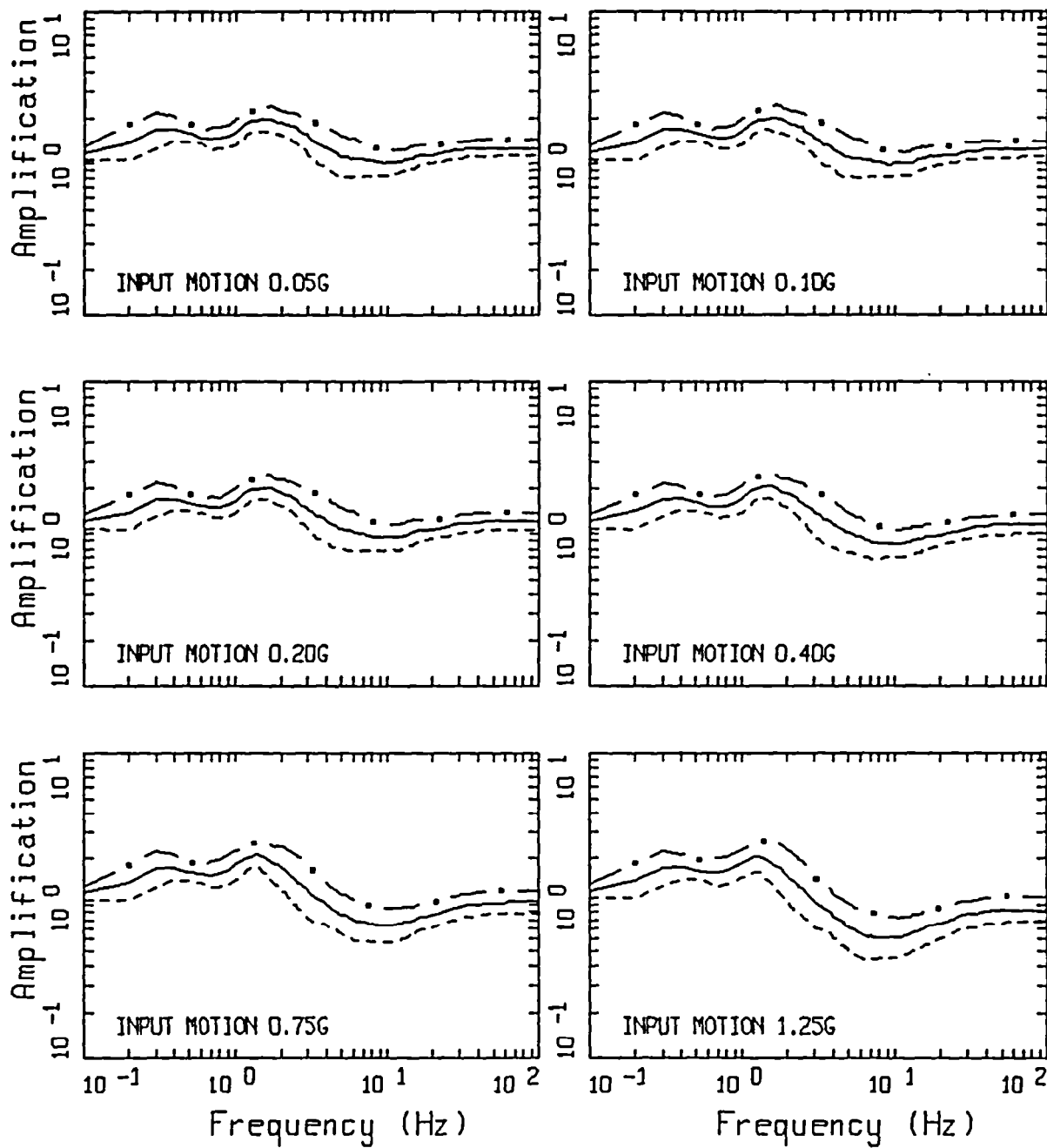
LA AMPLIFICATION

Ts



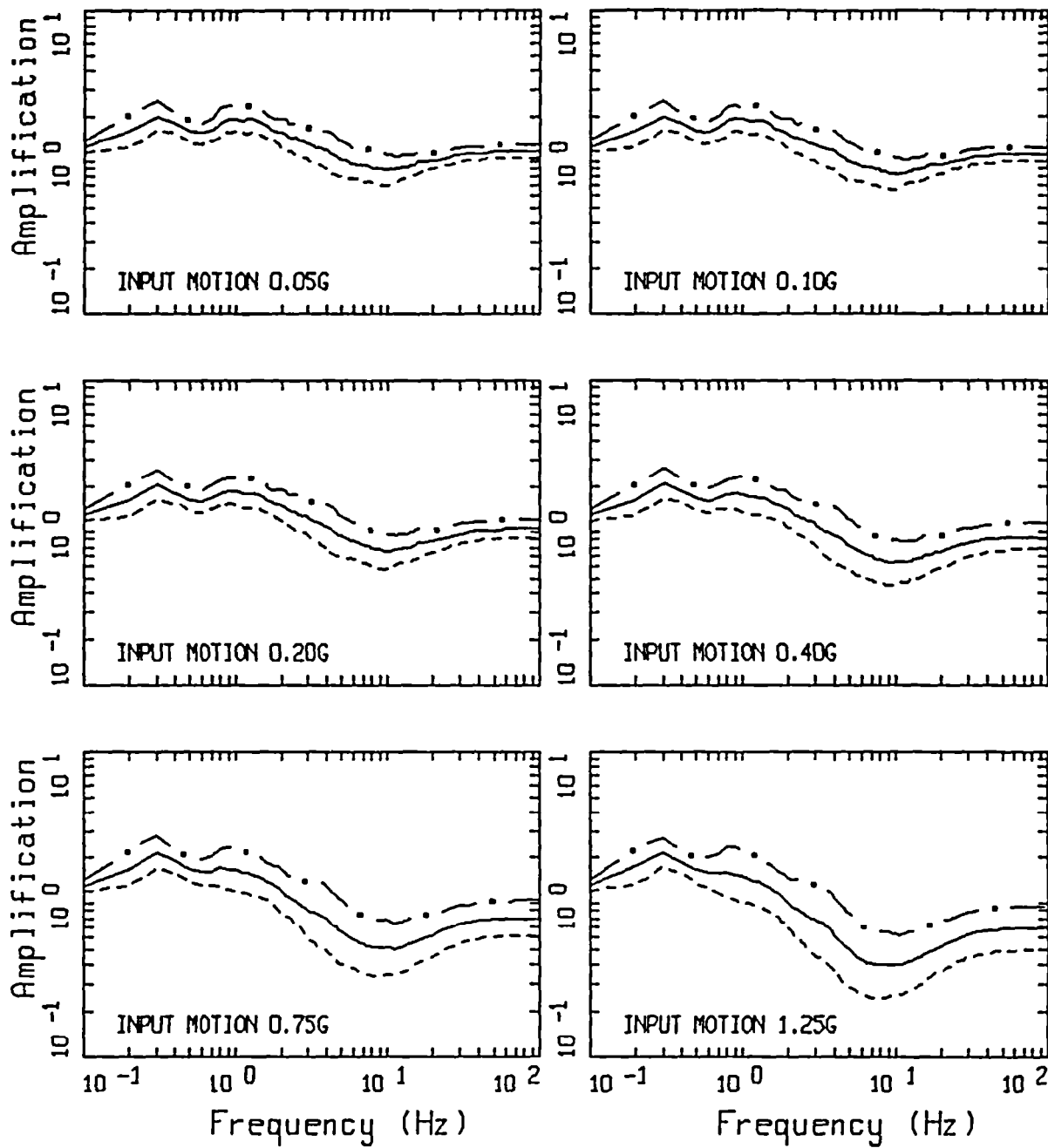
LA AMPLIFICATION

Saugus (Ts) (30 - 150 ft)



LA AMPLIFICATION

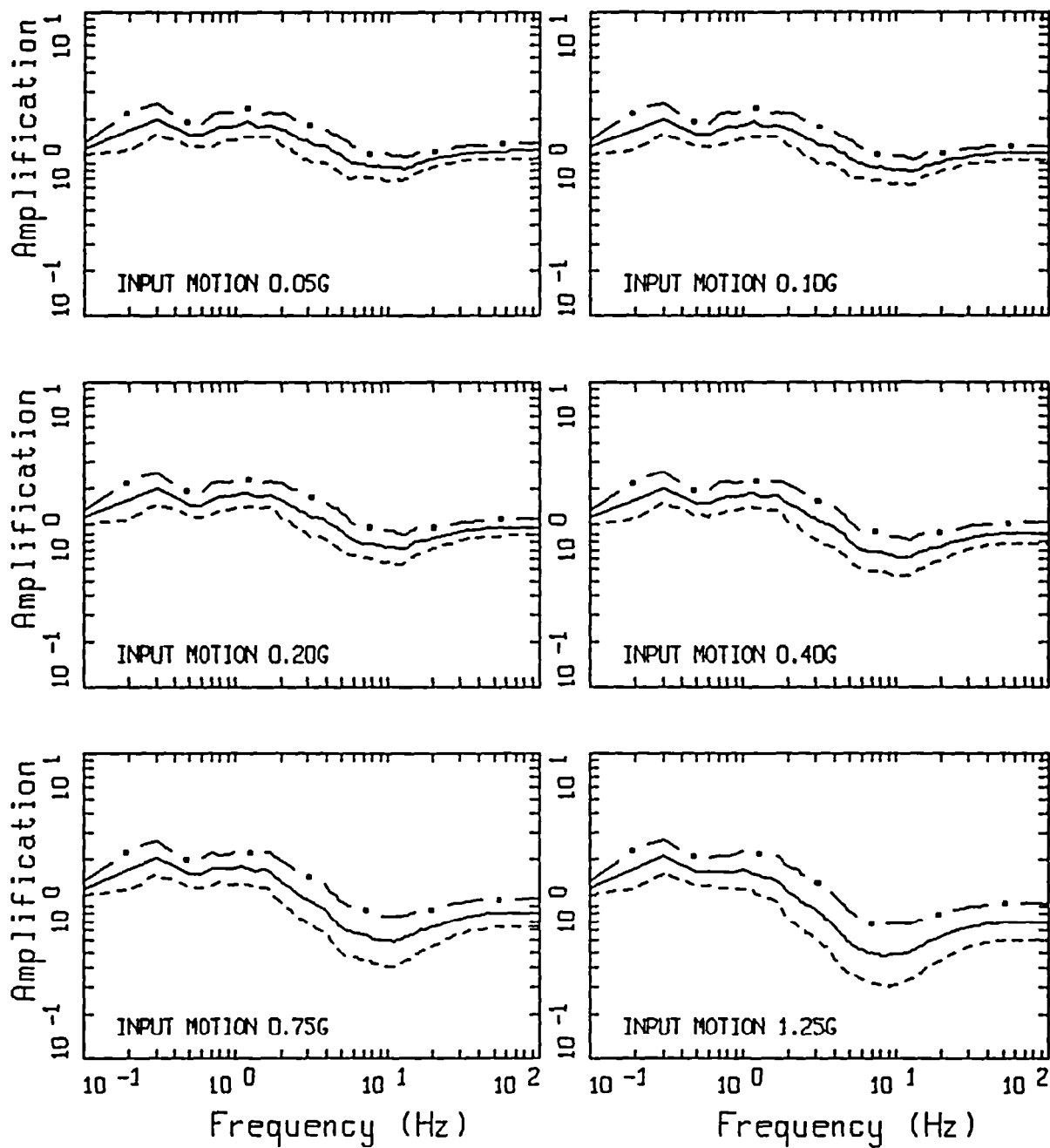
Saugus (Ts) (150 - 350 ft)



LA AMPLIFICATION

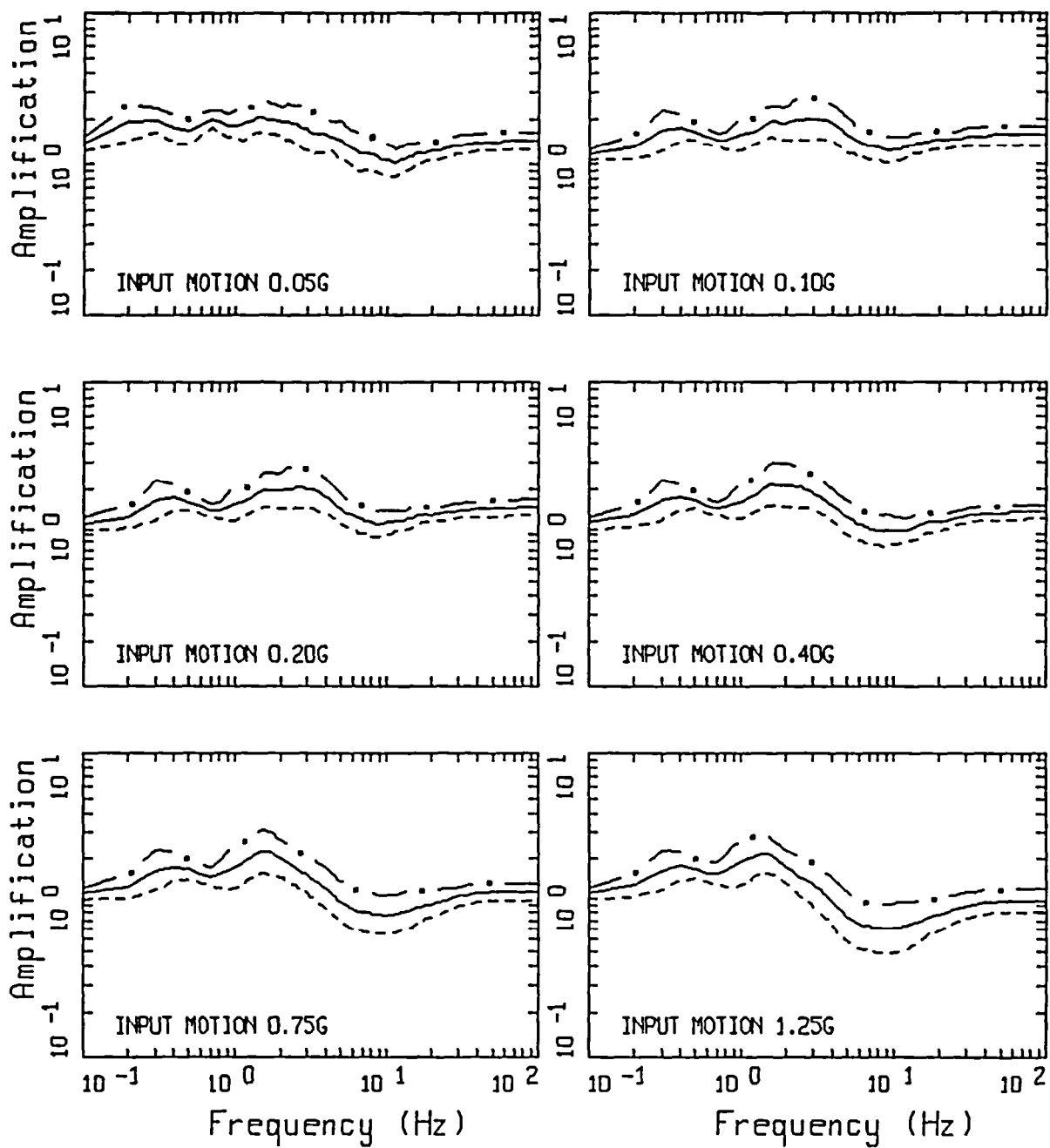
Saugus (Ts) (350 - 650 ft)



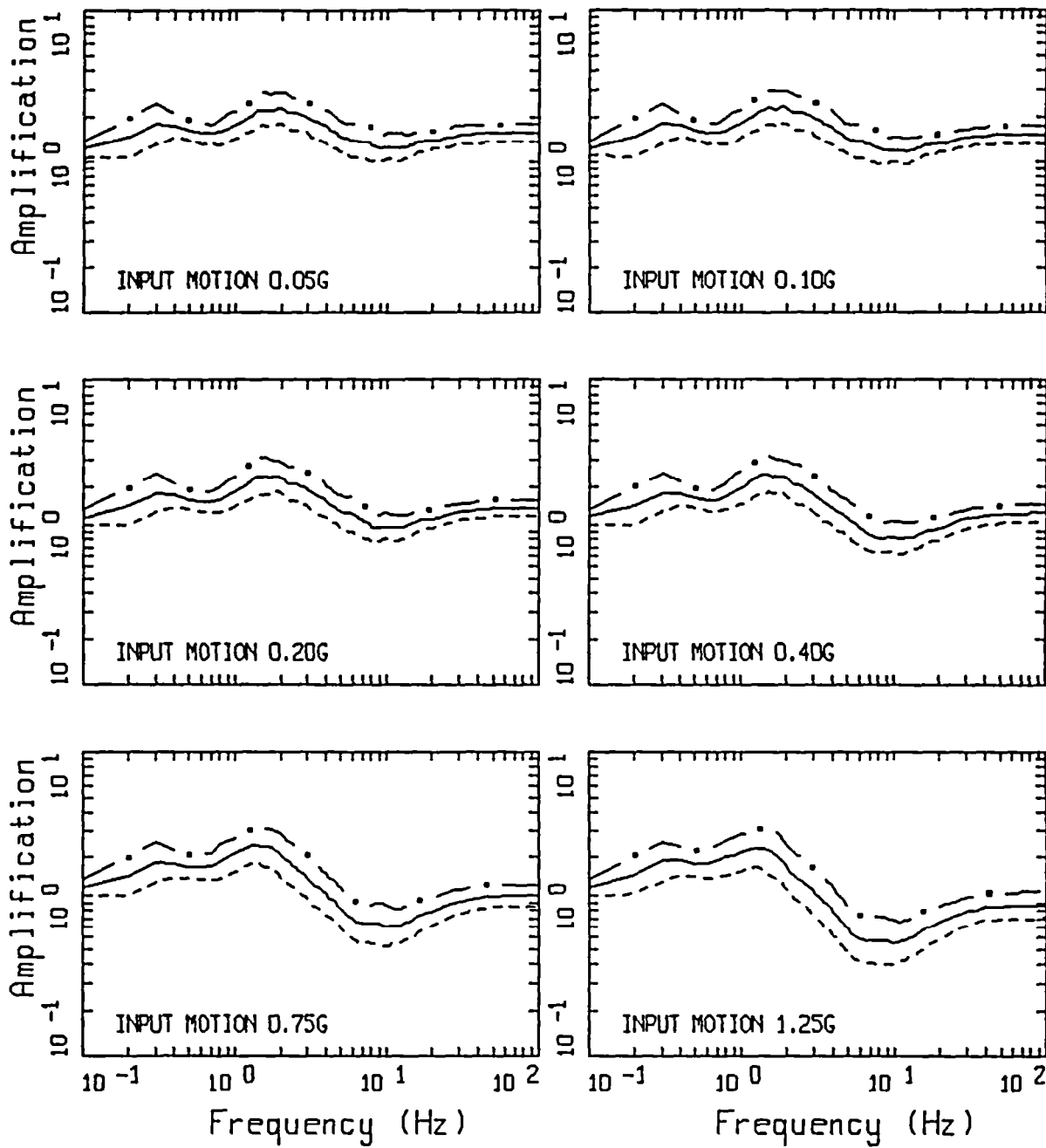


LA AMPLIFICATION

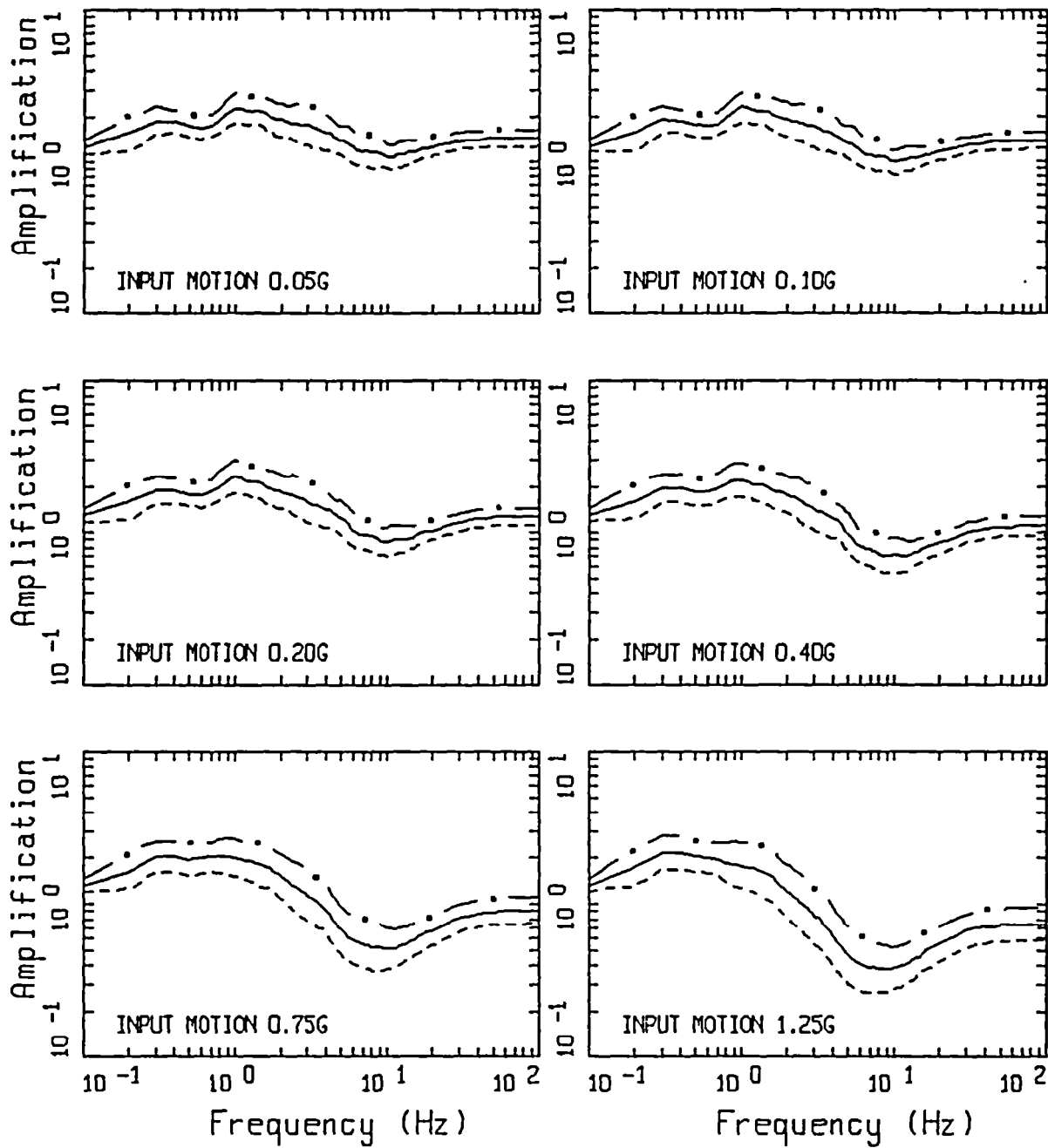
Saugus (Ts) (30 - 1000 ft)



LA AMPLIFICATION  
 $Q_0 + T_s$  (30 - 150 ft)

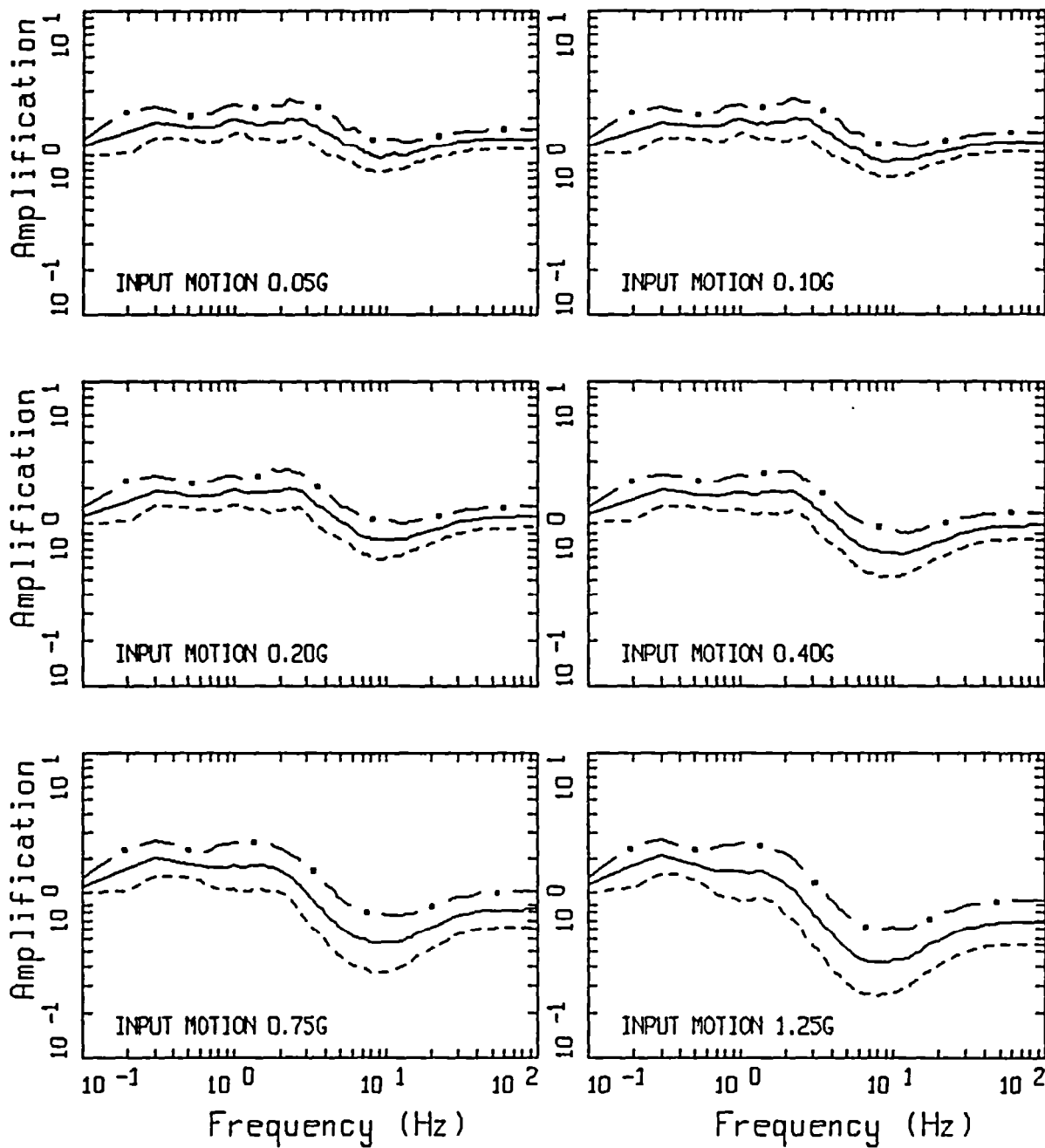


LA AMPLIFICATION  
 $Q_0 + T_s$  (150 - 350 ft)

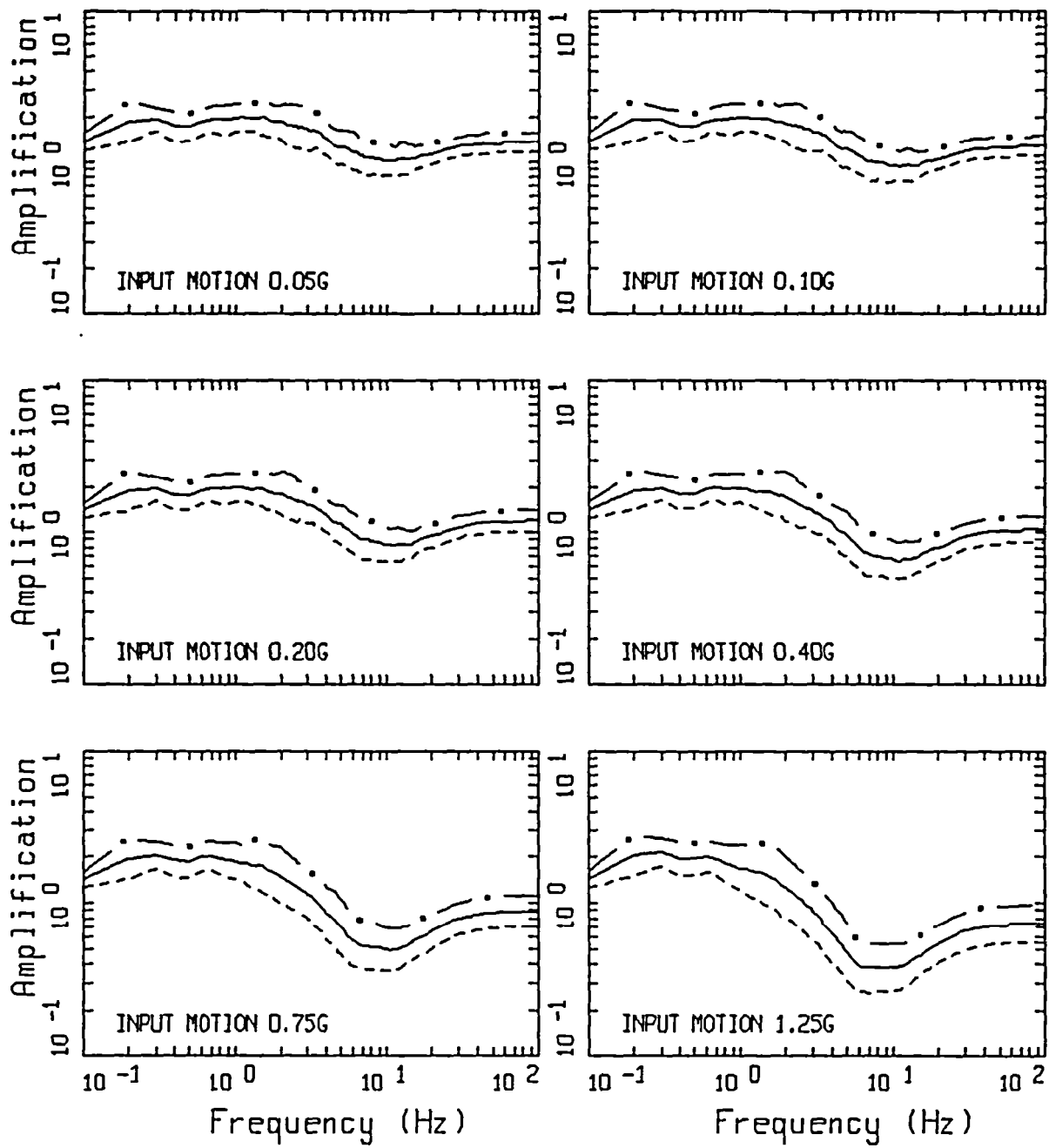


LA AMPLIFICATION

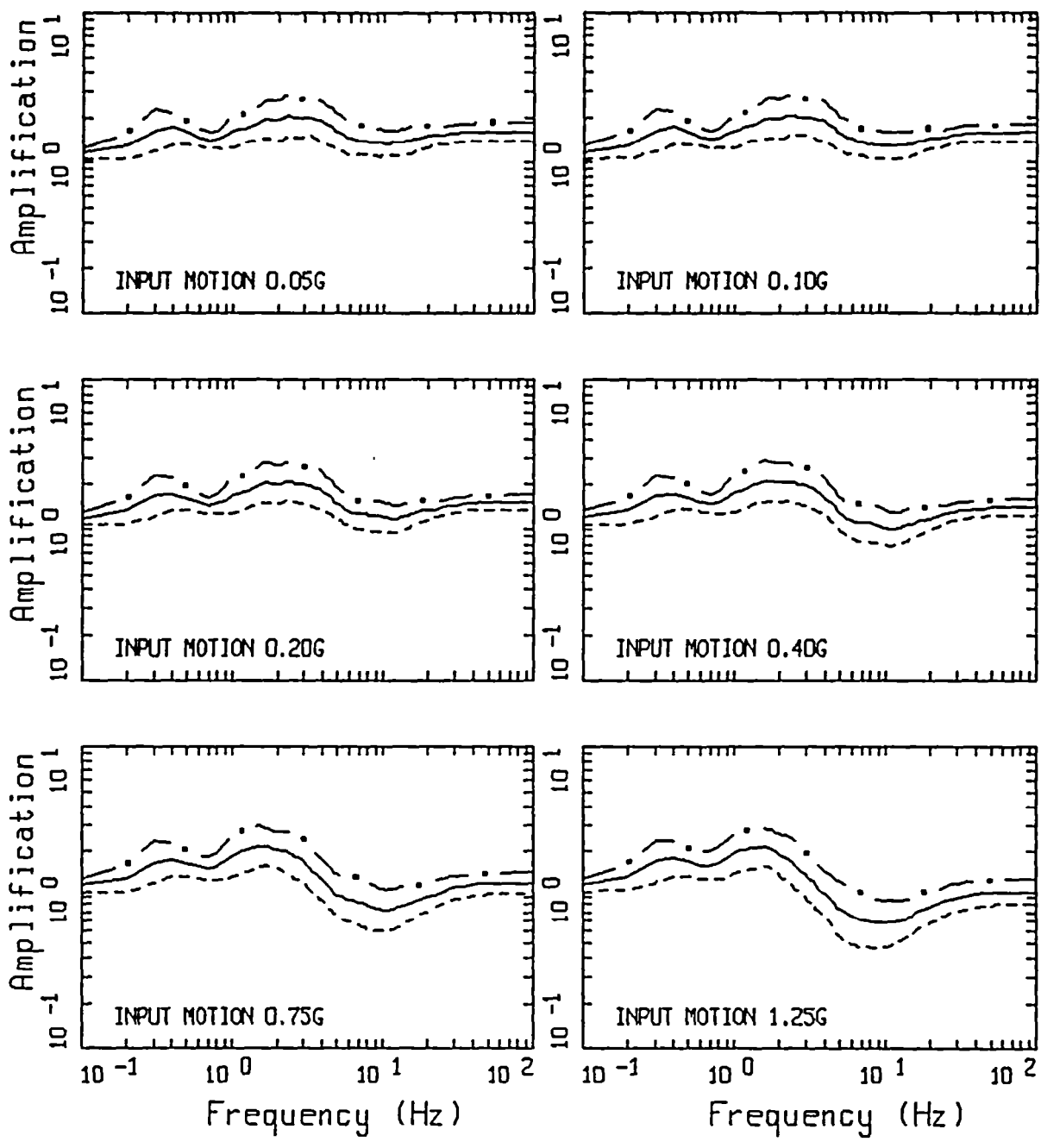
$Q_0 + T_s$  (350 - 650 ft)



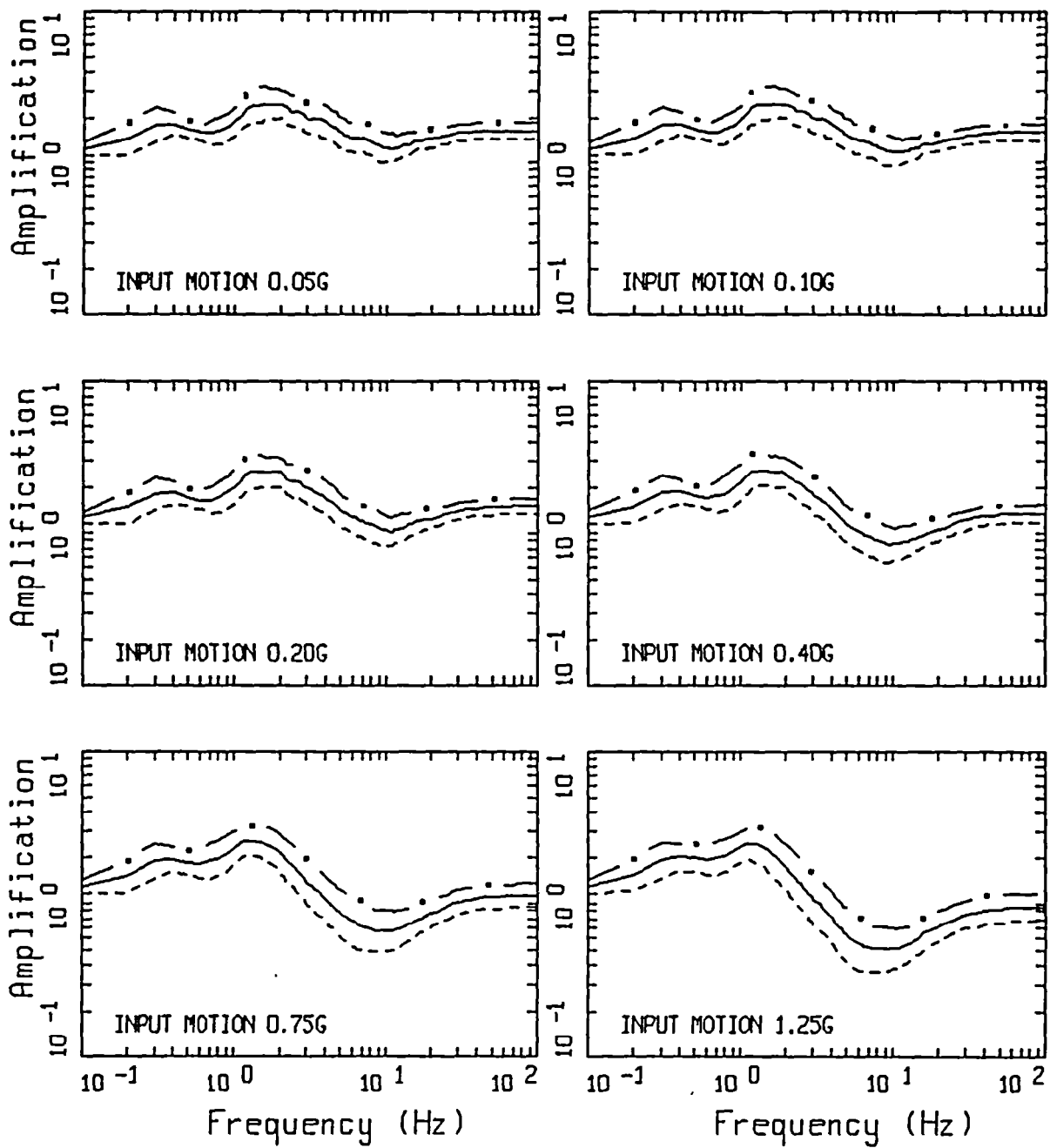
LA AMPLIFICATION  
 $Q_0 + T_s$  (30 - 1000 ft)



LA AMPLIFICATION  
 $Q_0 + T_s$  (500 - 1500 ft)

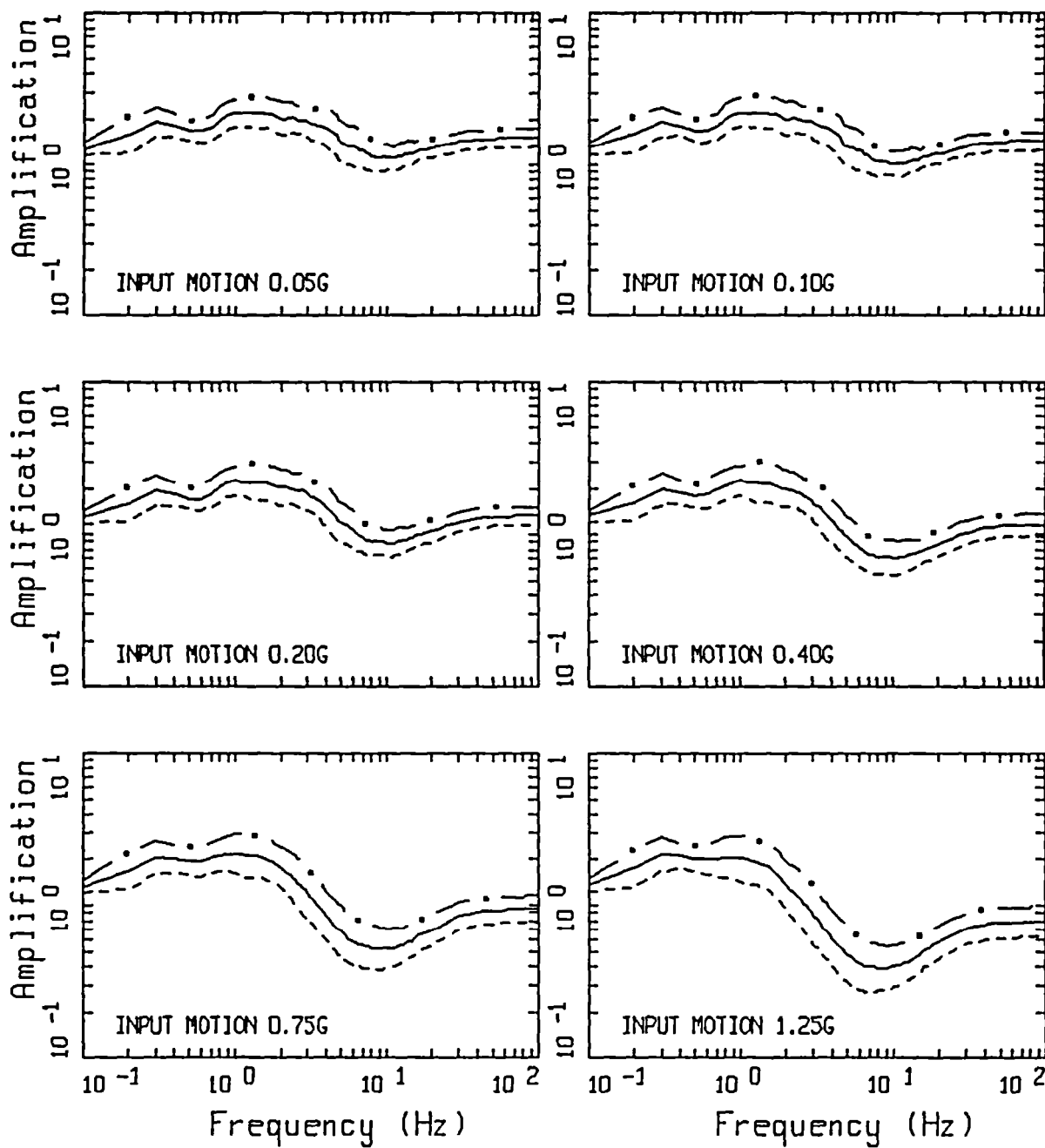


LA AMPLIFICATION  
 Q<sub>0</sub> (30 - 150 ft)

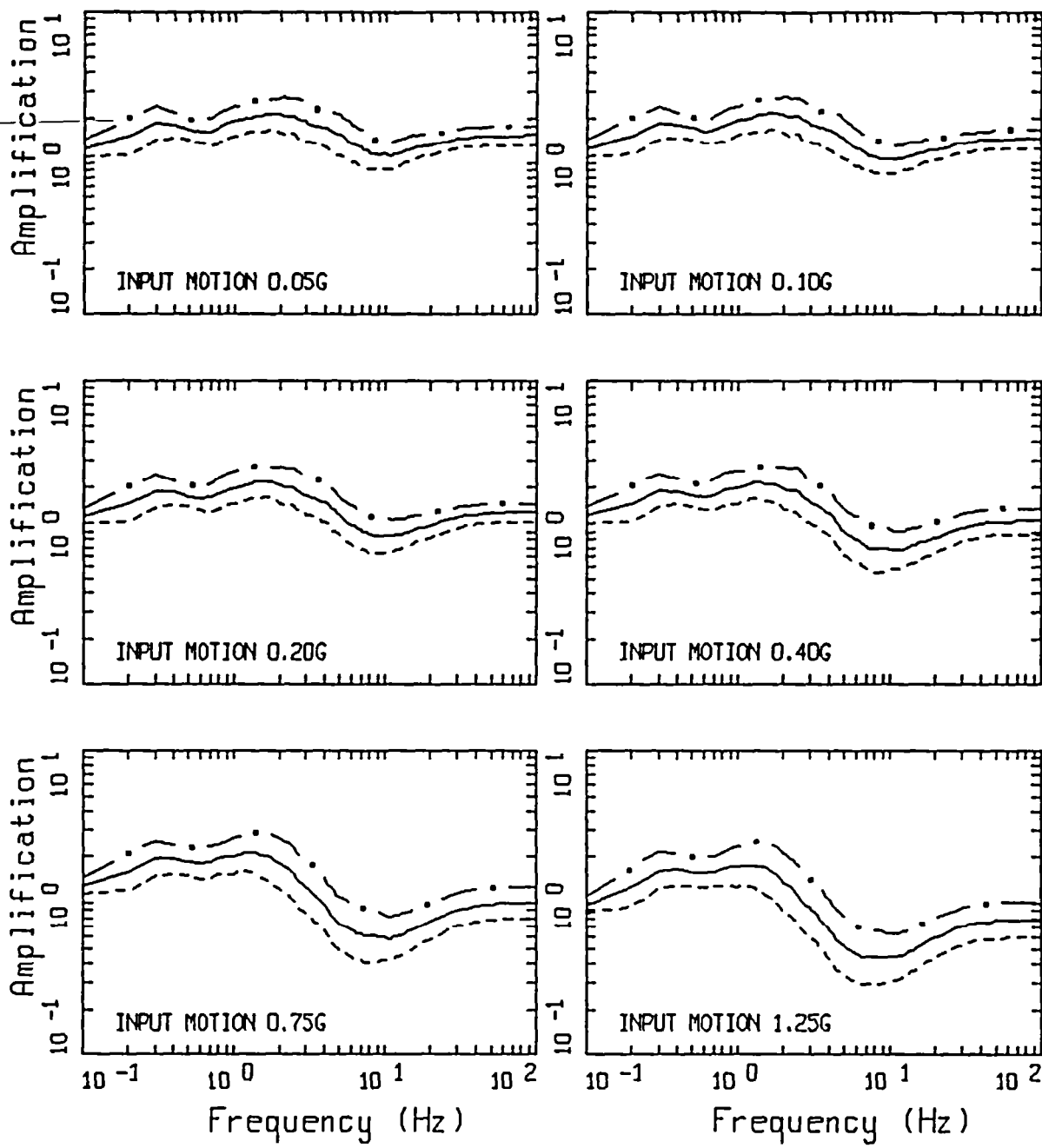


LA AMPLIFICATION  
 Q<sub>0</sub> (150 - 350 ft)

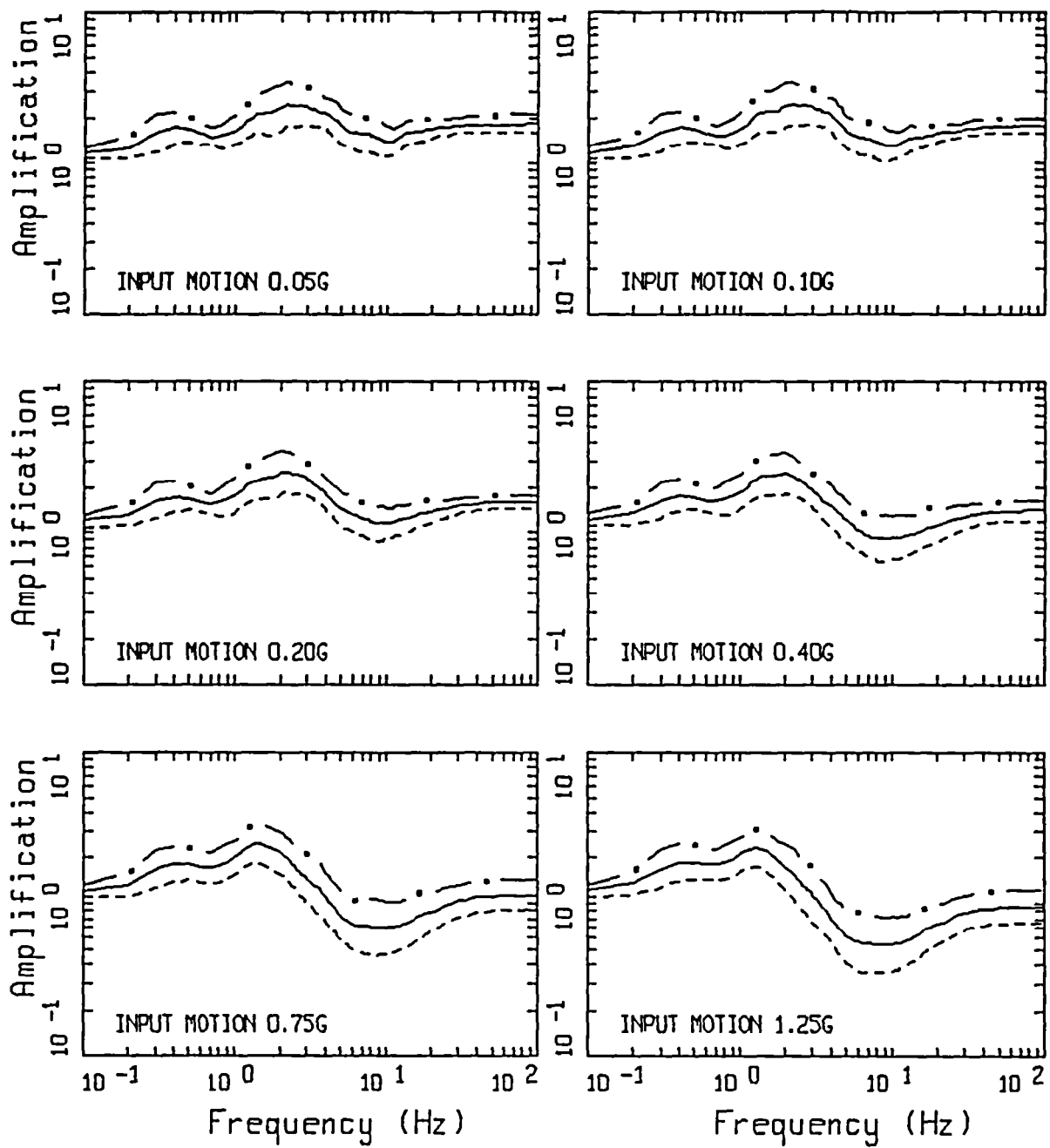




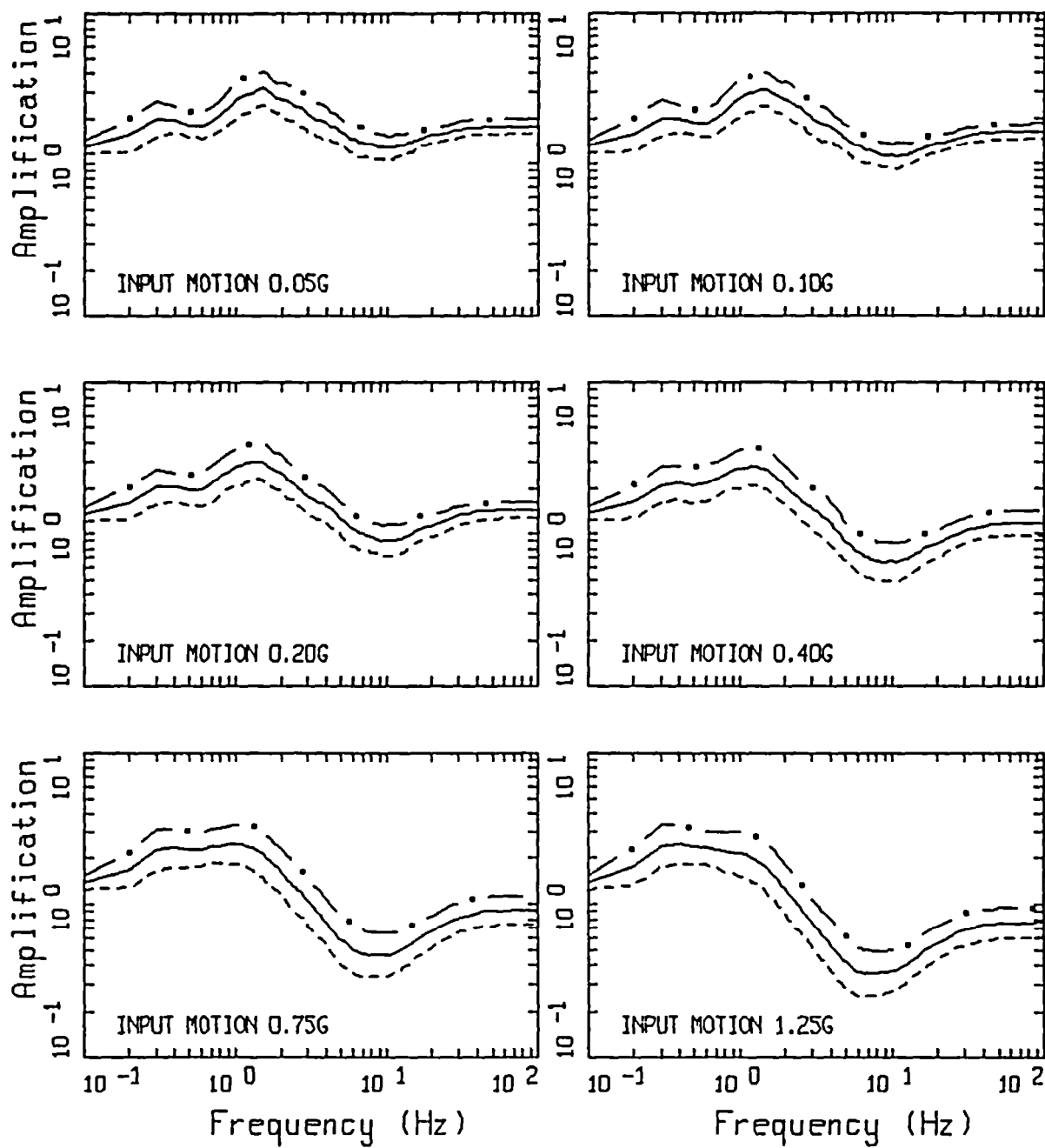
LA AMPLIFICATION  
 Q<sub>0</sub> (350 - 650 ft)



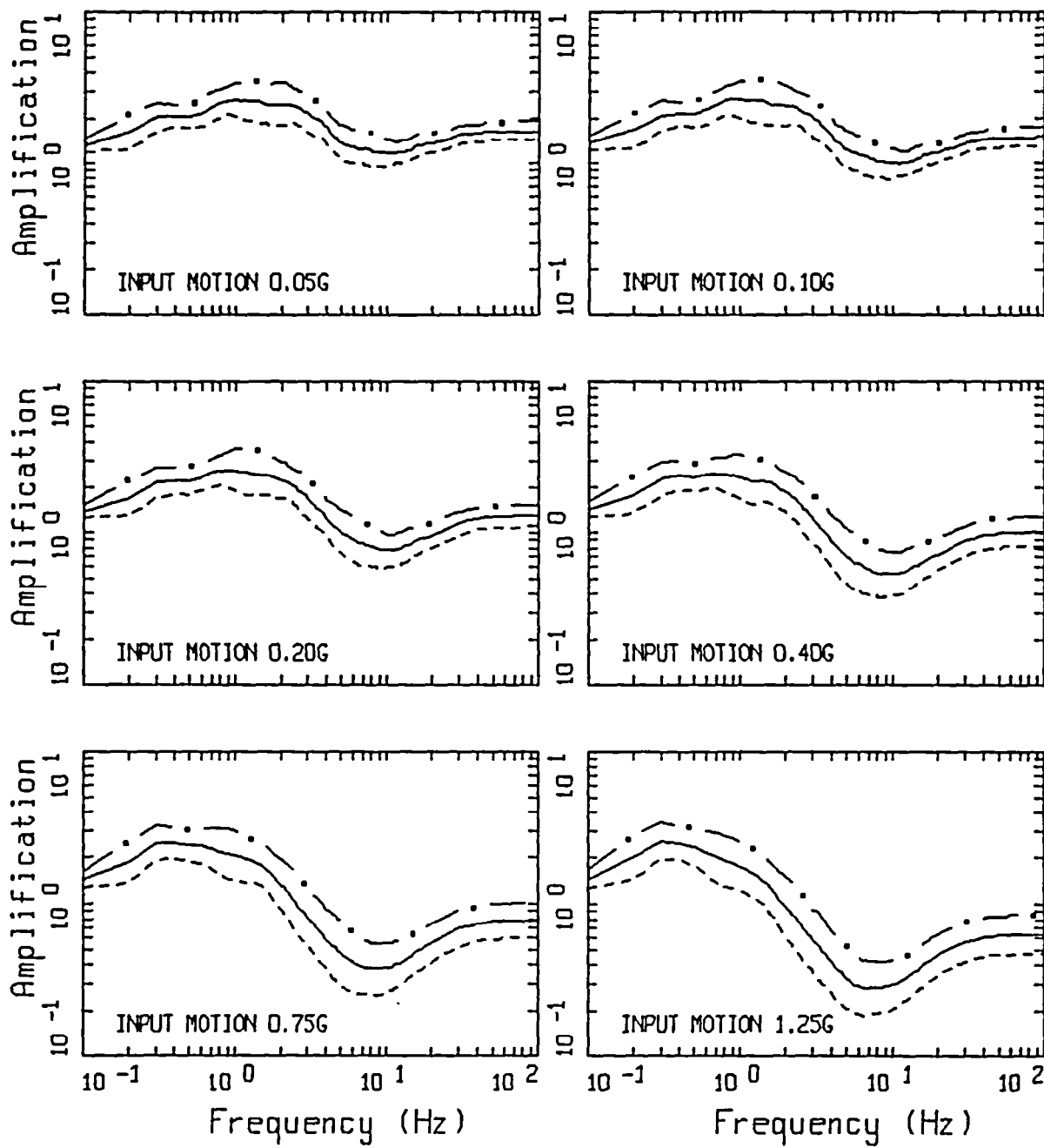
LA AMPLIFICATION  
Q<sub>0</sub> (30 - 1000 ft)



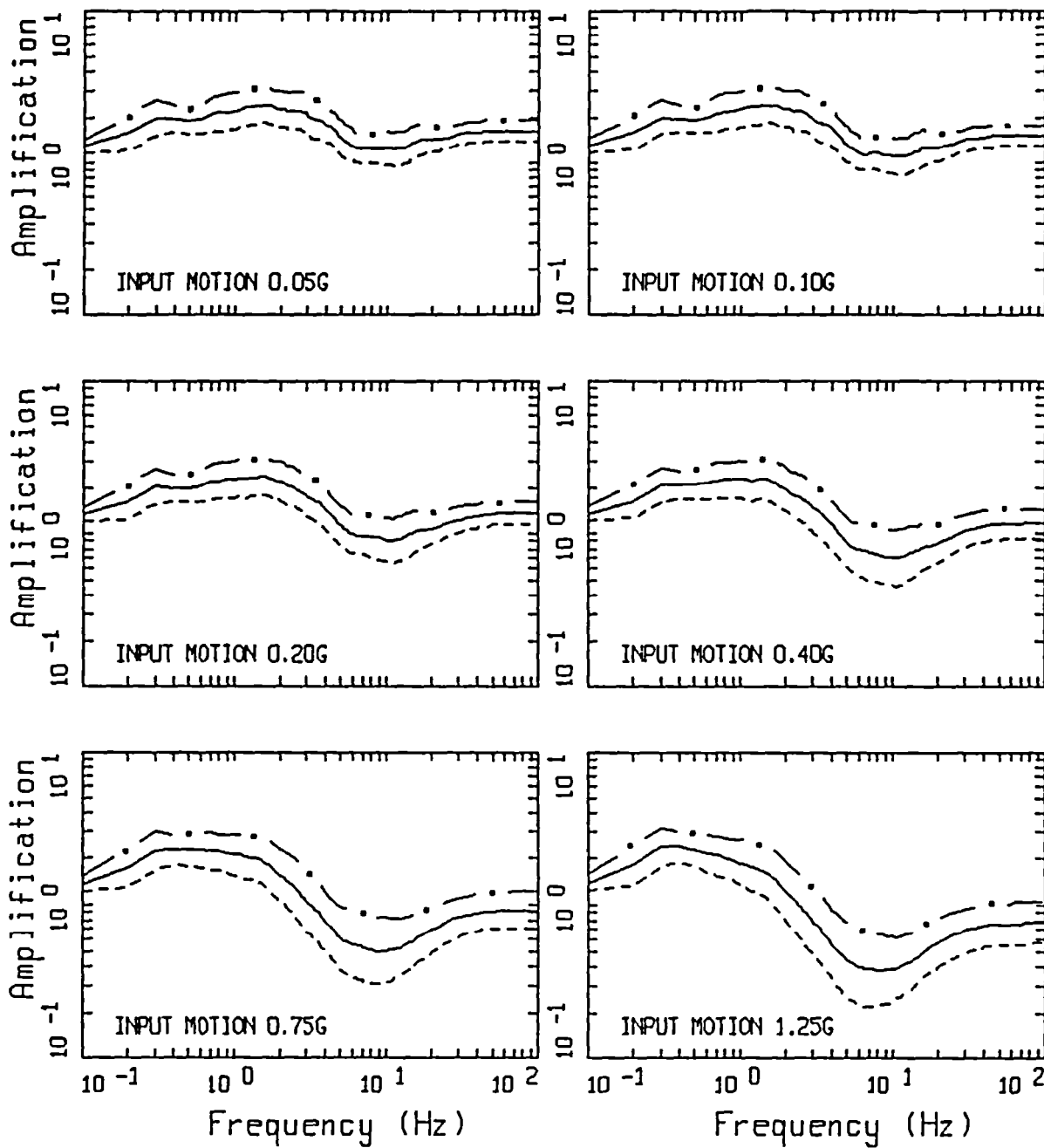
LA AMPLIFICATION  
 Q<sub>y</sub> (30 - 150 ft)



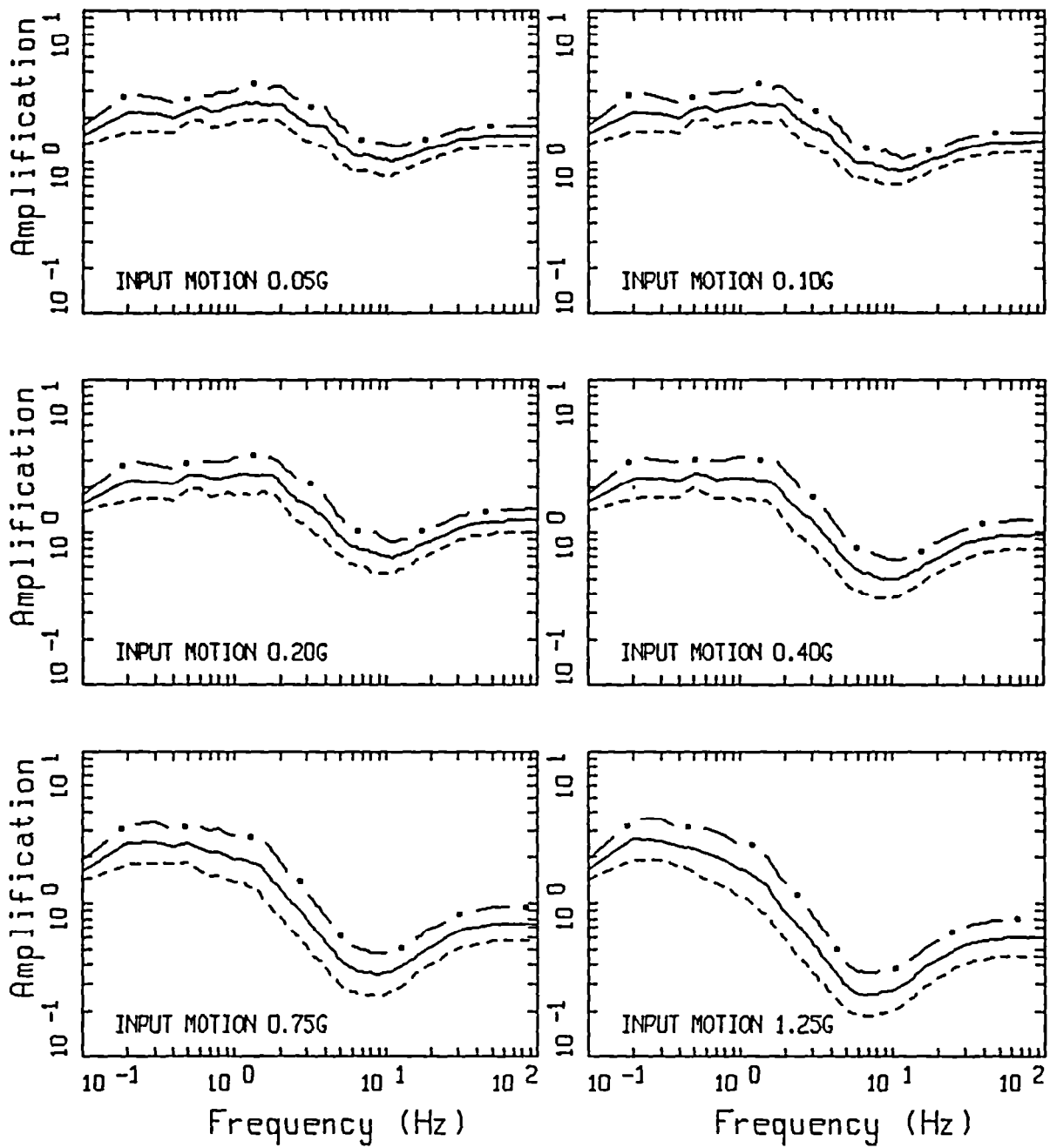
LA AMPLIFICATION  
 Q<sub>y</sub> (150 - 350 ft)



LA AMPLIFICATION  
 Q<sub>y</sub> (350 - 650 ft)



LA AMPLIFICATION  
 $Q_y$  (30 - 1000 ft)



LA AMPLIFICATION  
 $Q_y$  (500 - 1500 ft)